HIGH STRENGTH IRON COMPACTS CONTAINING CARBON, COPPER AND TIN.

A thesis submitted in application for the

degree of

Doctor of Philosophy

in

THE UNIVERSITY OF ASTON IN BIRMINGHAM

by

Paul Smith, B.Sc.

September 1974.

Department of Metallurgy,

The University of Aston in Birmingham,

Gosta Green,

Birmingham, B4 7ET.

Summary

The addition of five percent of copper + tin in various ratios to iron powder compacts produced a liquid phase at sintering temperatures of 900-950°C; considerably below the temperatures normally employed for sintering iron-copper compacts.

The mechanisms of liquid phase sintering in this system have been studied. Electron probe microanalysis of sintering models showed that the addition of tin to the iron-copper system progressively increased the solubility of iron in the liquid phase, and decreased the rate of copper diffusion into the iron. Likewise, the presence of copper during sintering decreased the rate of tin diffusion into the iron. This interaction between copper and tin results in the presence of a low melting-point liquid phase throughout the sintering process.

No evidence of stabilisation of the α-iron phase due to tin solution at 950°C was detected either metallographically or by electron probe microanalysis at Cu:Sn ratios of 3:2 to 15:2.

The addition of carbon to iron compacts containing five percent of copper + tin gave greatly improved mechanical properties when sintered in argon or carbon monoxide. As carbon is a γ-stabiliser, it is suggested that the major sintering mechanism is due to the enhanced iron solution rate in the liquid enabling dissolution and re-precipitation processes to occur, and not to any increased sintering rate due to stabilisation of the α-phase.

The sintering atmosphere employed was found to control the final mechanical properties of the sintered compacts. Compacts with low Cu:Sn ratios (high tin content) gave high strengths only

when sintered in pure hydrogen. Compacts with high Cu:Sn ratios yielded high strengths when sintered in various atmospheres.

Heat treatment of Fe-Cu-Sn or Fe-Cu-Sn-C compacts did not improve the mechanical properties to the same extent as did judicious choice of the optimum combination of copper-tin ratio, carbon content, and furnace atmosphere.

CONTENTS

Section 1 Introduction

1.1. Copper additions to iron powder compacts

Copper is frequently added to sintered iron (3-10%) for the purpose of improving the mechanical properties, and sintering is generally undertaken at temperatures above the melting point of copper, between 1100 and 1300°C. The time of sintering is usually comparatively short. In these alloys, the change of dimensions during sintering is of particular interest, as a precise control of these dimensional changes is of considerable economic importance.

The reason for the expansion of 1-1.5% commonly obtained with these alloys is that the copper diffuses into the iron during sintering, thereby enlarging the grains. The counteracting shrinkage due to the sintering process is not enough to offset the expansion effects during normal sintering times. It is found that additions of about one percent of tungsten, phosphorus, or carbon reduce this expansion. In the former case tungsten acts as a barrier to the diffusion of copper into iron; and in the latter two cases, the formation of lower melting-point eutectics may permit the growth changes to occur at an earlier stage of the sintering process, leaving more time for the subsequent shrinkage processes.

1.2. Copper and tin additions to iron powder compacts.

Additions to iron-copper compacts which have the effect of reducing the expansion, lowering the effective sintering temperature, and reducing the total amount of added alloying elements to iron while maintaining acceptable mechanical properties in the final sintered compact are obviously desirable from the economic viewpoint.

Small quantities of tin added to the copper used in many iron-base compacts has this effect. Total alloy additions to iron of 3% Cu and 2% Sn, and a sintering temperature of 900°C yielded an ultimate tensile

strength of 278 MN/m^2, elongation of 4%, and linear expansion of 0.5% after only ten minutes sintering[22]. The tin was thought to improve the mechanical properties of these compacts at 900-950°C primarily by activated sintering due to stabilisation of the α-phase.

1.3. The present work.

Following the original work carried out at the Tin Research Institute[20,21,22,25] and by Esper and Zeller[24,26] it was clear that the sintering mechanisms had not been satisfactorily explained, and that a wider range of alloys and sintering parameters should be studied in order to derive the major benefits that the Fe-Cu-Sn system could offer. In addition, the further possibility of strengthening by the addition of carbon was not to be overlooked, even though these additions would prevent any stabilisation of the α-iron during sintering.

Section II. Literature Review.

2.1. The Classical Theories of Sintering.

The sintering process is of importance to three separate disciplines; powder metallurgy, ceramics, and the agglomeration of ore fines. The theory of the sintering process has, however, not been studied in close detail prior to about 1920.

Sauerwald published a paper in 1922 [1] which was the first attempt at a rational theory of sintering. The temptation to treat it as a recrystallisation phenomenon must have been great, and this in fact is what he did. However, his clear concepts regarding the part played by surface characteristics laid the foundation for all other sintering theories.

Many investigations have been made into the influence of the numerous powder, pressing, and sintering parameters on the properties of the resulting sintered compact. This information, together with the principles determining the processes of atom transport were used to explain the sintering process.

It was not until 1945 with a paper published in Russia, that Frenkel [2] analysed the growth of individual contact zones theoretically, and this led to experimental observations via appropriate models.

2.1.1. Single Component Systems.

The driving force for sintering has long been accepted as the thermodynamic instability of powders compared to a 'perfect crystal'.

A decrease in free energy results from:-

1) Diminution of the specific surface area due to initiation and growth of contacts.

2) Decrease in pore volume and surface area.

3) Elimination of non-equilibrium states within the lattice.

The surface and lattice activities of a powder are mainly characterised during manufacture, and are affected only to a limited extent during the compacting cycle. Very fine powders are found to sinter at lower temperatures than coarse powders.

2.1.2. Multicomponent Systems.

2.1.2.1. Without mutual Solubility.

In this case, for sintering to commence, a decrease in free surface energy (γ_A, γ_B) is necessary for a mutually insoluble system.

If $\gamma_{AB} < \gamma_A + \gamma_B$ then sintering will occur, whereas if $\gamma_{AB} > \gamma_A + \gamma_B$ then no sintering of A-B contacts will occur, but A-A and B-B sintering is not affected.

According to Pines and Sukhinin [3] the sintering characteristics are a quadratic function of the mixing ratio. The number of A-A or B-B contacts, compared to the number of A-B contacts, determines the behaviour of the system exclusively.

The expected shrinkage, η, can be expressed as follows:-

$$\eta = \eta_A C_A^2 + \eta_B C_B^2 + 2\eta_{AB} C_A C_B \quad \ldots (i)$$

where $C_A + C_B = 1$

η_A and η_B signify the shrinkage hebaviour of A-A and B-B contacts respectively. Their number is a function of the square of C_A and C_B. The quadratic relationship (i) is also valid for the strength of sintered compacts, and has been verified on several systems (Cu-W, Cu-Mo, Cu-Fe).

2.1.2.2. Systems with mutual solubility.

In general, three aspects must be considered:

1) Sintering homogeneous solid solutions (no concentration gradient).
2) Sintering with simultaneous homogenisation.
3) Sintering with the decomposition of solid solutions.

Thümmler [4] dealt with the sintering of dilute, homogeneous solid solutions, in comparison with the pure base metal, and found that the sintering behaviour was closely related to the physical and thermodynamic properties of the solid solution. In the case of Fe-Mo, the higher energy for the formation of vacancies caused a marked inhibition of sintering by Mo. Solid solutions with a higher atomic mobility than the base metal would be expected to show enhanced sintering characteristics.

In the case of simultaneous formation of solid solutions, the sintering is controlled not by the solid solution formation, but by the different partial diffusion coefficients in each case producing a constant source of new vacancies, which in turn increases the atomic mobility of the system.

2.2. Liquid phase sintering.

In the case of a single component powder, sintered in an inert atmosphere, the only way in which sintering can proceed is via the neck contacts formed during pressing. If a liquid phase is present, however, the increased diffusion rate in melts; rapid dissolution and re-precipitation; and the possibility of re-ordering of the solid phase within the liquid matrix mean that the mechanisms of sintering in this case are rather different from those already discussed, at least in the initial stages.

Kingery [5-8] recognised three stages of liquid phase sintering:-

1) Rearrangement of the particles of the residual solid phase by viscous flow in the liquid phase. The random arrangement of the grains after mixing and pressing was improved, leading to shrinkage. A growing amount of liquid phase increased the shrinkage until theoretical maximum density was obtained with > 35 vol % liquid. The important factor in this shrinkage phenomenon was wetting of the

solid phase by the liquid. Solubility between the components still plays no part. The better the wetting effect, the more widely distributed will be the liquid phase. As the force of attraction between two spherical particles in the middle of which is situated a concave lenticular liquid is dependent upon the relative amounts, then it follows that coarse powder particles and small quantities of liquid should lead to greater forces of attraction.

2) Dissolution and Reprecipitation processes.

For these to take place, at least a limited solubility of the solid in the liquid phase is necessary. Densification occurs more slowly than in the rearrangement stage because material transport is via the liquid phase, necessitating dissolution and diffusion through the liquid. Small grains with highly convex curvatures disappear while the larger ones assume a more regular shape.

The driving force for material transport is the increased compressive stresses in the contact zones leading to a higher chemical potential and hence higher solubility in these regions. The dissolved material is then carried away and precipitated in regions of lower stress. This process would lead to shrinkage of the compact.

3) Coalescence.

Where there is complete wetting (angle of contact $\simeq 0$) then each solid particle will be separated by a thin membrane of liquid. If incomplete wetting occurs (angle of contact $< 90^{\circ}$) then the solid grains are only partially in contact without the complete interposition of the melt. After the conclusion of stage (1), processes similar to those found when sintering without a liquid phase take place, and subsequently become rate determining. This leads to slower densification and gradually falling driving force.

A non-wetting liquid phase (angle of contact $> 90^{\circ}$) is either ineffective, or, more probably, inhibiting and usually exudes partially from the sintered compact if present in sufficient quantity.

These three processes have been studied quantitatively by Kingery (loc. cit.). For the rearrangement stage, the relationship:

$$\frac{\Delta l}{l_o} = k r^{-1} t^{1+x} \qquad \text{applies with } (1+x) \leq 1$$

where $\frac{\Delta l}{l_o}$ is the change in length, t=time, minutes,

r = initial particle size, μm.

The corresponding relationship for the stage of dissolution and reprecipitation is:-

$$\frac{\Delta l}{l_o} = k' r^{-\frac{4}{3}} t^{\frac{1}{3}}$$

where r=original particle size, assuming diffusion in the liquid is rate determining, and a spherical grain shape is present.

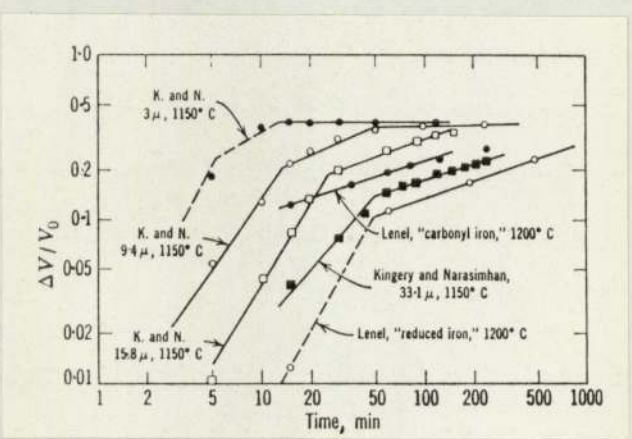

Fig. 1

When the liquid phase disappears during sintering, different conditions apply. This is the case in the systems Fe-Cu or Cu-Sn, where the liquid phase progressively dissolves into the solid phase until it disappears. Here, a growth component is found as well as a shrinkage, and has the technological advantage of enabling closer dimensional tolerances to be achieved in many instances.

The amount of expansion due to copper dissolving into iron can be controlled by adding carbon, which forms a ternary eutectic, increasing the amount of liquid phase, and decreasing the expansion.

2.3. Sintering models.

A large step forward in the understanding of the sintering process in the solid state was made by the work of Kuczynski [9,10] with models that allowed many simplifying assumptions to be made. He assumed the presence of spherical particles, circular cross sections, or cylindrical pores which enabled the mathematics to be simplified.

To study neck growth with time, the following models have been used: two spheres in point contact, a single sphere on a flat surface, and for the experimental study of a large number of individual contacts a bar-wire model, consisting of a wire spiral wound on a cylindrical bar. The contact widths are measured, after suitable metallographic preparation, on the micrograph.

According to Kuczynski, the first stage of sintering, characterised by formation of a neck between two particles, can be brought about by one or more of the following processes: viscous or plastic flow, evaporation and condensation, volume and/or surface diffusion. The relationships between the radii 'x' of the spheres, and 'a' of these spheres, time t, and temperature T can be described by the general

equation

$$\frac{x^n}{a^m} = F(T)t$$ where F(T) is a function of temperature only.

Thümmler and Thomma in their review of the sintering process [11] tabulate the results of Kuczynski and several other workers.

$$\frac{x^n}{a^m} = F(T)t \quad \text{or} \quad \frac{x}{a}\, n = F(T)ta^{n-m}$$

Mechanism	n	m	n-m	F(T)	Author	Ref.
Viscous or plastic flow	2	1	1	$3\gamma/2\eta$	Frenkel	
Evaporation and recondensation	3	1	2	$\sqrt{\frac{9\pi V_0 \gamma P_0}{2MRT}}$	Kuczynski	
	7	3	4	—	Pines	
Lattice diffusion	5	2	3	$K\frac{D_v V_0}{RT}$	Kuczynski Kingery & Berg	
	4	1	3	$K_1\frac{D_v \gamma V_0}{RT}$	Pines	
Surface diffusion	7	3	4	$56\frac{\gamma V_0 \delta}{RT} D_s$	Kuczynski Rockland	
	-	-	-	$X^6 \ln\frac{x}{2a} \sim t$	Pines	
	5	2	3	-	Cabrera Shwed	
	3	1	2	-	Shwed	

It can be seen that conclusions regarding the dominant factor in transport can be drawn from the time dependence of neck growth, but that these conclusions are not consistent. The experimentally determined exponent is frequently liable to uncertainties of $\pm$ 0.5, and also appears to be temperature dependent. The validity of n=2 for flow processes, and n=3 for evaporation and condensation are not doubted today. Also the balance of evidence favours a value of n=5 for volume diffusion.

2.3.1. The application of models to liquid phase sintering.

The models discussed above have been used in several studies of the liquid phase sintering process. The amount of success obtained was variable, due to the very complex conditions which existed. The more reactive the liquid phase, the more difficult it was to obtain reproducible results. Eisenkolb[12] used the 'rod and wire' method of Kuczynski to assess the effect of various liquids upon the sintering of carbonyl iron and Armco iron. Melts of lead, boric acid, and borax, as well as mixtures of calcium and sodium chloride and of potassium and sodium fluoride were used. The contact areas were considerably enlarged in some cases, and the general conclusion was that transport of material was promoted by chemical processes. After these model experiments, Eisenkolb made up powder compacts to assess the mechanical properties of a wide range of additions including copper alloys and hard solder. The mechanical tests did not always follow the results of the model experiments, because of unfavourable brittle phases produced. Hence it was quite possible for some additions to increase the rate of sintering significantly but not to improve the mechanical properties.

G. Matsumura [13] sintered iron wires in the presence of a

liquid phase, using the spool models of G.A. Geach and F.O. Jones[14] and B.H. Alexander and R.W. Balluffi[15]. Sulphur and phosphorus additions to iron are known to accelerate the sintering process. Small additions of these two elements were made separately to iron spool models to investigate their effect quantitatively. In addition, the eutectic of fayalite ($2FeO\text{-}SiO_2$) and wüstite (FeO) (eutectic temperature 1177°C and composition ~24 wt % SiO_2) was found to be effective for the acceleration of the sintering of iron. The mechanism of this accelerating process was also studied.

The rate of neck growth in the case of the fayalite-wüstite eutectic was determined, and a relationship of

$$\left(\frac{x}{a}\right)^5 = \frac{K}{a^2} t \quad \text{was obtained}$$

where x = half neck width

a = radius of the wire

t = sintering time

K = a constant

As the mechanism of sintering or iron in fayalite-wüstite eutectic was based upon the dissolution and precipitation of iron, and no mutual diffusion between iron and the liquid phase was expected, then this mechanism was similar to that of evaporation and condensation. For this process Kuczynski[loc. cit.] derived the following equation:

$$\left(\frac{x}{a}\right)^3 = \frac{K}{a^2} t$$

Since the fifth power relationship was observed rather than the third power, it was concluded that the rate determining step was not the speed of the dissolution of iron into the liquid phase, but rather

the diffusion of iron ions through the liquid phase.

2.4. Sintering of iron.

2.4.1. Sintering in the α- phase.

The sintering mechanisms of α - iron have received very little attention, although they are of practical and fundamental interest. In industrial practice most iron powders are sintered in the austenite range, but fine iron powders sinter rapidly at temperatures below the transition point.

Fischmeister and Zahn[16] initially studied the growth of necks in iron wire spools made of 100 µm diameter carbonyl iron wires. These were sintered in dry hydrogen at various temperatures. In all cases the results yielded a seventh power rate law for neck growth, which indicates a mechanism of surface self-diffusion for material transport. The exponent n=7 is constant throughout the ferrite range, but changes gradually to a value of n=5 in the austenite range, and remains at this value into the δ - range (Fig. 2).

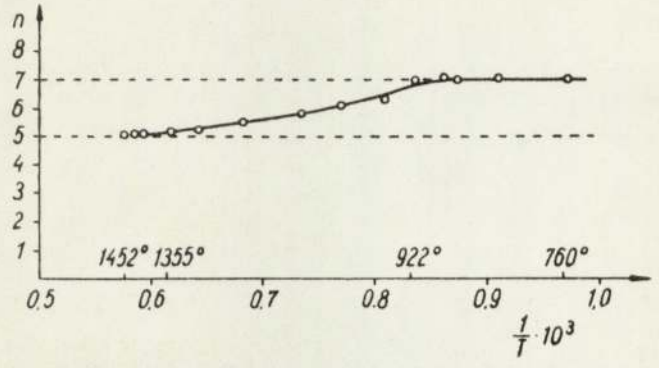

Fig. 2. The exponent of the rate law of neck growth as a function of temperature.

Fig. 2.

These results indicate that two opposing mechanisms can operate: surface self-diffusion at low temperatures, and volume self-diffusion at higher temperatures.

Many criticisms of Kuczynski's derivation of the exponent 7 for surface diffusion have been made, but Fischmeister and Zahn have compared the surface diffusion constant obtained from wire spool experiments with the same constant derived from scratch healing and thermal grooving experiments. Fig. 3 shows that the results are complementary, so that the exponent value of 7 seems to be accurate for surface diffusion.

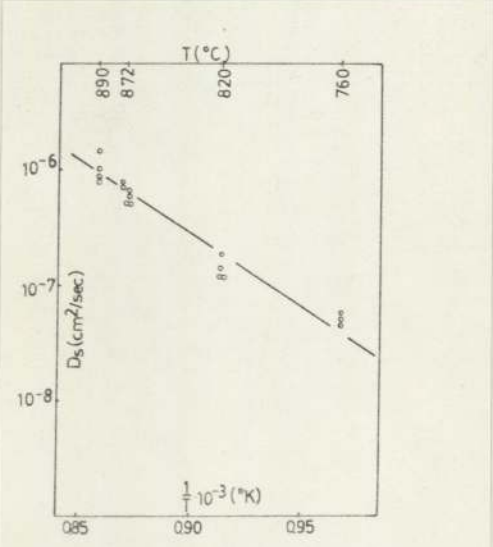

Surface diffusion constant *vs.* inverse temperature from wire models.

Fig. 3

The later stages of sintering, accompanied by a marked shrinkage, are due to volume diffusion since it can be shown that surface diffusion on its own cannot lead to a shrinkage. However, the experimental results illustrated above indicated a surface diffusion mechanism, but shrinkage was observed also. Fischmeister and Zahn explain these

observations by saying that different transport mechanisms are operative depending upon the size of the particles.

J. Backmann and G. Cizeron[17] considered the sintering mechanisms of carbonyl iron powder in the α - phase. A dilatometric approach was used, and the rates of shrinkage measured during heating to determine the activation energy of sintering. The measurements were made between 450-950°C in hydrogen for the phases of shrinkage corresponding to the first two stages of sintering. The value of the activation energy obtained in this range was close to that for intergranular self-diffusion. Their use of this rate method verified that volume diffusion becomes predominant when the residual porosity is essentially within the grains; the final stage of sintering.

2.5. Furnace atmospheres.

2.5.1. Atmospheres for carbon control.

In the sintering of ferrous alloys containing carbon, the atmosphere also serves to control the carbon concentration. Changes in carbon content occur by reaction of the added graphite with surface oxides or furnace gases.

For example,

$$2CO \rightleftharpoons CO_2 + C \qquad K_1 = \frac{P^2_{CO}}{P_{CO_2}}$$

$$CO + H_2 \rightleftharpoons H_2O + C \qquad K_2 = \frac{P_{CO} P_{H_2}}{P_{H_2O}}$$

$$CH_4 \rightleftharpoons 2H_2 + C \qquad K_3 = \frac{P_{CH_4}}{P^2_{H_2}}$$

When the reactions proceed to the right, solid carbon is produced

and when they proceed to the left, carbon is removed from the solid phase. In determining the equilibrium constants K_1, K_2 and K_3, it is assumed that the carbon is present as graphite, and has an activity of unity. In the presence of iron, the carbon may go into solution in the iron, and the activity of the carbon is < 1, at a value dependent upon its concentration. Thus the equations and equilibrium constants become modified to:

$$2CO + Fe \rightleftharpoons CO_2 + C \text{ (in Fe)} \qquad K_4 = \frac{P^2_{CO}}{P_{CO_2}} \cdot \frac{1}{a_c}$$

where a_c = activity of the carbon in iron.

Coult and Munro[18] show how the equilibrium concentration of carbon in iron at a given temperature varies with the CO/CO_2 and CH_4/H_2 gas ratios of the atmosphere employed. This data is shown in Fig. 4.

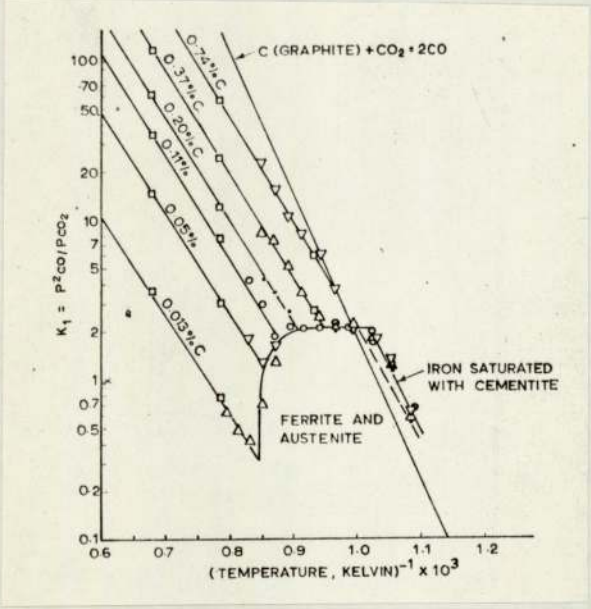

Fig. 4

To control the carbon levels in the compacts, the CO/CO_2 ratio or the CH_4/H_2 ratio must be closely controlled. This control is usually obtained by metering either the amount of CO_2 or H_2O in the furnace gases. Could and Munro found that for iron and iron + 7% Cu compacts sintered in an atmosphere of 0.5% Carbon potential showed little pick-up of carbon during sintering. They also exhibited little loss of carbon from the 0.5% level on sintering in an atmosphere of 0.2% carbon potential. The copper-bearing compacts were superior to the plain iron compacts in holding their initial carbon content. Presumably this is because the presence of a liquid phase prevents the ingress of carburising or decarburising gases to the inside of compacts. For short sintering times it seems that carbon control is not difficult for powder samples as long as the carbon potential of the sintering atmosphere is close to the added carbon level of the compacts.

2.5.2. Neutral atmospheres.

Brownlee, Edwards and Raine[18] classify furnace atmospheres as follows:-

1) Reducing atmosphere with decarburising conditions.

2) Reducing atmosphere with carburising conditions.

3) Neutral atmosphere.

In the case of iron powder metallurgy, the only neutral atmospheres under all conditions are the inert gases. They have the advantage of being easily dried and in the case of argon, reasonably cheap for specialist applications. They have no effect upon the sintering reactions taking place except in the latter stages on sintering with closed pores. In this case, the pores can only grow smaller until the surface tension forces are balanced by the gas pressure inside the pore. In the case of hydrogen, however, its diffusivity is high in solid metals, and pore

shrinkage can continue throughout sintering.

2.5.3. Atmospheres for activated sintering.

Most atmospheres for activated sintering make use of chemical reactions between the atmosphere and the compact to increase the sintering rate. Hydrogen will react chemically with any iron oxide in the iron compact to yield clean surfaces for the sintering reactions. This reaction is on a very limited scale, and is not termed 'activated' sintering.

Eudier[19] cited a true activated sintering process where an elongation at fracture of 10% in iron of density 5.7 g/cm^3 was obtained by incorporating small traces of a hydrogen halide in the sintering atmosphere. Salts can be formed on the surface of the iron, and if fusible, formed at the corners of the pores with the result that the pores were rounded. When the salts were decomposed at higher temperatures or by a change of atmosphere, the metal atoms agglomerated and the pores retained their rounded form. The considerable notch effect of irregular voids was thus eliminated, giving higher ductility values.

2.6. Sintering in the System Fe-Sn-Cu.

A.B. Shelmerdine and D.A. Robins[20] added small amounts of tin ($<1\%$) to steel containing 0.07 or 0.3% carbon and conducted mechanical tests on the alloys after both hot and cold reduction of the ingot into wire. Also they added tin to mild steel containing 0.15% carbon. In all cases an increase in yield point, UTS and hardness was noted, and a decrease in ductility as shown in Fig. 5.

The nature of the fractured surface showed increasing intergranular fracture as the tin content approached 0.6%. Upon quenching samples from 650°C however, impact properties were improved as the ductile/brittle

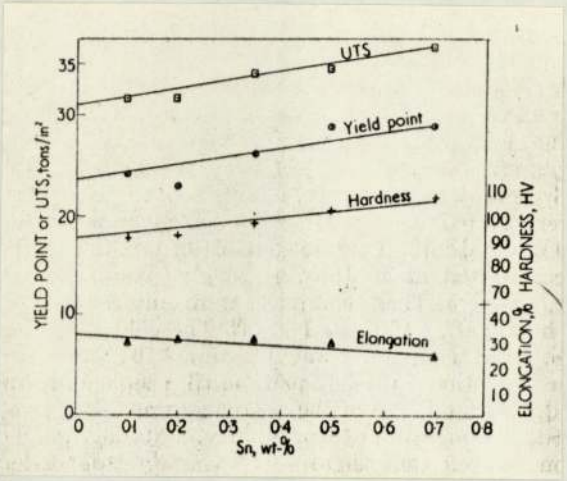

Fig. 5

transition temperature was lowered. The mechanism of embrittlement due to tin was not elucidated, but by using radioactive tin it was shown that tin or a tin-rich phase did not segregate in the grain boundaries even at low temperatures.

An attempt to reduce the sintering temperature of iron-copper compacts was made by R. Duckett and D.A. Robins[21]. Normally iron containing a few percent of copper is sintered at approximately 1150°C, above the melting point of the copper. The authors initially produced compacts containing 2% of -56 µm atomised tin, the rest -56 µm Swedish sponge iron powder. These were sintered at 1000°C for one hour in three types of hydrogen to assess the effect of water vapour:

1) Cylinder hydrogen

2) Oxygen-free dry hydrogen

3) Hydrogen saturated in water vapour at room temperature

The first two atmospheres gave compacts with tensile strengths between 247-263 MN/m^2 (16-17 tons/in^2) whereas the third atmosphere gave tensile strengths of only 185-201 MN/m^2 (12-13 tons/in^2). Cylinder hydrogen was used for the remainder of the investigation.

Figs. 6-9 illustrate the results obtained.

Tensile strength and hardness of compacts sintered for 1 hour:

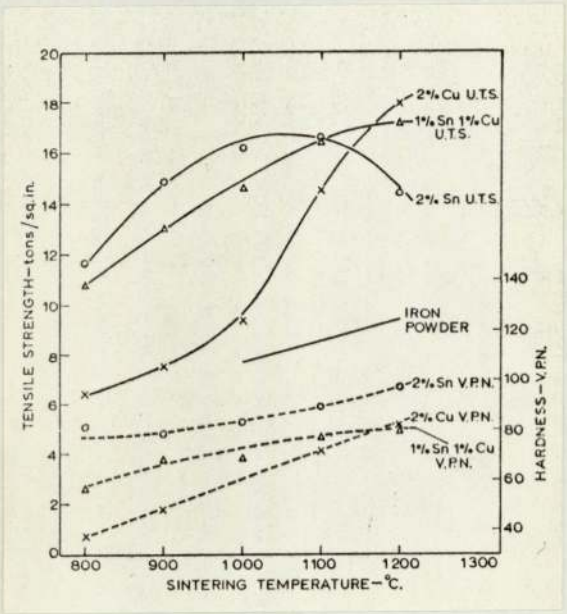

Fig. 6

Density and shrinkage of compacts sintered for 1 hour:

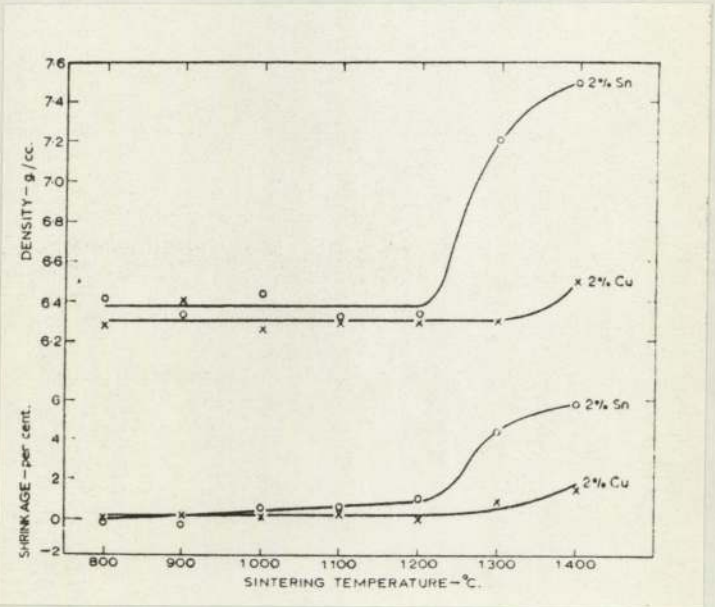

Fig. 7

Tensile strength and hardness of compacts sintered at 1000°C:

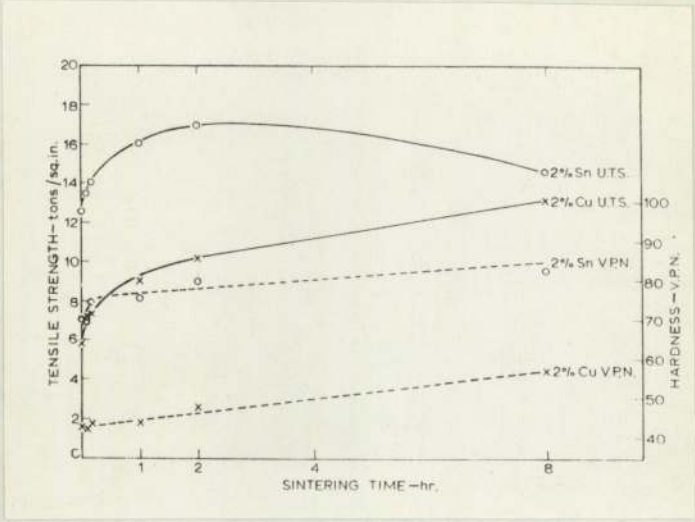

Fig. 8

Tensile strength and hardness of compacts sintered at 1100°C:

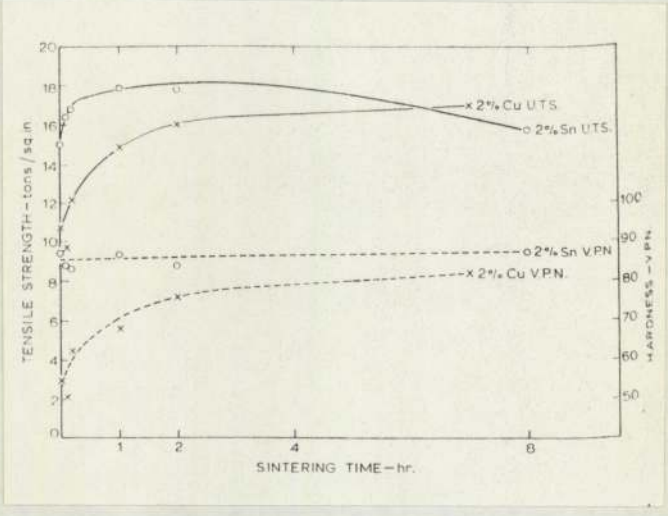

Fig. 9

They concluded that the addition of 2% tin considerably aided the sintering process, being more effective than copper in this respect. They showed that by using tin at least in place of some of the copper, lower sintering temperatures could be employed for equivalent strengths, or shorter times.

The mechanism by which tin activated the sintering process was thought not to be due to the presence of transient concentration gradients or compound formation, but to be some function of tin in homogeneous solid solution within the iron.

Further experiments were done by S.K. Barua, P.A. Ainsworth and D.A. Robins[22] using the same powder materials as previously, and an atmosphere of oxygen-free, dry hydrogen.

Many results were obtained in terms of the final mechanical properties, and the pertinent ones are shown in Fig. 10.

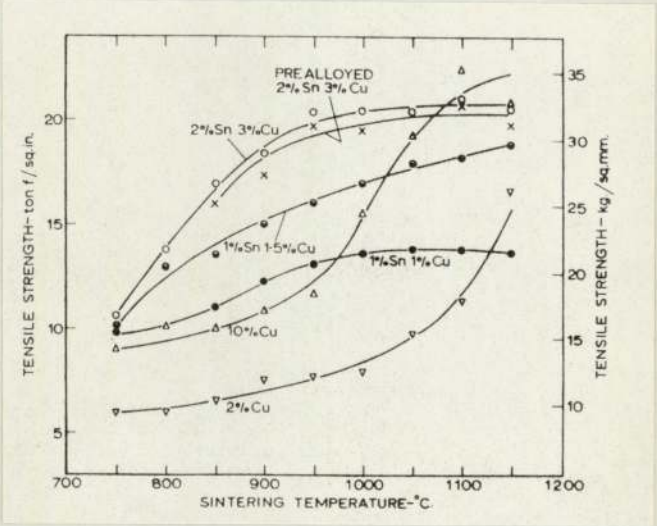

Fig. 10

The recommendation made after this series of experiments was that 2% Sn + 3% Cu in elemental form gave maximum improvement of properties. A less effective, but none the less important improvement can be obtained by additions of 1% Sn + 1½% Cu. The sintering temperature to be employed could be 900-950°C. Shrinkage varied from +0.7% to -0.3% depending upon additions. It was concluded that the change in properties was due to a rearrangement of the total porosity rather than its reduction.

The mechanisms by which sintering was aided by copper and tin additions were not established, but several ideas were presented.

Tin on its own goes easily into solid solution in the iron, and affects surface energy and self diffusion rates in iron. In the presence of copper, at low copper:tin ratios, the tin can still diffuse predominantly into the iron, and the above processes occur. Even with copper: tin ratios of 3:2, where the Cu_3Sn liquid phase is present in larger quantities, it was concluded that it was the tin only which enhanced the sintering process by increasing self-diffusion rates and lowering surface tension.[23]

An investigation into the reactions occurring in the Fe-Cu-Sn system was carried out by F.J. Esper, K.H. Freise and R. Zeller,[24] following the work of Robins et. al. [20-22] Dilatometric measurements were made for various iron-rich alloys. The sintering reactions of Fe-Sn compositions with 2% and 5% of Sn are shown in Fig. 11. When sintered compacts with 3% Sn were cooled from 1200°C, no dilation due to the $\alpha \rightarrow \gamma$ transition was observed. This is in agreement with the binary phase diagram (Appendix A).

In the case of Fe-Cu-Sn compositions, reaction occurred at a temperature as low as 230°C, when liquid tin reacted with copper.

Sintering reaction in Fe Sn-compositions (2 to 20 wt-% Sn)

Dilatometer-results		*X-ray-diffraction analysis*
Temperature-range $\triangle$ t °C	Probable reaction	Phase composition of the sintered specimen at room-temperature
~ 235 to ~ 420	β-Sn → Liq.	α-Fe, β-Sn
~ 420 to ~ 460	Liq. + α-Fe(s) → $FeSn_2$(s)	α-Fe β-Sn, $FeSn_2$
~ 460 to ~ 495	$FeSn_2$(s) + + α-Fe(s) → FeSn(s)	α-Fe FeSn, $FeSn_2$
~ 495 to ~ 530	Liq. + α-Fe(s) → FeSn(s)	α-Fe FeSn
~ 530 to ~ 600	no reaction	α-Fe FeSn
~ 600 to ~ 660	FeSn(s) + α-Fe(s) → Fe_3Sn_2(s)	α-Fe + α-Fe (solid solution) FeSn, Fe_3Sn_2
> ~ 660	$FeSn_x$(s) + + α-Fe(s) → α-Fe (solid solution)	α-Fe(s) + α-Fe (solid solution)
~ 660 to ~ 765	no additional reaction	α-Fe + α-Fe (solid solution) Fe_3Sn_2
~ 765 to ~ 880	Fe_3Sn_2(s) + + α-Fe(s) → Fe_3Sn(s)?	5 wt—% Sn: 850 °C: traces of FeSn, Fe_3Sn_2 H : α-Fe (solid solution)
> ~ 880	→ Fe_3Sn(s) + + α-Fe(s) → α-Fe (solid solution)	5 wt—%Sn: α-Fe (solid solution)

Fig. 11

Characteristic temperatures from the dilatometer diagrams at which changes of the dimensions were recorded, agreed with temperatures of phase changes in the binary Cu-Sn system (Appendix A).

S.K. Barua and C.J. Thwaites[25] published a further paper concerned with the mechanisms of Fe-Cu-Sn sintering. They also looked at longer sintering times, and the effect of a decarburising atmosphere - the only time that these workers considered an atmosphere other than pure hydrogen.

The powders used were elemental, and mixed with a binder of stearic acid dissolved in CCl_4, which was then evaporated. These were pressed at 40 Kg/mm^2 into square section bars. Sintering was carried out initially in a tube furnace with an atmosphere of dry oxygen-free hydrogen. Heating was carried out in two stages, the first stage comprising 5 minutes at 400°C to burn off the binder, followed by pulling the specimens into the hot zone for the required sintering time. Rapid cooling was ensured by pulling the specimens into the cold water-cooled end of the furnace tube.

The effect of sintering time is illustrated in Fig. 12.

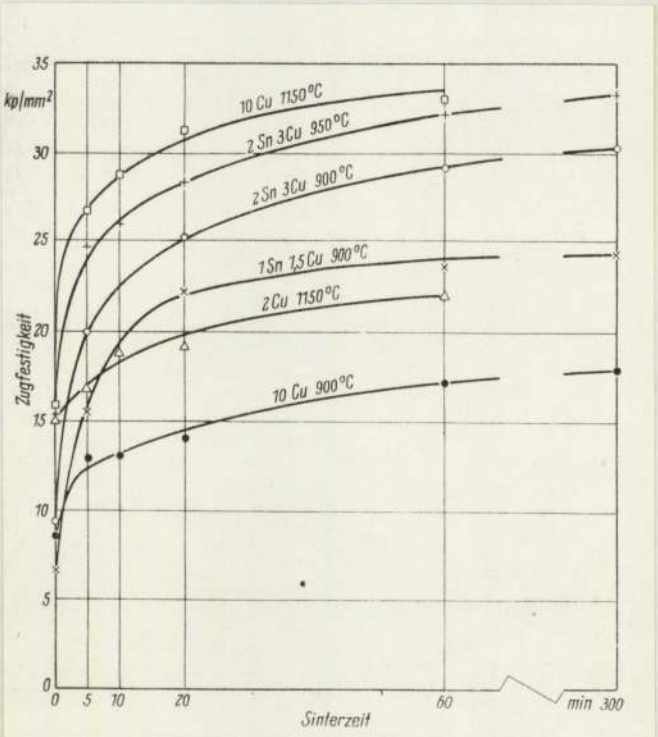

Fig. 12

This shows that the ultimate tensile strength rises with sintering time, and that after only 20 minutes at 950°C, adequate strength levels for many applications can be obtained from the copper-tin containing samples. Dilation of these specimens showed only an expansion of about 0.6% when sintered at 900°C or 950°C, whereas a 10% copper addition to iron gives a linear expansion of up to 2.3% when sintered at 1150°C. The explanation for this was given as being due to the large amount of Cu dissolution into the iron matrix in the latter case.

Following the conclusions of other workers[20-22] Barua and Thwaites then employed a sintering atmosphere of 90% H_2 + 10% CO_2 to give more decarburising conditions.

The increase in tensile strength for Cu/Sn bearing compacts was about 29.5 MN/m^2 ($3Kg/mm^2$), or ten percent. The 10% copper material did not show this dependence on atmosphere. This small improvement was judged to be due to removal of some of the carbon present in the iron powder during sintering.

An attempt to confirm this influence of carbon was made. Up to 0.8% graphite was added in elemental form to 3% Cu 2% Sn 95% Fe compacts. These were sintered at 1000°C in hydrogen and the final compacts gave the results shown in Fig. 13.

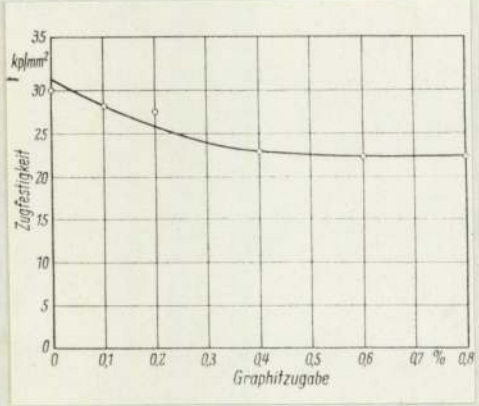

Fig. 13

The fall in tensile strength with increasing graphite level was thought to be due to carbon decreasing the beneficial effect of tin on the sintering process. No micrographs were available for examination.

An interesting attempt to improve the mechanical properties of this system was made by F.J. Esper and R. Zeller[26] who applied a heat treatment procedure subsequent to the sintering process. This procedure, they found to be dependent upon the copper/tin ratio. The brittleness of Fe-Cu-Sn sintered compacts has always offset the advantage of their low sintering temperature, so that Esper and Zeller looked at compositions ranging from copper:tin ratios of 1:3 to 1:9. Increasing ductility was found to occur with leaner tin additions as shown in Fig. 14.

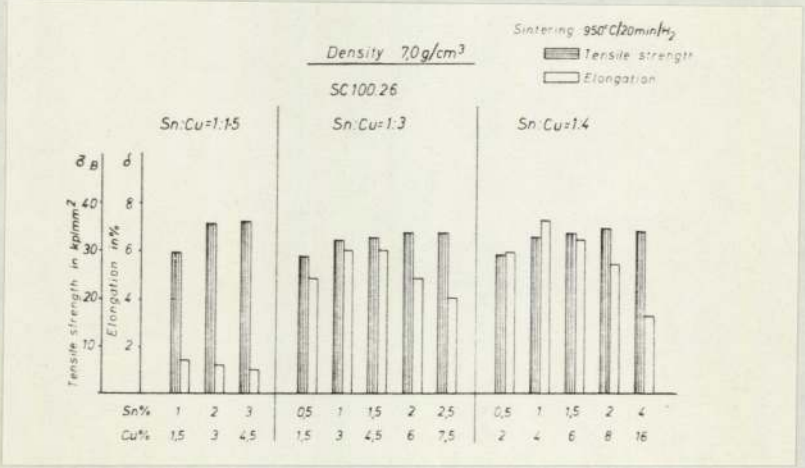

Fig. 14

High UTS values correspond to high as-pressed density as will be shown in the experimental results. This factor also greatly improves the ductility of the compacts over and above the improvement caused by higher Cu:tin ratios.

Heat treatment was carried out upon samples containing 4%Cu 1%Sn balance iron. Some samples were cooled at 10°C/min from the sintering temperature to room temperature. Others were cooled at 22 deg C/min from 950°C to a given temperature, then quenched in water. The slowly cooled samples were tempered between 550°C and 700°C for 2 hours. The results are shown in Fig. 15.

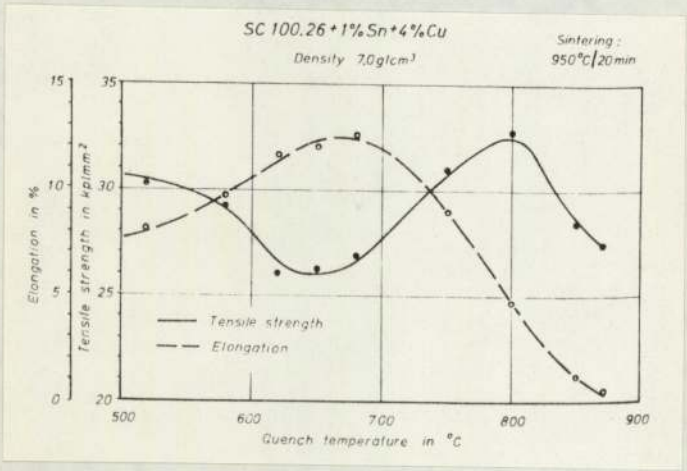

Fig. 15

X-ray and microprobe examinations were used to correlate mechanical properties with the phases present in the samples. In addition to

α -iron, two phases were present, probably Cu/Sn phases. One was fcc and the other bcc. The total amount of both of these phases was in the first approximation constant, but the amount of each individual phase was dependent upon heat treatment. The maximum amount of the fcc phase corresponded to the high elongation values, while those samples with a high level of the bcc phase had high tensile strength. The two phases could not be identified, but it was assumed that the fcc phase was a supersaturated solution of tin in copper, and the bcc phase corresponded to the solution of tin in β-copper in the temperature range above 650°C. The microprobe analysis showed that mainly copper diffused into the iron grains, and it did not detect any tin in the solution within the iron at a copper:tin ratio of 4:1.

In a further paper[27] Esper and Zeller continued their heat treatment experiments, and even carbonitrided some samples in an Ibsen kiln, and in a muffle furnace using Endogas. In both cases the temperature was 850°C for 80 minutes. Quenching was carried out in oil.

Briefly, the results indicated that whereas heat treatment can be beneficial in the case of copper:tin ratios of 1:3 to 1:9, in the case of 3:2 ratio, heat treatment leads to poor mechanical properties. Only a cooling rate of < 10 deg C/min guaranteed a tensile strength ≥ 30 kp/mm^2 together with an elongation $> 5\%$. The explanation was given in terms of excessive precipitation of Cu Sn compounds within the iron at tin-rich ratios when slowly cooled. This precipitation caused the iron to become more ductile. Carbonitriding did not give enhanced properties at a copper:tin ratio of 3:2, due, the authors stated, to the lack of iron-iron contacts when this copper:tin ratio was employed. Therefore the state of the iron - martensitic or

otherwise - had little bearing upon the strength of the compacts if the fracture mechanism was controlled by the intergranular CuSn compound.

Section III. Experimental Procedure.

3.1. Selection of experimental conditions.

In this investigation, it was necessary to use procedures and materials readily available commercially, so that any results could easily be translated into commercially profitable operations.

Certain restraints, however, had to be imposed in order to obtain meaningful results. For instance, closer control of furnace atmosphere had to be obtained in the laboratory than is common in industry so that sintering reactions could be studied in depth and yield reproducible results. Also, the decision to use an admixed lubricant in the laboratory depended more upon the effect the lubricant would have upon the variables to be studied, rather than the enhanced die life associated with this procedure. For investigations into sintering mechanisms no lubricant was added to the powder at all, but die wall lubrication was used throughout. This, it was felt, would be beneficial for the simple reason that the number of variables involved would be lowered.

The choice of dies, compaction techniques and pressures was made with commercial practice in mind, with slight modifications in mixing and die-filling to obtain the most consistent green compacts possible. The mechanical tests were carried out upon compacts conforming to BS 2590. These tests included tensile testing on a Denison machine, which measured ultimate tensile strength, and elongation. The yield point in no case was measurable from stress-strain curve, due to the effect of the porosity present upon the mode of deformation and fracture.

More details of the chosen experimental techniques follow in

the relevant sections.

3.1.1. Powder materials.

In ferrous powder metallurgy there is a very wide choice of powders available which can be categorised according to their methods of manufacture, their shape; their chemical composition, surface activity; or their compressibility performances.

Domtar and Höganäs powders tend to be porous, have fairly high residual oxygen levels due to their method of production, whereas carbonyl powders are spherical, dense and not easily compressed.

An easily available and commonly used powder, ROSPA MP32, made by the Domtar process was chosen for the main part of the investigation because of its well-tried and tested performance in a wide range of powder matallurgical fields. It yielded compacts with adequate green strength even at low compaction pressures, and gave higher density compacts at increased loads without any trouble.

The copper and tin powders used were water atomised powders. Particle Size Analysis and residual oxygen levels of all three powders appear in the results section.

3.1.1.1. Blending.

The powders were initially weighed out on an electronic balance. This worked well for small amounts, < 100g, and larger amounts were weighed on a weighted pendulum-type balance with a top-pan which was accurate to $\pm$ 0.5g.

Blending was carried out for small quantities (< 300g) in cylindrical glass jars placed in a mixing machine which revolved the jars about their longitudinal axis at 60 revs/min. At this speed, the powder mixes without lubricant additions were found to exhibit a minimum

amount of sticking friction to the glass walls, so two ceramic balls about 1.5 cm diameter were added to the powders in the jar, and caused much improved mixing by the tumbling action of the powder over the balls, and vice versa. A mixing time of 45 minutes was found to be adequate for all compositions containing about 5% of Cu + Sn, the balance iron.

3.1.1.2. Compaction.

A double-acting die was used to produce compacts conforming to BS 2590. This is shown in Fig. 16. A range of smaller cylindrical double-acting dies, and larger rectangular double-acting dies was available. The die was arranged upon the bottom platen of a Denison 300 ton hydraulic compression machine. The bottom platen was built onto a spherical bearing so that any slight misalignment between bottom and top platens was automatically removed during compaction. Any misalignment within the die housings was removed by careful adjustments by the technical staff. The resulting compacts were then substantially parallel along their length with no more than ± 0.002" discrepancy at either end.

Side view of double-acting die conforming to BS 2590:

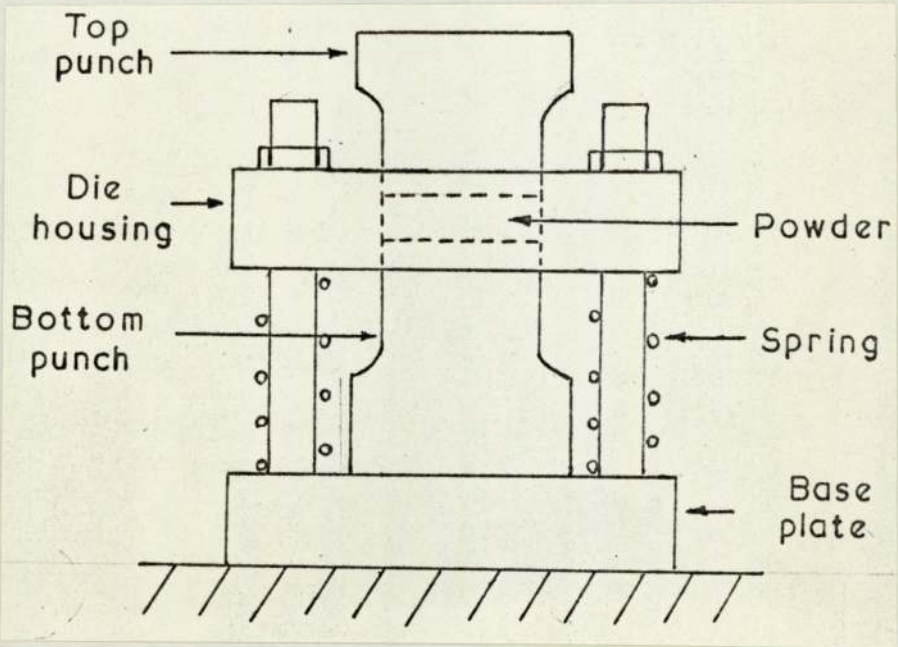

Fig. 16

Die wall lubrication consisted of squirting a solution of 1% stearic acid in ether into the die cavity, then lowering the die housing until the ether spilled out of the bottom punch. The top surface was then cleaned with rags, including the flush bottom punch. The assembly was released from load, the housing rose again, and the powder was introduced.

It was found that more segregation of dissimilar powders occurred if the die was filled without care than if the powders had been mixed very little prior to their introduction into the die.

20g batches of the mixed powder were used for each sample. If the powder was introduced into the die via a folded paper, for instance, then the heavier copper particles and much finer tin particles segregated to the bottom of the die. This was overcome as much as possible by compressing the die housing until the bottom punch was nearly level with the top surface. Then by slowly and carefully introducing the powder via a glass tube containing the requisite amount, and simultaneously allowing the die housing to return to its original position, the powder had very little distance to fall, and was consequently much less segregated. Finally the top surface of the powder was levelled with a straight edge flush with the top surface of the die, and the load removed. The top punch was inserted, and the load applied slowly via an oil bypass valve to the value required. Here it was held for approximately 3-5 seconds, and then reduced evenly to zero. The whole compaction cycle from the start (load beginning to rise) to the end took approximately twenty seconds. The load dials on the Denison were calibrated in KN, and could be read to the nearest 1 KN.

With the top punch removed, the compact was ejected smoothly.

The pressure needed to initiate this operation never exceeded $30MN/m^2$ as measured upon the dial.

3.1.2. Sintering.

After compaction of the samples, sintering was usually carried out immediately. If this progression could not be scheduled, then the compacts were stored as-pressed in glass dessicators until required.

The sintering furnace employed is illustrated in Fig. 17:

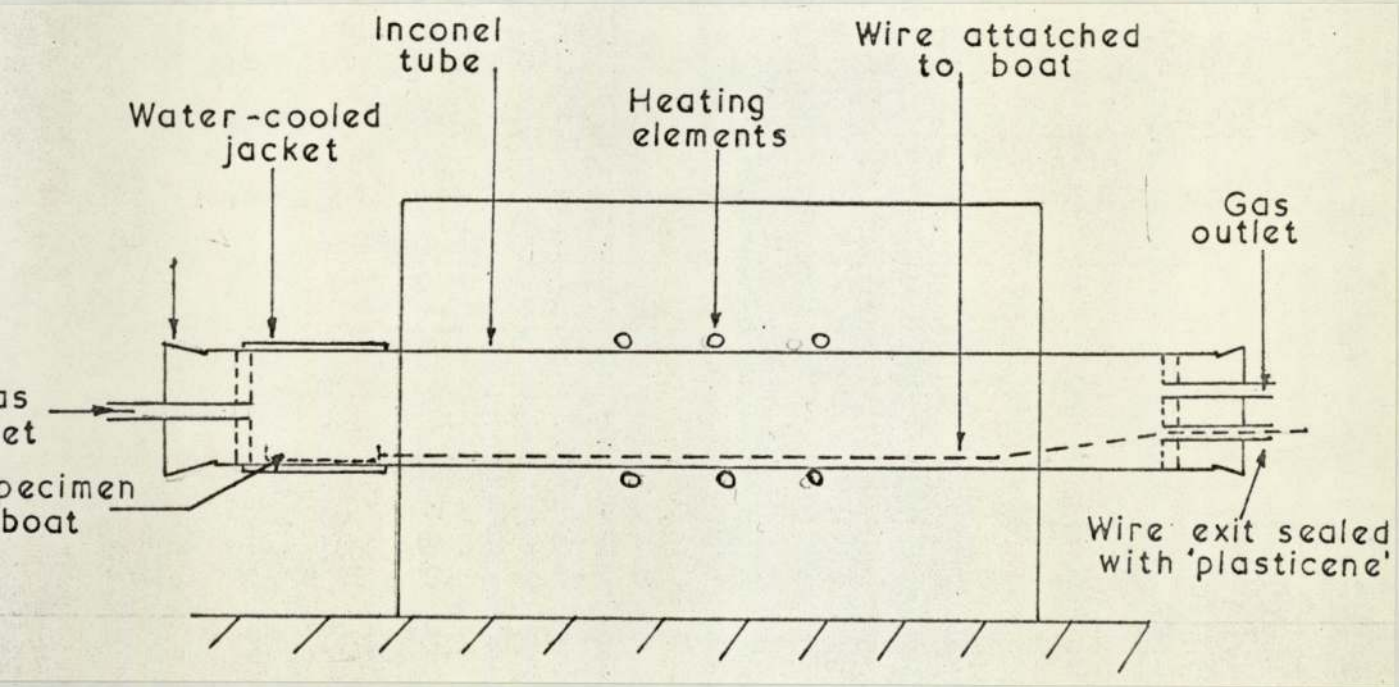

Fig. 17

It consisted of an Inconel tube 80mm in diameter and 3mm thick. Six silicon carbide ceramic heating elements were used, three each above and below the tube. This gave a hot zone of 150mm long $\pm 5^{\circ}C$. at a temperature of 900-1100°C. The ends were sealed with rubber bungs protected internally with circular asbestos discs. Glass tubes on the inlet side enabled the gas to enter from cylinders via the drying

train. This train consisted of a 50mm dia. glass tube containing an H_2 catalyst which converted any oxygen present to water vapour. Then came a section of silica gel, and finally a section of magnesium perchlorate on the furnace side. The three sections were separated by wads of cotton wool. The outlet rubber bung contained two glass tubes; one leading via a flowrate meter to the outlet pipe, and the other containing the Inconel wire with which the boat was pulled into the hot zone after adequate purging of the tube. This latter tube was sealed with plasticene enabling the boat to be pulled into the hot zone without ingress of air. The heating elements were controlled by a variable-tap transformer, and a Transitrol control unit enabling a temperature $\pm 5^{\circ}C$ of that set to be obtained. A separate Pt/Pt:Rh thermocouple was used in conjunction with a potentiometer to set the hot zone temperature accurately before sintering commenced.

After sintering was completed, the boat was pulled into the cold zone of the furnace, which was watercooled. A time of 20-30 minutes was then required in the cold zone to bring the sample temperature down to about room temperature. The samples, up to about eight in number, could then be removed if the furnace atmosphere was not explosive or poisonous. If it was, purging with a mixture of 90% N_2 10% H_2 was carried out once the samples were cool.

3.1.3. Atmosphere control.

The use of cylinder gas meant that mixing of gases was unnecessary. The drying train removed oxygen and water, and the flow rate meter controlled how much gas passed per unit time. A water bubbler at the outlet gave a slight positive gas pressure, and if the gas was momentarily turned off, the positive pressure would fall very slowly

indicating that the bungs were a very good fit and that very little air, if any, could gain access to the inside of the furnace.

High purity cylinder argon and hydrogen, and commercially pure cylinder carbon monoxide and 90% N_2 10% H_2 atmospheres were used.

3.2. Determination of the variables to be studied.

Early work carried out in the Department by the author and C. Fletcher[28] using the powders already discussed yielded a series of results which are illustrated graphically in Figs. 22-33 in the results section. Various copper/tin ratios were investigated as well as sintering temperature, time, particle size, and the amount of alloying elements added to the basis iron powder.

These results will be fully discussed in the relevant section, but certain observations were found to differ considerably from those obtained by TRI[21,22,25] and illustrated in Section II.

Furthermore, it was found that the published behaviour of FeCu-Sn compacts could be replicated in our laboratory by using an atmosphere of pure dry hydrogen and by adding small amounts of lubricant to the metal powders. These results are included and compared with work by TRI[22,25] and Esper and Zeller[26,27].

3.2.1. TRI results.

Experimental results obtained at the Tin Research Institute are well documented[loc. cit.] and led the workers to suggest a copper-tin ratio of 3:2 with a 5% total addition of these elements to iron. The sintering time advised was about 20-30 minutes in the temperature range 900-950°C. Advantages of this system were shown to be:

1) A lowering in the temperature used for sintering iron-base

powder components.

2) A lowering in the time used for sintering.

3) A saving in the overall production cost of the alloy components.

3.2.2. University of Aston results.

The experiments were carried out in a sintering atmosphere with a lower hydrogen content at all times. The TRI components were sintered in pure, dry hydrogen, whereas the author's sintering atmosphere consisted of a ready-mixed 90% N_2 + 10% H_2 which was dried before use. The reason for this choice was that this atmosphere corresponded more closely to the type of atmosphere which would be used industrially. No powder metallurgy producer employs pure hydrogen as an atmosphere for sintering common iron-base components.

These initial results showed that a higher Cu-Sn ratio gave better strength levels when the components were sintered in the 90% N_2 - 10% H_2 atmosphere, together with increased ductility with essentially the same sintering parameters of compaction pressure, time and temperature.

3.2.3. Computer analysis of TRI and University of Aston results.

The physical properties of Fe-Cu-Sn compacts were shown to be variable depending on the sintering conditions. For this reason a series of experiments was carried out in conjunction with TRI with the aim of determining the most important variables.

The method chosen was to perform a multiple regression analysis upon results obtained by changing one or more of the processing variables. The easiest way for this form of analysis was to replicate experiments both at Aston and at TRI, using identical Cu:Sn ratios, sintering time and temperature, and atmospheres; and in addition to

compare the different powders used and the mixing and compaction methods. When all results were collated, they were precessed by the University computer and yielded a multiple regression equation showing the relative influence of the different variables. This procedure was carried out both at the 95% and 5% significance levels.

The results of this analysis showed which variables were most important in controlling the strength of the Fe-Cu-Sn sintered compacts, and therefore which variables were worthy of study in determining the sintering mechansisms involved. The regression equation showed that the most important variables were as follows (in order of the relative effect upon the ultimate tensile strength of the compacts):

1) The sintering atmosphere employed.

2) The copper/tin ratio.

3) The sintering temperature (within the range of 950°C and 1150°C)

During discussions with the TRI workers several possible reasons were put forward to account for the low mechanical properties of the 3:2 Cu:Sn ratio iron compacts sintered in 90% N_2 10% H_2. These were based on the possible difference in powder characteristics, and to the fact that 0.5% zinc stearate was added to the TRI compacts before mixing and compaction. No previous consideration of furnace atmospheres had been made by the TRI workers. In order to decide if it was the zinc stearate additions which changed the properties achieved using lubricant-free compacts, the following experiments were conducted, using both 90% N_2/10% H_2 and pure H_2.

3.3. Zinc Stearate Additions.

3.3.1. Using a sintering atmosphere of 90% N_2 10% H_2.

The effect of the initial 'burn-off' period of fifteen minutes

at 300-500°C prior to sintering was investigated.

Three sets of three samples were prepared of composition 95% Fe 3% Cu and 2% Sn. Two sets contained no zinc stearate, and the third set contained 0.5% of this lubricant. The first set was sintered at 950°C for 30 minutes. The second set was sintered as before after a 15 minute simulated 'burn-off' period at a temperature of 300-500°C. The third set containing the lubricant was treated as for the second set.

Tensile strength and elongation were measured after sintering. The effect of lubricant additions upon the green density was noted.

3.3.2. Using a sintering atmosphere of pure H_2.

In this series, two sintering temperatures (1100 and 950°C) were employed, and copper-tin ratios of 3:2, 6:2, and 8:2 all at the 5% addition level were studied. Each sample contained 0.5% zinc stearate added as powder before mixing. These conditions and compositions were chosen to enable direct comparison to published work[26,27].

These experiments compared well with similar work carried out elsewhere, and showed that the addition of zinc stearate, although increasing the tensile strength and ductility as may be expected, did not do so to the required degree, in the case of those sintered in 90% N_2 10% H_2, to explain the considerably lower properties which are obtained in this case.

In the following section covering a study of the sintering mechanisms involved, no zinc stearate additions were made, to keep the system as simple as possible.

To study the sintering mechanisms involved in the Fe-Cu-Sn system, experiments were designed to elucidate the diffusion mechanisms operating.

The TRI workers proposed that the major sintering mechanism was stabilisation of the α-iron phase by tin during sintering. If this were true, then carbon additions could only prove to be detrimental due to the opposing influence of carbon stabilising the γ-iron phase. Early work[29] indicated that carbon additions to iron-Cu-Sn compacts could improve the strength of these compacts after sintering at 1150°C.

So it was proposed to use diffusion experiments to study the way in which liquid copper+tin alloys react with iron with and without the presence of carbon. As the regression analysis showed the sintering atmosphere to be of great importance, this also was studied in detail.

3.4. Diffusion Experiments.

3.4.1. Study of the reaction between 60% Cu 40% Sn alloy with steel of varying carbon content.

Five samples of steel with carbon contents varying from zero to 0.8% were made by vacuum melting pre-reduced Domtar iron powder with graphite additions. Pre-reduction of the powder was carried out by heating in H_2 for 30 minutes at 900°C. The vacuum furnace contained a fused alumina crucible heated by a tungsten heating element. The whole assembly could be tilted within the vacuum chamber to cast the melt into a copper mould. The iron powder + graphite in the required amounts were compacted initially into cylinders with a ~~surface~~ cross-sectional area of 645 mm^2 and about 15 mm deep. This procedure was adopted to fill the crucible with enough material. After casting, the steel was annealed in argon at 50°C above the A_{c_3} temperature for one hour and normalised to refine the cast structure. They were then machined as shown in Fig. 18.

0.3g of pre-alloyed 60% Cu 40% Sn alloy powder was introduced

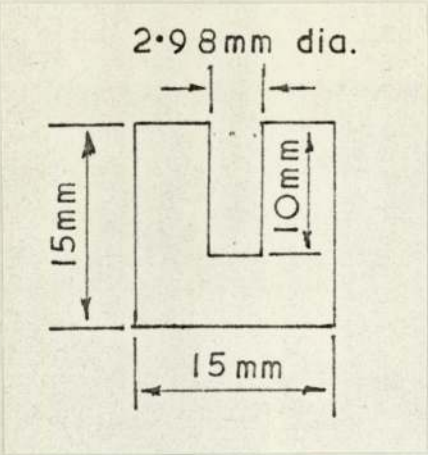

Fig. 18

into the hole in each sample, and the whole heated to 1100°C for one hour under an atmosphere of pure, dry argon. The specimens were then carefully sectioned and studied metallographically and by electron microprobe analysis. The amount of copper or tin diffusion into the iron was measured. A third dendritic phase present within the original Cu/Sn liquid was analysed and proved to be nearly pure iron. Microhardness tests were carried out at the interface to check on the degree of interdiffusion of the three metallic species.

3.4.2. Microprobe analysis.

3.4.2.1. Technique.

Microprobe analysis was employed during the above experiments and also at various other stages of this project to study the extent of reaction between microscopic components within the specimens.

Very briefly, in this technique a finely focussed beam of electrons was aimed onto the surface of the specimen. The energy of the electron beam governed the depth of penetration, and hence the volume of material which generated x-rays. Lower beam energies gave smaller spot sizes,

but less intense x-ray generation.

The samples were set in electrically conducting Bakelite so that charges built up on the surface of the specimen could be dissipated. In addition the samples were ground and polished flat so that the angle of incidence of the electron beam, and hence the angle of the emitted x-rays entering the spectrometers was held constrant.

The generated x-rays were detected by a geiger counter after being diffracted via a suitable crystal set to the appropriate Bragg angle for the K_{α} emissions of the element in question. A variety of crystals was available to cover a large number of elements. The lower limit of this range was set by the transparency of the counter window to the x-rays produced by low atomic number elements.

3.4.2.2. Spot analysis and line scans.

Spot analyses were made of areas upon the sample surface by using a stationary electron beam, and recording the number of counts detected by the geiger counter per unit time (ten seconds). The counts were measured on an electronic decade counter connected to the geiger counter. Due to a lag in counting efficiency at very high frequencies, a 'dead-time' correction was employed. The background noise was then measured for the same unit time and subtracted from the total. This noise was randomly generated within the equipment, and due to the very high sensitivity of the counter amplifiers, could not be eliminated. Finally a check was made to ensure that there were no elements present which could mask the reading of that element under observation.

The same corrections and precautions had to be made to line scans. These scans were made by moving the electron beam at a set

velocity of 40 μm per minute across the required area, and instead of counting the number of geiger tube discharges, the results were obtained on an X-Y recorder linked in the X-direction proportionately to the movement of the electron beam across the sample, and in the Y-direction to the output of the geiger counter. Dead time and background noise corrections were then made to the resulting scans after which they yielded quantitative information.

3.4.3.

The results of these experiments showed that copper and tin diffusion into the iron was limited under the experimental conditions, and not dependent upon the carbon content of the iron. Also at least a small amount of iron dissolution into the liquid Cu/Sn alloy had occurred.

Because these results were not directly applicable to the reactions to be found in powder compacts, a further experiment was designed as follows:

Domtar iron powder was pre-reduced in pure hydrogen for 90 minutes at 800°C, and ground. The powder then had a total oxygen content of 0.35%. 1% carbon was added as graphite, and the mix was pressed into a cylindrical form at a compacting pressure of 463MN/m^2 (30 tsi). This was sintered at 950°C for 30 minutes in argon after which the structure was entirely pearlitic. A hole 0.325 mm in diameter was drilled into the block and filled with pre-alloyed 60% Cu 40% Sn powder. This specimen was sintered for 30 minutes at 900°C in argon, and then sectioned. The resulting microstructure was examined metallographically and by microprobe analysis.

The results of this experiment showed that very little tin had

diffused into the iron at all, as pearlite was present up to the solid/liquid interface (as little as 3% tin is required to stabilise the α - phase). Also no iron was detected metallographically within the original liquid phase, but microprobe analysis showed iron to be present within this phase.

No evidence at all for α- phase stabilisation had been obtained at this stage, and because of this, it was decided to study more closely the dissolution of iron by the liquid. If a dissolution and re-precipitation sintering mechanism could be predominant, then carbon additions would be effective in increasing the strength of the Fe-Cu-Sn compacts.

3.4.4. The effect of Cu/Sn ratio on the dissolution of iron at 1100°C.

To study the dissolution of iron by liquid copper tin alloys, the following procedure was adopted.

A block of vacuum-cast 0.1% carbon steel was drilled with holes 3.2 mm in diameter similar to that shown in Fig. 18, but containing five holes. Copper and tin powders were mixed in compositions ranging from pure copper through various alloys to pure tin, and placed individually in the various holes within the steel sample. This specimen was heated for 30 minutes at 1100°C in an atmosphere of pure, dry argon. The block was then sectioned and studied metallographically and by microprobe analysis. The microstructures observed were correlated to the line scans obtained by microprobe analysis.

The amount of iron which dissolved into the liquid Cu/Sn alloy varied in proportion to the amount of tin present. Up to 15% or iron in the 60/40 Cu/Sn phase had been detected at various stages in this project, therefore thermal analysis was employed to determine the

effect of this amount of iron upon the solidification characteristics of the copper/tin phase present within powder samples. If the effect of the dissolved iron was to raise the solidification temperature of the Cu/tin alloy, then a detrimental effect upon the sintering rate may be expected, due to removal of some of the liquid phase early in the sintering process.

3.5. Thermal analysis

3.5.1. The equipment

A vertical metal tube furnace was employed, connected to gas cylinders to provide the atmosphere. Within this furnace was suspended an alumina crucible containing the alloy under investigation. A thermocouple contained in a thin-walled silica sheath was embedded in the alloy and connected to an electric recorder. A linear cooling rate was achieved by comparing the output of a thermocouple within the hot zone, but not in contact with the cooling alloy, with the output of an electronic slope generator which could generate a linear voltage slope of the order of that produced by the thermocouple. The difference between these voltages was used to control the gate of a triac power control unit feeding the furnace heating elements. In this way linear cooling rates of less than $1^{\circ}C$ per minute were easily obtained.

3.5.2. Experimental procedure.

The samples were prepared by mixing 60% Cu and 40% Sn powders to give the 3:2 Cu/tin ratio. Iron powder was added to this mix at 5%,10% and 15% levels. These mixtures were heated in an atmosphere of 90% N_2 10% H_2 and the heating rate followed by the specimen thermocouple. The reaction between tin and Cu on heating was exothermic, but at about $1100^{\circ}C$ the mixture was molten. After holding at this temperature for about 60 minutes to ensure complete mixing, the cooling

cycle was commenced. An electric switch was employed to turn off the equipment at such a time as the sample was completely solid. The resulting cooling curves showed that up to 15% iron had little effect upon the solidification characteristics of the Cu/Sn alloy.

3.6. Low temperature experiments.

After the diffusion experiments described in section 3.4. were carried out, low temperature experiments were designed to study the way in which the tin and copper react both together and with iron prior to reaching the sintering temperature of 950°C. Esper and Zeller[26] carried out dilatometric work combined with x-ray diffraction to list the reactions occurring during the heating up cycle. The object of this series of experiments was to determine if the tin could react with the iron before being dissolved by the copper.

Samples containing 95% Fe, 3% Cu and 2% Sn were mixed and pressed at 463MN/m^2 (30 tsi), and sintered for 15 minutes in 90% N_2 10% H_2. The sintering temperatures employed were 400,500,600,700,800,900°C. The sintered samples were infiltrated under vacuum with liquid 'Araldite' and allowed to set, because the low-temperature specimens were too friable to be mechanically polished. The specimens were then studied metallographically, and areas of interest were located accurately with microhardness indentations so that subsequent electron microprobe analysis could be directed to a line between these indentations. The magnification and orientation of the specimens was adjusted within the microanalyser by studying the back-scattered electron image. Thus it was possible to obtain a trace for both copper and tin contents which could be coupled accurately to a photomicrograph of the relevant area.

3.7. Additions of pre-alloyed 60% Cu 40% Sn powders.

After the results of mechanical tests upon samples containing 3% Cu + 2% Sn added in elemental form, and a study of the modes of reaction during heating up of these compacts; a series of experiments was carried out to compare the final sintered mechanical properties with those properties of similar composition samples produced using pre-alloyed copper/tin powder. In this way it was possible to reach the sintering temperature without any of the low temperature reactions occurring.

The pre-alloyed 60% Cu 40% Sn powder was produced by melting the required amounts of Cu + Sn powders in an alumina crucible under an atmosphere of pure hydrogen. The powders were pre-mixed and heated together at 950°C for 30 minutes. The material when cool proved to be extremely brittle, as it was composed mainly of the intermetallic compound Cu_3Sn. The solid was ground down to -152 μm (-100#) in an agate mortar, and 5% was added to iron powder. The mixture was pressed and sintered normally.

The mechanical properties of the compacts containing pre-alloyed 60/40 Cu:Sn powder as opposed to elemental powders proved to be very similar, indicating that the reactions which occur during heating of the elemental tin and copper within the iron compact had little effect upon the sintering process.

3.8. Wire spool experiments.

The previous experiments yielded a lot of information on the sintering process, but an attempt to get quantitative information was instigated. This seemed to be the only way to tie up the effect of furnace atmosphere upon the sintering process, apart from observations

of the mechanical properties and oxygen contents of compacts.

The wire spool technique originated by Kuczynski[9,10] on sphere models was chosen. Matsumura[13] obtained encouraging results using wire spool models and a liquid phase composed of Wüstite/fayalite eutectic. This eutectic had a solubility for iron, and so was similar to the system Fe-Cu-Sn in this respect.

The formers for the wire spools were produced from a rod of Armco iron which was drawn down from 15.8mm dia. to 5.0mm dia. Intermediate anneals were carried out when the wire showed any signs of excessive work hardening. The formers consisted of annealed pieces of this rod about 3 cm long. Pure iron wire 0.305 mm in diameter was wound closely on the formers as carefully as possible under a constant load of about 150 g obtained by hanging a weight on the end of the wire during the winding operation. The completed spools were placed in ceramic boats and a mixture of 3:2 or 15:2 mixed Cu/Sn powders sprinkled on top of the windings. The whole was heated to 950°C for five minutes under a selected protective atmosphere and cooled. The resultant sample was then carefully filed to remove any excess Cu/Sn alloy from the windings, which could cause excessive iron dissolution at the outside. The samples were then resintered at 950°C for the required time using either pure H_2 or 90% N_2 10% H_2 as an atmosphere. Sectioning of wire spools heated for 5 minutes at 950°C in either atmosphere showed the liquid to have completely infiltrated the windings. After the required time at temperature, the samples were cooled and sectioned. Spark machining was employed in the case of the 3:2 Cu/tin - infiltrated spools because of the brittleness of this phase, which tended to break up upon any method of mechanical sectioning. After polishing the samples were

studied metallographically for signs of neck growth. Microprobe analysis was performed to determine the extent of iron solution into the original liquid. This procedure was used because of the certainty of a deep region in the centre of the Cu/Sn regions free of any iron particles. This is not so in powder compacts, and due to the penetration of the electron beam, the measurement of iron content within the Cu/Sn alloy in the latter case was not as certain.

3.9. Furnace atmospheres and carbon additions.

To study the effect of the sintering atmosphere upon the sintering mechanisms operating within a powder compact is difficult. The physical parameters which can be studied are the residual porosity after sintering; structure of the final sintered compact, or the mechanical properties after sintering.

A series of experiments was designed to determine the effect of sintering atmosphere upon the residual porosity of various iron-copper-tin compacts, and also to compare the mechanical properties of these compacts after sintering in one of four atmospheres: pure hydrogen, 90% N_2 10% H_2, pure argon, or carbon monoxide.

Samples contained either 0.8% or 1.2% carbon added as graphite. In addition two Cu/Sn ratios were investigated, either 3:2 or 15:2. The total addition of Cu + Sn was 5 wt% in all cases. Mixing and pressing of the compacts was as described using a compaction pressure of 30 tsi to produce samples conforming to B.S. 2590. In each instance sintering was continued for 30 minutes at 950°C with a fairly rapid cool after sintering obtained by pulling the boat containing the samples into the cold zone of the furnace.

3.9.1. Porosity measurement.

The technique employed could be used on either green or sintered compacts, and determined the total amount of porosity, the open porosity, and by difference, the closed porosity present in the compact.

Initially the compact was weighed in air to one thousandth of a gram. The volume of the compact was measured. For the B.S. 2590 die employed, the top surface area of the compact was accurately formed to one square inch. The most accurate measure of volume was then obtained by measuring the thickness of the compact along its length with a micrometer.

The average density of the solid material within the compact was calculated from the known densities and amounts of iron, copper and tin present. The overall porosity was then given by

$$\% \text{ porosity} = \frac{\frac{A}{B}}{Y} \times 100\%$$

where A = weight of the compact in g.

B = volume of the compact in cm^3.

Y = true density of the compact material in g/cm^3.

This value was checked by an Archimedian principle which also gave the relative amount of open porosity. The compact was immersed in oil of accurately determined specific gravity at room temperature, $20^{\circ}C$. The oil-impregnated compact was placed in a vacuum chamber connected to a rotary pump, and the pressure lowered. Bubbles of air frothed out of the sample, and continued to do so for some time. Pumping was stopped as soon as the bubble production finished. Air

was then admitted to the system whereupon the oil completely filled the available pore spaces. The samples were then removed from the oil, and excess oil carefully wiped off. These infiltrated specimens were then accurately weighed in air, and again when immersed in water.

The interconnected porosity is given by the expression:

$$\%_{Int} = \frac{B-A}{(B-C) \times \rho_{oil}}$$

where A = weight of compact in air

B = weight of compact + oil in air

C = weight of compact + oil in water

ρ_{oil} = density of oil at room temperature

The total porosity is given by

$$\% \text{ total} = \frac{(B-C) - \frac{A}{\rho_x}}{(B-C)}$$

where ρ_x = the average density of the solid material of the compact.

3.9.2. Samples for mechanical testing.

Carbon additions of 0.2, 0.6, 0.8 or 1.2% carbon were made to iron compacts containing 5% of Cu + Sn in the ratios of 3:2 or 15:2. The same four atmospheres were employed as with the porosity experiments, namely pure H_2, 90% N_2 10% H, pure argon, or pure carbon monoxide. All samples were sintered for 30 minutes at 950°C.

3.9.2.1. Tensile testing.

Tensile testing was carried out in two ways. The Hounsfield tensometer was employed initially for samples showing lower strengths. For samples with higher strengths, and those containing carbon, a

Denison wire-testing machine was used because the grips in the Hounsfield tensometer could not cope with the higher loads.

3.9.2.2. Elongation measurement.

Elongation measurements were made on the tensile test specimens. The gauge length chosen was one inch, conforming closely to the British use of

$$\text{Gauge length} = 5.65 \sqrt{\text{area}}.$$

Two gauge lengths were marked on the specimen as shown in Fig. 19:

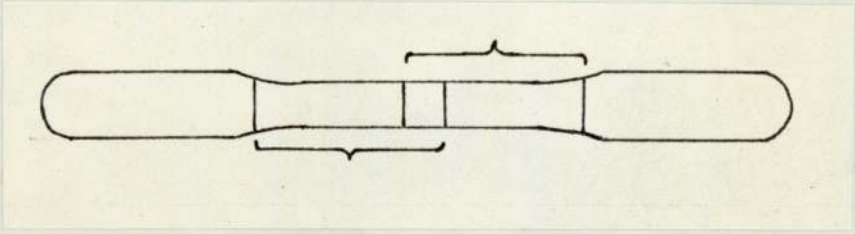

Fig. 19

This overlap meant that a meaningful reading could be obtained wherever the sample fractured during testing.

3.9.2.3. Hardness measurement.

Hardness measurements were made upon the tensile test specimens to determine the effect of the sintering atmosphere upon the carbon content of the specimens. Overall hardness measurement was performed using the Vickers, Brinell, and Rockwell tests. For reproducibility and ease of performance the Rockwell test employing a conical diamond was found to be best, and this test was used throughout for overall hardness measurements.

These tests showed that the atmosphere used was critical to the mechanical properties obtained in carbon-bearing compacts. The original work carried out in conjunction with the TRI showed that the atmosphere used was also critical to the mechanical properties of carbon-free Fe-Cu-Sn compacts.

Because the only variable in the atmosphere in this corroborative work was the partial pressure of hydrogen, it was proposed to carry out experiments to determine the amount of reduction of the various oxides within the powders by either pure hydrogen, or 90% N_2 10% H_2.

3.10. Oxygen content of the metal powders and of various sintered compacts.

3.10.1. Balzers Exhalograph.

This apparatus could measure the oxygen content of metallic powders by fusing them into a nickel bath contained in a carbon crucible held at a temperature of 1800°C, whereupon the dissolved oxygen present reacted with carbon to form CO.

The amount of CO evolved was measured by an infra-red analyser and converted into wt % oxygen content of the powders.

Loose powders were first compacted into samples about 1-2 g in weight in a screw press prior to testing. Sintered samples were cut directly from the specimens. The size of the sample had to be dependent upon the expected oxygen content to keep within the limits of the equipment.

3.10.2. Oxygen content of the powders and compacts.

The iron, copper and tin powders used throughout this investigation were analysed for oxygen content in the 'as-received' states. In addition the iron and tin powders employed at the TRI

were also analysed in the same condition.

Samples were then prepared containing 5% of Cu + Sn in the ratio of 15:2 or 3:2, with a compacting pressure of 463MN/m^2 (30 tsi). These were sintered at 950°C and 1150°C in either H_2 or 90% N_2 10% H_2 for 30 minutes. Samples obtained from the TRI in the sintered condition were also analysed for oxygen content.

3.10.3. Use of an industrial sintering furnace employing cracked ammonia.

In addition to the effect of both H_2 and 90% N_2 10% H_2 atmospheres upon the residual oxygen content and mechanical properties of Fe-Cu-Sn compacts, it was thought that an industrial furnace should be employed for sintering these specimens to determine the effect of an intermediate hydrogen partial pressure in an atmosphere used quite commonly for sintered iron parts.

For this reason powder compacts containing 5% of Cu + Sn at either the 3:2 or 15:2 Cu:Sn ratios were prepared and sent to the BSA Sintered Components Division for sintering in a mesh belt-type furnace employing an atmosphere of cracked ammonia. Both our own powders, and those supplied by TRI were employed, and the results of oxygen analysis and mechanical tests compared.

The furnace was set at a temperature of 1130°C, and being of the continuous type, the total sintering time was approximately 40 minutes.

3.10.4. Additions of tin oxides (SnO or SnO_2).

The above work showed that pure hydrogen would reduce the final level of oxygen within the compacts to a lower value than could be obtained with either 90% N_2 10% H_2 or cracked ammonia. The use of tin oxide additions was made in order to artificially introduce oxygen

to the compact in order to study its effect upon the microstructure and the mechanical properties. Copper oxides were not employed because they are very easily reduced by a small partial pressure of hydrogen even below the sintering temperature.

The compositions of the compacts were made at either the 3:2 or 15:2 Cu:Sn ratios allowing of course for the additional oxygen content of the tin oxide powder. The total alloy addition was 5% in all cases.

Sintering of these compacts was carried out at 950°C for 30 minutes in H_2 or 90% N_2 10% H_2. The microstructures were examined to reveal the extent of unreduced oxide in each case. Mechanical tests as already described were performed upon these samples and compared to the results one would expect from samples originally containing metallic tin as opposed to the oxides.

A carefully weighed amount of either SnO or SnO_2 was reduced in an alumina crucible under exactly the same conditions, and the effectiveness of the reduction measured by weight loss.

The results of these experiments were similar in mechanical property terms to those one would expect using metallic tin in place of the oxides. The structure of the 3:2 samples containing SnO_2 and sintered in N_2/H_2 showed large amounts of unreduced tin oxide. An attempt to find if the final mechanical properties could be related to the final oxygen content of the compact, or to the initial sintering conditions, was carried out.

3.10.5. <u>The influence of a second sintering operation upon samples already sintered for 30 minutes in H_2 at 950°C.</u>

Twelve samples were prepared containing 3% Cu and 2% Sn, the

balance iron. The 3:2 ratio was chosen because it was found that this ratio was more sensitive to sintering atmosphere than was the 15:2 Cu:Sn ratio.

The samples were pressed at 463 MN/m^2 (30 tsi) and sintered in pure H_2 for 30 minutes at 950°C. Sets of three samples were then re-sintered in either H_2, 90% N_2 10% H_2, argon, or carbon monoxide for the same time and temperature. Mechanical tests were carried out to determine how the final properties were dependent upon the original hydrogen sinter, or the secondary sinter in a different atmosphere.

3.11. Heat treatment of Fe-Cu-Sn and Fe-Cu-Sn-C compacts.

After it had been shown that carbon additions can be beneficial to this system contrary to the views of some workers[22,24,25,26,27], a series of experiments was carried out to study the effects of quenching these materials from the sintering temperature, followed by annealing procedures.

In order to quench samples rapidly from the sintering temperature with a minimum of oxidation, a vertical tube furnace was employed. This furnace was capable of running under vacuum or any selected atmosphere. 90% N_2 10% H_2 was chosen for the sintering atmosphere because pure H_2 is explosive and could not be employed if the furnace tube was to be opened to allow quenching of the samples from the sintering temperature. The quench operation was carried out by increasing the flow rate of the gas through the tube, under a slight positive pressure of about 2 lb/in^2. The bottom plate was then unscrewed and the radiation shields quickly removed. The samples were immediately dropped into the quench medium by means of a lever arrangement fitted through the top plate which released the basket containing

the samples. Both oil and water at room temperature were used as quenching media.

3.11.1. Fe-Cu-Sn compacts.

Samples containing 5% of Cu + Sn in the ratios of 3:2 or 15:2 were made up using a compacting pressure of 30 tsi. These were sintered at 950°C for 30 minutes in 90% N_2 10% H_2 and quenched in either water or oil. The hardness, tensile strength and elongation were measured in the as-quenched state, and also after an annealing treatment consisting of 30 minutes at 700 or 800°C.

3.11.2. Fe-Cu-Sn-C compacts.

Samples were prepared identical to those in the preceeding section except for carbon additions of 0.4, 0.8 or 1.2%, added as graphite. These were again sintered at 950°C for 30 minutes but argon was used instead of N_2/H_2 mixture because hydrogen can react with carbon in the presence of small traces of water vapour to produce methane at these temperatures. After quenching mechanical tests showed the compacts to have no strength at all due to a very high degree of brittleness. An annealing procedure of 30 minutes at 500°C was carried out after quenching, and prior to mechanical testing. The effect of various annealing temperatures was determined upon carbon-bearing samples with a Cu:Sn ratio of 15:2. The 3:2 ratio was not considered due to the brittleness of the intermetallic compound formed from the originally liquid Cu/Sn phase.

Section IV. Experimental Results.

4.1. Powder materials.

4.1.1. Sieve analysis of MP 32 iron powder.

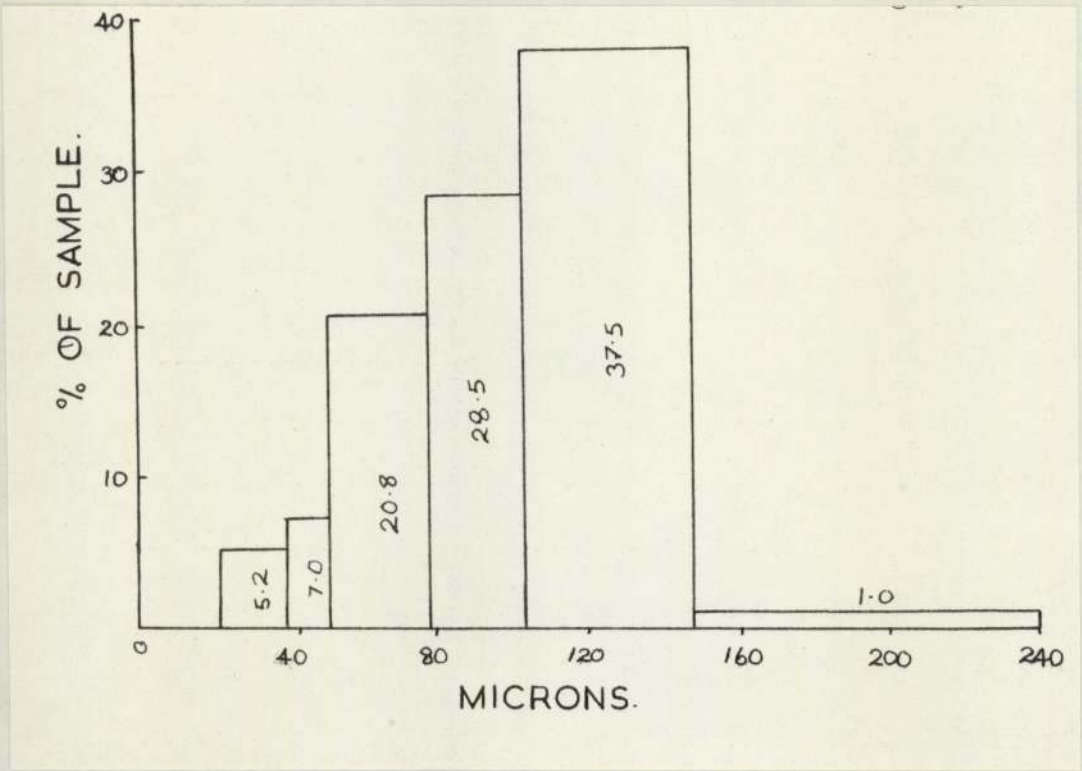

Fig. 20

4.1.2. Sieve analysis of atomised copper powder.

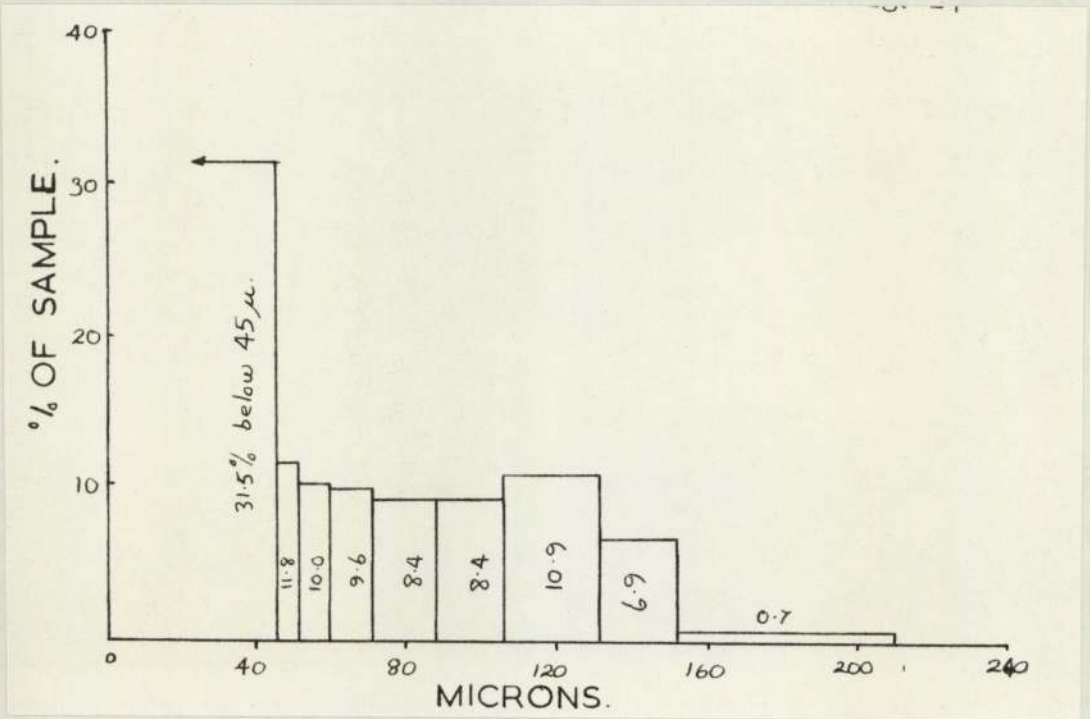

Fig. 21

4.1.3. Sieve analysis of atomised tin powder.

The atomised tin powder was spherical in shape, and all of it passed through a -53 μm (-300#) sieve.

4.2. The initial results of mechanical tests carried out on various Fe-Cu-Sn compacts.

4.2.1. The ultimate tensile strength of iron compacts containing copper or tin sintered for 30 minutes in 90% N_2 10% H_2.

Table 1.

Compaction pressure = 463 MN/m^2 (30tsi)
-152 um copper additions to iron.
Sinter temperature = 1100°C.

% addition	UTS_2 MN/m^2
zero	188, 190, 196 → 191
1.0	234, 218 → 226
1.5	231, 228 → 229
3.0	250, 243 → 247
3.5	232, 247 → 240
5.0	255, 231, 232 → 239
8.0	241, 266, 255 → 254
10.0	275, 252, 258 → 262

Table 2.

Compaction pressure 463 MN/m^2
-152 um copper additions to iron
Sinter temperature 900°C

% addition	UTS_2 MN/m^2
zero	180, 159, 166 → 168
2.0	156, 170 → 163
4.0	179, 177 → 178
8.0	173, 195 → 184
10.0	191, 181 → 186

Table 3.

Compaction pressure = 463 MN/m^2
-53 um copper additions to iron
Sinter temperature 1100°C

% addition	UTS$_2$ MN/m^2	
zero	188 190 196	191
4.0	280 294 277	284
10.0	309 283 280	291

Table 4.

Compaction pressure 463 MN/m^2
-53 um tin additions to iron
Sinter temperature 1100°C.

% addition	UTS$_2$ MN/m^2	
zero	188 197 179	188
2.0	57.6 69.0	63.3
4.0	61.9 8.8	35.5
8.0	9.1 2.5	5.8
10.0	22.4 9.1	15.7

Table 5.

Compaction pressure 463 MN/m^2
-53 um Sn additions to iron
Sinter temperature 900°C.

% addition	UTS$_2$ MN/m^2	
zero	145 145 134	141
2.0	90 32	61
4.0	13.6 21.3	17.5
8.0	7.7 25.6	16.7
10.0	31.3 6.5	18.9

Table 6.

Compaction pressure 386 MN/m^2
-53 um Sn addition to iron
0.5% zinc stearate added.
Sintering temperature 1008°C.
Atmosphere H_2.

% addition	UTS$_2$ MN/m^2	
zero	170 164	167
2.0	269 267	268
6.0	137 102	119

4.2.2. The dimensional change of Fe-Cu and Fe-Sn compacts sintered in 90% N_2 10% H_2.

Table 7.

Compaction pressure 463 MN/m^2
-152 um copper additions to iron
Sinter temperature 1100°C.

% addition	% dimensional change	
zero	-0.1 -0.1	-0.1
1.0	0.35 0.57	0.46
1.5	0.61 0.83	0.72
2.5	1.23 0.70	0.97
3.0	1.27 1.31	1.29
3.5	1.31 1.31	1.31
5.0	2.38 1.25	1.82
8.0	2.58 2.48	2.53
10.0	2.73 3.11	2.92

Table 8.

Compaction pressure 463 MN/m^2
-53 um tin additions to iron
Sinter temperature 1100°C.

% addition	% dimensional change	
zero	-0.1 -0.1	-0.1
2.0	0.1 0.1	0.1
4.0	0.1 0.15	0.125
8.0	0.98 1.00	0.99
10.0	1.10 1.28	1.19

Table 9.

Compaction pressure 463 MN/m^2
-53 um tin additions to iron
Sinter temperature 900°C.

% addition	% dimensional change	
zero	-0.1 -0.1	-0.1
2.0	0.1 0.1	0.1
4.0	0.49 0.67	0.58
8.0	1.00 1.05	1.02
10.0	1.27 1.40	1.34

Table 10.

Compaction pressure 463 MN/m^2
-152 um copper additions to iron
Sinter temperature 900°C.

% addition	% dimensional change	
zero	-0.1 -0.1	-0.1
2.0	-0.09 -0.05	-0.07
4.0	0.09 0.09	0.9
8.0	0.15 0.09	0.12
10.0	0.15 0.08	0.12

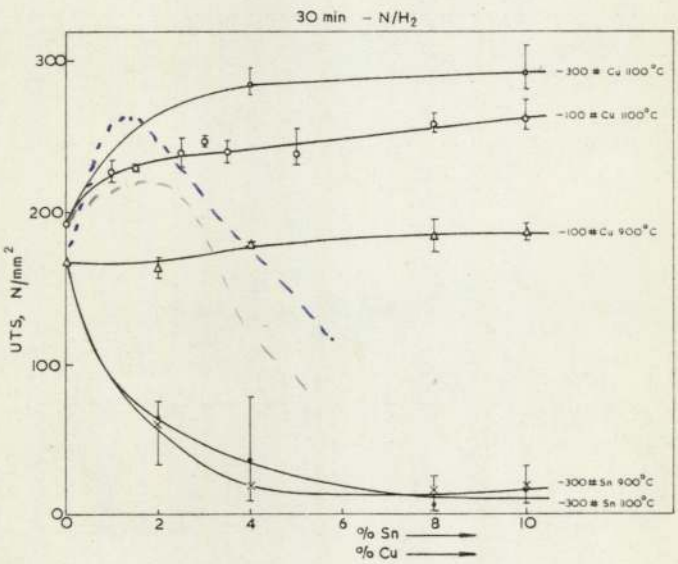

UTS vs. individual copper and tin additions for samples sintered for ½ h.

Fig. 22

4.2.3. The UTS and elongation of compacts containing 2% of Cu + Sn in various ratios.

Table 11.

Compaction pressure 463 MN/m^2.
-152 um Cu and -53 um Sn additions to iron.
Sinter temperature 1100°C.

Cu:Sn ratio	UTS MN/m^2		Elongation %	
Sn only	57.6 64.6 69.0	63.7	0 0 0	
3:2	182 168 114	155	0.5 0.5 0.5	0.5
4:2	142 126 196	155	0.5 0.5 0.5	0.5
5:2	210 219 204	211	1.0 2.0 1.5	1.5
7:2	255 239 233	242	4.0 2.0 2.5	3.0
10:2	238 238 232	236	3.5 2.5 2.5	3.0
15:2	239 252 264	252	4.0 3.0 3.0	3.3
20:2	232 236 260	243	6.0 6.0 4.0	5.3
Cu only	246 261 242	250	6.0 4.0 5.0	5.0

Table 12.

Compaction pressure 463 MN/m^2
-152 um Cu and -53 um Sn additions to iron.
Sinter temperature 900°C.

Cu:Sn ratio	UTS MN/m^2		Elongation %	
Sn only	89.9 32.0 51.4	57.6	0 0 0	
3:2	127 69	98	1.0 1.5	1.25
4:2	114 159	137	1.0 2.0	1.5
5:2	154 96	125	2.0 2.0	2.0
7:2	161 139	150	1.0 1.0	1.0
10:2	174 178	176	1.5 2.5	2.0
15:2	185 186	185	4.0 3.5	3.75
20:2	181 188	184	4.0 6.0	5.0
Cu only	156 170	163	5.0 7.0	6.0

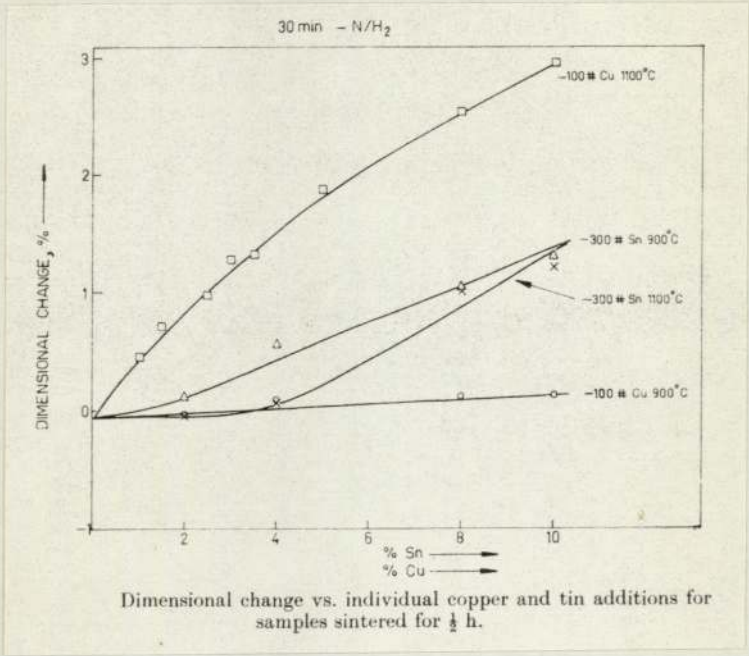

Dimensional change vs. individual copper and tin additions for samples sintered for ½ h.

Fig. 23

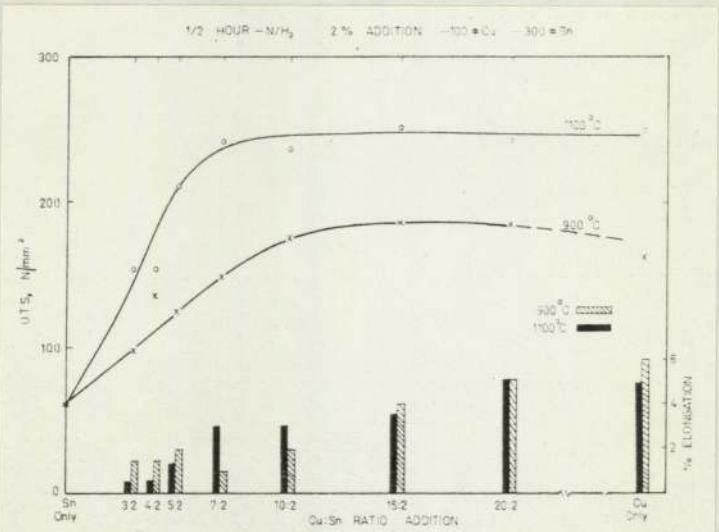

UTS and elongation % vs. Cu:Sn ratio for 2% alloy addition of – 100 mesh Cu and – 300 mesh Sn powder after sintering for ½ h at 900 and 1100°C.

Fig. 24

4.2.4. The UTS and elongation of compacts containing 4% of Cu + Sn in various ratios.

Table 13.

Compaction pressure 463 MN/m^2
-152 um Cu and -53 um Sn additions to iron.
Sinter temperature 1100°C.

Cu:Sn ratio	UTS MN/m^2		Elongation %	
Sn only	77.4 20.7 8.8	35.6	0 0 0	
3:2	127 91 76	98	0.5 1.0 0.0	0.75
4:2	162 193 101	152	1.0 1.0 1.0	1.0
5:2	256 226 233	238	2.0 1.0 0.5	1.0
7:2	218 215 255	230	2.0 1.0 1.5	1.5
10:2	256 279 249	261	5.0 5.0 3.5	4.5
15:2	299 297 284	293	3.0 3.5 4.0	3.5
20:2	275 306 306	296	4.0 4.0 2.0	3.3
Cu only	247 270 257	258	6.0 4.0 5.0	5.0

Table 14.

Compaction pressure 463 MN/m^2
-152 um Cu and -53 um Sn additions to iron.
Sinter temperature 900°C.

Cu:Sn ratio	UTS MN/m^2		Elongation %	
Sn only	13.6 21.3	17.5	0 0	
3:2	113 71	92	1.5 1.5	1.5
4:2	74 108	91	1.5 1.5	1.5
5:2	188 216	202	2.0 1.0	1.5
7:2	171 192	181	1.0 2.0	1.5
10:2	227 195	211	2.0 2.0	2.0
15:2	209 213	211	5.5 4.5	5.0
20:2	241 234	237	5.0 5.0	5.0
Cu only	179 177	178	7.0 5.0	6.0

4.2.5. The UTS and elongation of compacts containing 8% of Cu + Sn in various ratios.

Table 15.

Compaction pressure 463 MN/m^2
-152 um Cu and -53 um Sn
additions to iron.
Sinter temperature 1100°C.

Cu:Sn ratio	UTS MN/m^2		Elongation %	
Sn only	9.1 2.5	5.8	0 0	
3:2	108 164 97	123	0.5 1.0 0.0	0.5
4:2	102 201 167	157	0.5 0.5 0.5	0.5
5:2	203 224 152	193	1.5 0.5 1.0	1.0
7:2	261 247 272	260	2.0 1.5 1.5	1.7
10:2	289 290 281	287	5.0 4.0 6.0	5.0
15:2	302 298 285	295	4.0 3.0 3.5	3.5
20:2	313 273 270	285	5.0 3.0 2.5	3.5
Cu only	241 235 208	228	3.5 4.0 3.0	3.5

Table 16.

Compaction pressure 463 MN/m^2
-152 um Cu and -53 um Sn
additions to iron.
Sinter temperature 900°C.

Cu:Sn ratio	UTS MN/m^2		Elongation %	
Sn only	7.7 25.6	16.6	0 0	
3:2	63.3 27.8	45.5	1.5 1.5	1.5
4:2	154.0 97.3	125.6	2.0 1.0	1.5
5:2	162 197	179.5	1.5 1.5	1.5
7:2	171 193	182	2.5 0.5	1.5
10:2	227 195	211	1.0 2.0	1.5
15:2	241 243	242	4.0 4.0	4.0
20:2	238 246	242	4.5 5.5	5.0
Cu only	179 177	178	6.0 5.0	5.5

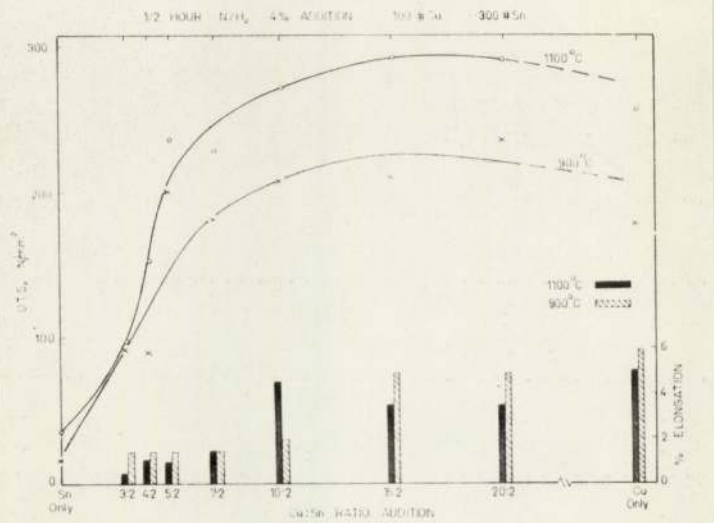

UTS and elongation % vs. Cu:Sn ratio for 4% alloy addition of −100 mesh Cu and −300 mesh Sn powder after sintering for ½ h at 900 and 1100°C.

Fig. 25

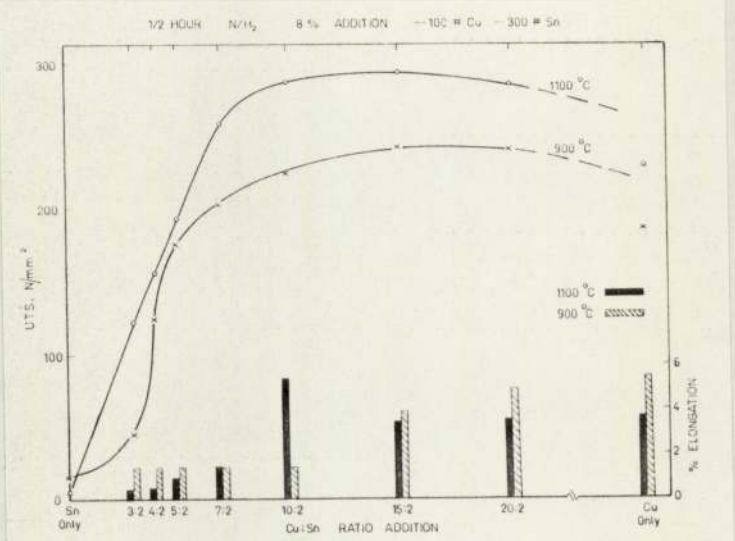

UTS and elongation % vs. Cu:Sn ratio for 8% alloy addition of −100 mesh Cu and −300 mesh Sn powder after sintering for ½ h at 900 and 1100°C.

Fig. 26

4.2.6. The UTS and elongation of compacts containing 10% of Cu + Sn in various ratios.

Table 17.

Compaction pressure, 463 MN/m^2
-152 μm Cu and -53 μm Sn
additions to iron.
Sinter temperature 1100°C.

Cu:Sn ratio	UTS MN/m^2	Elongation %
Sn only	22.2, 9.1 } 15.7	0.0, 0.0
3:2	117, 137, 158 } 137	0.5, 0.5, 0.0 } 0.35
4:2	156, 196, 94 } 149	2.0, 1.0, 1.5 } 1.5
5:2	208, 137, 144 } 163	0.5, 0.5, 0.5 } 0.5
7:2	253, 264, 270 } 262	2.5, 3.0, 3.0 } 2.8
10:2	276, 279, 275 } 277	5.0, 4.0, 6.0 } 5.0
15:2	312, 290, 286 } 296	2.5, 3.0, 5.0 } 3.5
20:2	289, 269, 305 } 288	3.0, 3.0, 5.0 } 3.6
Cu only	235, 253, 216 } 235	4.0, 4.0, 4.0 } 4.0

Table 18.

Compaction pressure, 463 MN/m^2
-152 μm Cu and -53 μm tin
additions to iron.
Sinter temperature 900°C.

Cu:Sn ratio	UTS MN/m^2	Elongation %
Sn only	31.3, 6.5 } 18.9	0.0, 0.0
3:2	92, 123 } 108	1.5, 1.5 } 1.5
4:2	126, 158 } 142	2.0, 1.0 } 1.5
5:2	137, 162 } 150	1.5, 1.5 } 1.5
7:2	217, 219 } 218	2.0, 1.0 } 1.5
10:2	219, 287 } 253	5.0, 4.0 } 4.5
15:2	267, 282 } 275	7.0, 5.0 } 6.0
20:2	253, 232 } 243	5.0, 5.0 } 5.0
Cu only	191, 181 } 186	6.0, 6.0 } 6.0

4.2.7. The UTS and elongation of compacts containing 4% and 10% of -53 um Cu + -53 um Sn in various ratios.

Table 19.

Compaction pressure, 463 MN/m^2,
Sinter temperature 1100°C,
4% addition.

Cu:Sn ratio	UTS MN/m^2		Elongation %	
Sn only	77.2 20.7 8.8	35.6	0 0 0	
1:2	98.2 66.1 59.9	74.7	2.0 0.5 0.0	0.8
2:2	64 156 154	125	1.0 1.0 1.0	1.0
3:2	230 127 209	189	0.0 0.0 1.0	0.3
5:2	230 213 236	226	3.0 2.0 4.0	3.0
10:2	273 264 281	273	3.0 2.0 2.0	2.3
16:2	260 256 306	274	2.0 3.0 1.0	2.0
20:2	290 294 262	282	1.0 2.0 1.0	1.3
Cu only	280 294 277	284	1.0 1.0 1.0	1.0

Table 20.

Compaction pressure 463 MN/m^2,
Sinter temperature 1100°C,
10% addition.

Cu:Sn ratio	UTS MN/m^2		Elongation %	
Sn only	22.2 9.1 15.4	15.6	0 0 0	
1:2	26.3 36.3 42.7	35.1	0.0 2.0 1.0	1.0
2:2	112 109 105	109	2.0 2.0 1.0	1.7
3:2	136 133 114	128	1.0 0.0 1.0	0.7
5:2	275 243 233	250	1.0 0.0 0.5	0.5
10:2	280 296 282	286	4.0 3.0 3.0	3.3
16:2	310 307 290	302	3.0 2.0 4.0	3.0
20:2	264 286 275	275	2.0 4.0 3.0	3.0
Cu only	309 283 279	290	1.0 1.0 2.0	1.3

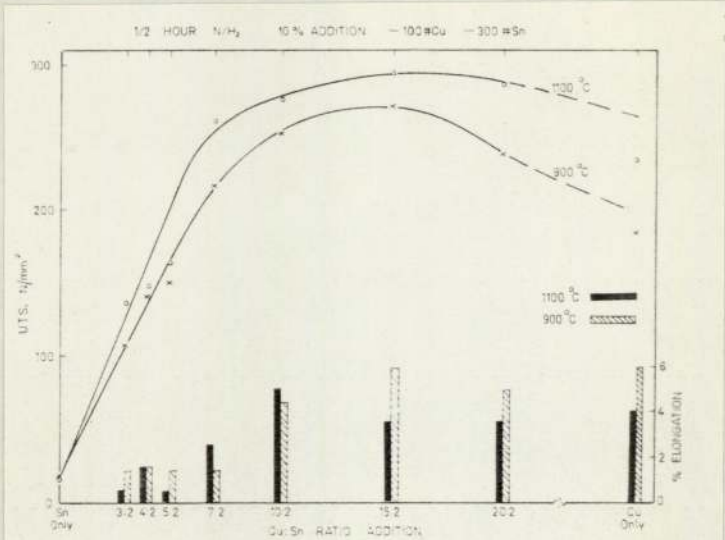

UTS and elongation % vs. Cu:Sn ratio for 10% alloy addition of — 100 mesh Cu and — 300 mesh Sn powder after sintering for ½ h at 900 and 1100°C.

Fig. 27

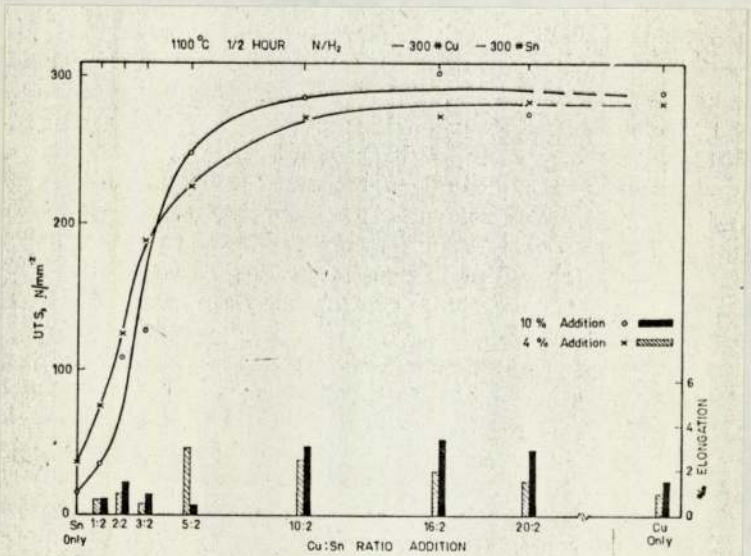

UTS and elongation % vs. Cu:Sn ratio for 4% and 10% alloy additions of —300 mesh Cu and —300 mesh Sn powder after sintering for ½ h at 1100°C.

Fig. 28

4.2.8. The dimensional change (percent) of various samples sintered for 30 minutes at 900°C in 90% N_2 10% H_2.

Table 21.

Cu:Sn ratio	Addition			
	2%	4%	8%	10%
Pure Sn	0.15 0.09 } 0.1 0.12 0.05	0.70 0.52 } 0.56 0.58 0.42	1.26 0.98 } 1.02 0.87 0.97	1.58 1.43 } 1.34 0.99 1.36
3:2	0.15 0.17 } 0.22 0.41 0.15	0.35 0.35 } 0.34 0.29 0.35	0.70 0.46 } 0.54 0.46 0.55	0.46 0.52 } 0.41 0.37 0.29
4:2	0.12 0.17 } 0.15 0.12 0.20	0.20 0.38 } 0.34 0.41 0.38	0.55 0.46 } 0.46 0.37 0.55	0.46 0.52 } 0.45 0.37 0.43
5:2	0.26 0.20 } 0.20 0.20 0.15	0.55 0.20 } 0.54 0.67 0.73	0.75 0.49 } 0.56 0.52 0.49	0.52 0.49 } 0.46 0.37 0.46
7:2	0.23 0.15 } 0.19 0.18 0.21	0.49 0.37 } 0.46 0.55 0.43	0.52 0.67 } 0.59 0.52 0.64	0.73 0.58 } 0.73 0.75 0.90
10:2	0.35 0.35 } 0.28 0.23 0.20	0.49 0.49 } 0.41 0.49 0.17	0.78 0.52 } 0.70 0.73 0.75	0.73 0.73 } 0.80 0.90 0.75
15:2	0.46 0.15 } 0.26 0.12 0.29	0.43 0.32 } 0.38 0.46 0.29	0.43 0.61 } 0.62 0.75 0.70	0.73 0.67 } 0.65 0.73 0.49
20:2	0.29 0.12 } 0.21 0.29 0.15	0.20 0.15 } 0.24 0.20 0.41	0.46 0.49 } 0.49 0.43 0.58	0.67 0.67 } 0.69 0.70 0.73

4.2.9. The dimensional change of various samples sintered for 30 minutes at 1100°C in 90% N_2 10% H_2.

Table 22.

Cu:Sn ratio	Addition			
	2%	4%	8%	10%
Sn only	0.10 0.15 0.10 0.05 } 0.10	0.10 0.07 0.20 0.23 } 0.15	0.97 1.23 0.81 1.00 } 1.00	1.34 1.20 0.97 1.23 } 1.19
3:2	1.05 0.98 0.81 0.84 } 0.92	0.90 0.73 0.73 0.84 } 0.80	0.81 1.05 1.02 1.05 } 0.98	1.05 0.96 0.81 1.05 } 0.97
4:2	0.67 0.75 0.61 0.49 } 0.63	0.75 0.96 0.87 0.94 } 0.88	1.07 0.84 0.78 0.87 } 0.89	0.78 0.87 1.02 0.90 } 0.89
5:2	0.44 0.38 0.40 0.44 } 0.41	0.80 0.73 0.73 0.79 } 0.76	0.75 0.67 0.70 0.71 } 0.71	0.63 0.70 0.75 0.73 } 0.70
7:2	0.53 0.49 0.40 0.70 } 0.52	0.75 0.49 0.70 0.73 } 0.67	0.75 0.97 0.87 0.81 } 0.85	0.73 0.70 0.63 0.73 } 0.70
10:2	0.55 0.38 0.40 0.40 } 0.43	0.78 0.78 0.78 0.78 } 0.78	0.90 1.05 0.78 1.02 } 0.94	1.02 1.16 0.96 1.02 } 1.04
15:2	0.62 0.48 0.45 0.55 } 0.53	1.00 1.25 0.93 0.93 } 1.03	1.21 1.24 1.31 1.27 } 1.26	1.00 1.69 1.58 1.46 } 1.43
20:2	0.59 0.52 0.41 0.65 } 0.54	0.96 1.14 1.00 0.82 } 0.99	2.31 1.89 1.52 1.80 } 1.88	2.34 1.83 2.24 1.79 } 2.05

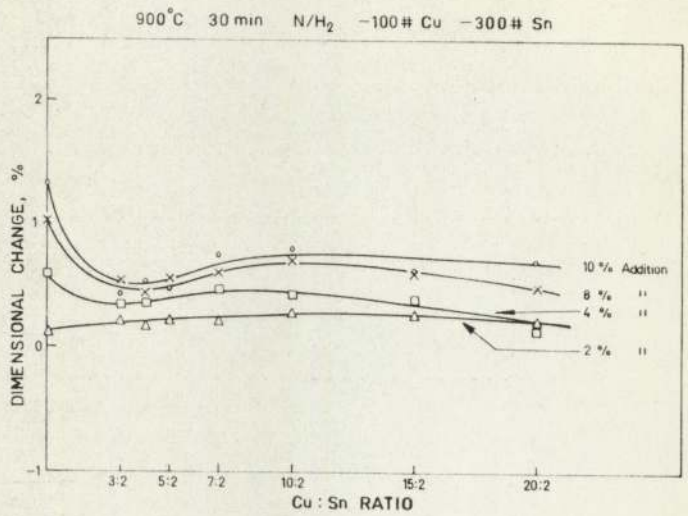

Dimensional change vs. Cu:Sn ratio for 2, 4, 8, and 10% alloy additions of −100 mesh Cu and −300 mesh Sn powder after sintering for ½ h at 900°C.

Fig. 29

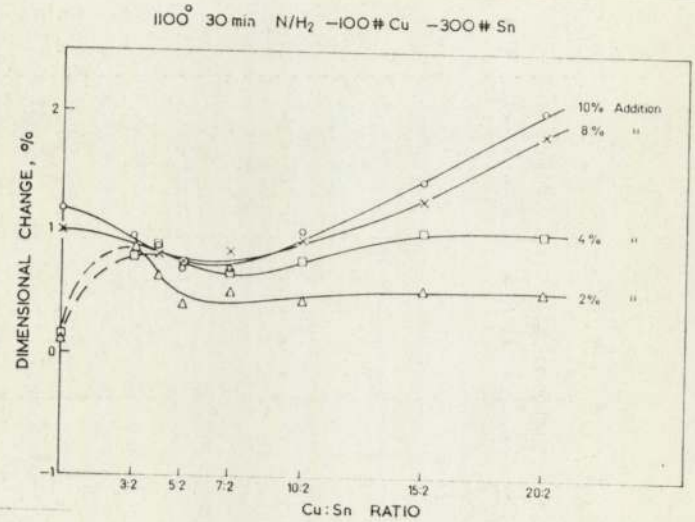

Dimensional change vs. Cu:Sn ratio for 2, 4, 8, and 10% alloy additions of −100 mesh Cu and −300 mesh Sn powders after sintering for ½ h at 1100°C.

Fig. 30

4.2.10. The dimensional change of various samples sintered at 1100°C using -53 µm Cu and -53 µm Sn.

Table 23.

Cu:Sn ratio	Addition		Cu:Sn ratio	Addition	
	4%	10%		4%	10%
Sn only	0.10, 0.07, 0.20, 0.23 } 0.15	1.34, 1.20, 0.97, 1.23 } 1.19	10:2	0.73, 0.67, 0.76, 0.60 } 0.69	1.02, 0.73, 0.81, 1.02 } 0.89
2:2	0.67, 0.55, 0.84, 0.88 } 0.73	0.73, 0.87, 0.87, 1.02 } 0.87	15:2	0.43, 0.73, 0.96, 0.70 } 0.70	1.02, 1.42, 1.36, 1.12 } 1.23
3:2	0.90, 0.84, 0.64, 0.67 } 0.76	0.64, 0.70, 0.78, 0.90 } 0.76	20:2	0.87, 0.95, 1.02, 0.93 } 0.94	1.65, 1.36, 2.03, 1.60 } 1.66
5:2	0.60, 0.51, 0.43, 0.52 } 0.52	0.70, 0.73, 0.70, 0.63 } 0.69			

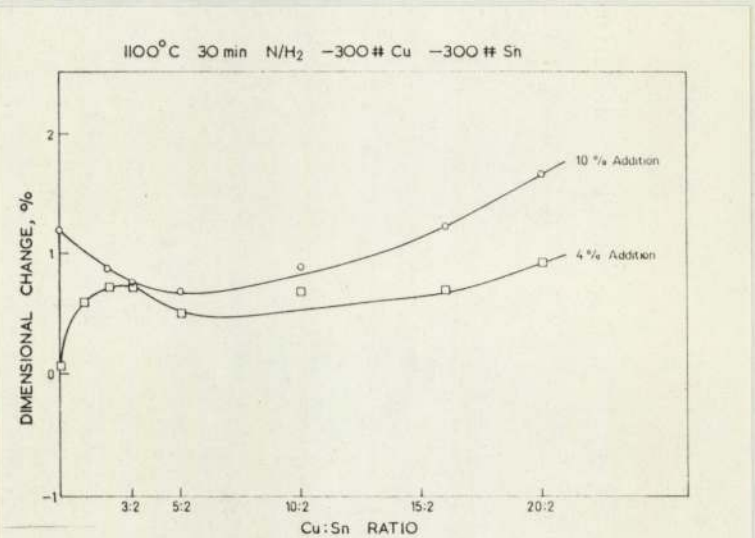

Dimensional change vs. Cu:Sn ratio for 4 and 10% alloy additions of −300 mesh Cu and −300 mesh Sn powders after sintering for ½ h at 1100°C.

Fig. 31

4.2.11. The UTS of compacts containing 4% and 10% alloy additions of 15:2 Cu + Sn powder after sintering for 30 minutes.

Table 24.

4% Addition		10% Addition	
Sinter temperature °C	UTS MN/m^2	Sinter temperature °C	UTS MN/m^2
800	137) 138)136 132)	800	125) 134)133 139)
900	217) 203)203 193)	900	234) 219)236 254)
1000	262) 264)261 257)	1000	263) 261)263 266)
1100	287) 294)292 295)	1100	289) 289)284 273)
1150	303) 315)314 324)	1150	317) 318)310 295)

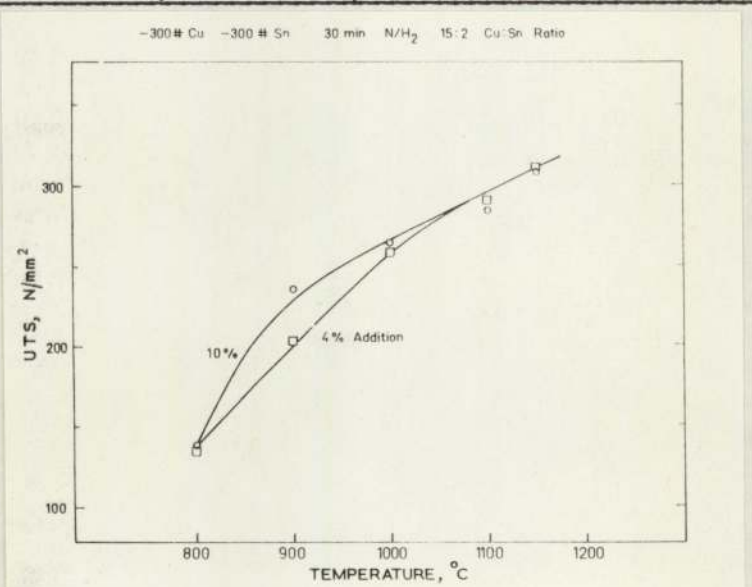

UTS vs. temperature for 4 and 10% alloy additions of 15:2 Cu:Sn (−300 mesh Cu, −300 mesh Sn) powder after sintering for ½ h.

Fig. 32

4.2.12. The dimensional change of compacts containing 15:2 Cu + Sn after sintering at various temperatures.

Table 25.

Values are the average of six results:

4% Addition			10% Addition	
Sinter temperature, °C	Dimensional change		Sinter temperature, °C	Dimensional change
800	0.14		800	0.30
900	0.37		900	0.80
1000	0.60		1000	0.80
1100	0.76		1100	1.57
1150	0.69		1150	1.19

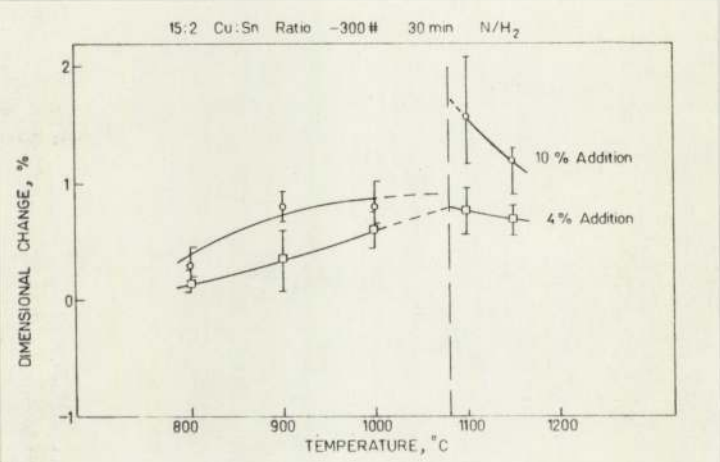

Dimensional change vs. temperature for 4 and 10% alloy additions of 15:2 Cu:Sn (−300 mesh Cu, −300 mesh Sn) powders after sintering for ½ h.

Fig. 33

Table 26.

Experimental sequence, and furnace atmosphere →	TRI POWDER TRI MIXPRE TRI SINT H_2	U/A POWDER U/A MIXPRE U/A SINT H_2	TRI POWDER TRI MIXPRE U/A SINT N_2 H_2	TRI POWDER U/A MIXPRE U/A SINT N_2 H_2	U/A POWDER U/A MIXPRE U/A SINT N_2 H_2	U/A POWDER U/A MIXPRE TRI SINT H_2	
3:2 950°C 30 min	19.3) 24.5)23.0 23.2)	24.9) 22.4)23.0 21.7)	10.3) 10.3)10.75 11.6)	10.5) 11.8)10.1 8.0)	7.5) 5.2) 6.6 7.4)	20.0) 24.0)23.0 25.0)	3:2 950°C 30 min
3:2 1150°C 30 min	16.6) 23.0)20.3 21.3)	26.2) 24.2)24.6 23.3)	11.8) 17.0)15.0 16.2)	16.1) 16.3)16.1 15.9)	15.2) 17.0)16.4 17.0)	21.0) 24.0)24.3 28.0)	3:2 1150°C 30 min
15:2 950°C 30 min	14.0) 17.0)15.9 16.6)	21.6) 20.5)21.0 20.9)	13.9) 17.5)16.0 16.6)	16.7) 18.4)17.9 18.6)	20.0) 22.0)20.6 20.0)	23.0) 25.0)23.3 22.0)	15:2 950°C 30 min
15:2 1150°C 30 min	23.6) 17.3)20.1 19.5)	28.3) 30.1)29.1 29.1)	19.6) 23.7)21.6 21.6)	27.2) 25.0)26.1 26.2)	27.5) 27.0)27.3 27.5)	24.0) 26.0)26.0 28.0)	15:2 1150°C 30 min

↑ copper/tin ratio, sinter temperature, and time

Abbreviations:
TRI = Tin Research Institute
U/A = University of Aston
MIXPRE = Mixing and pressing
SINT = Sintering

Table 26 cont.

Experimental sequence, and furnace atmosphere → / copper/tin ratio, sinter temperature, and time ↑	U/A POWDER TRI MIXPRE TRI SINT H_2	U/A POWDER TRI MIXPRE U/A SINT H_2	U/A POWDER TRI MIXPRE U/A SINT N_2 H_2	TRI POWDER U/A MIXPRE TRI SINT H_2	TRI POWDER U/A MIXPRE TRI SINT N_2 H_2	
3:2 950°C 30 min	10.0 17.0 10.7 8.8	20.6 12.2 17.8 20.7	10.8 7.9 8.2 5.9	21.3 20.3 20.1 20.9	13.6 15.1 15.3 17.4	3:2 950°C 30 min
3:2 1150°C 30 min	11.1 13.2 12.2 12.2	21.6 16.1 19.2 20.0	15.6 19.4 18.0 19.0	20.0 26.5 24.0 25.6	22.0 21.8 21.5 20.8	3:2 1150°C 30 min
15:2 950°C 30 min	15.7 15.7 15.2 14.2	23.5 19.5 17.8 10.3	12.3 17.0 14.6 14.4	15.2 16.0 16.0 17.0	15.2 15.8 13.9 10.7	15:2 950°C 30 min
15:2 1150°C 30 min	17.9 18.5 18.2 18.2	23.6 22.4 24.2 26.4	21.9 25.1 23.0 21.8	21.8 23.2 22.4 22.4	22.2 23.3 21.5 19.2	15:2 1150°C 30 min

4.3. Regression Analysis

4.3.1. Experimental results in conjunction with TRI.

Table 26 shows the results obtained of collaborative work both at this University and at the Tin Research Institute. Both establishments worked together closely by carrying out the sequence of operations shown at the top of the table. Compaction pressure was 463 MN/m^2 (30 tsi) in all cases with no lubricant added to the powders. The values shown are for the ultimate tensile strength in kg/mm^2. Each value is the average of three tests.

The final regression equation obtained from table 26 was:

$$UTS = 23.14 + 9(\text{mix/press}) - 29(\text{gas atmosphere}) - 9.5(\text{Cu/Sn ratio}) - 3.2(\text{mixing x sinter}) + 4.6\ (\text{sinter x ratio}) + 3.8(\text{gas x ratio}) + 0.175(\text{Temp}^{\circ}\text{C}).$$

This result was obtained both at the 95% and the 5% significance levels.

4.4. Lubricant additions to the powder mixes

4.4.1. Mechanical properties of compacts sintered in 90% N_2 10% H_2

Table 27.

Compaction pressure 386 MN/m^2

Comp.	zinc stearate addition %	green density g/cm^3	UTS MN/m^2	% El.	sintering treatment
95% Fe 3% Cu 2% Sn	0.0 0.0 0.0	6.65) 6.62)6.61 6.55)	84.9) 57.1) 67.9 61.8)	0.0 0.0 0.0	30 min at 950°C
95% Fe 3% Cu 2% Sn	0.0 0.0 0.0	6.58) 6.62)6.58 6.53)	119) 83)103 107)	0.0 0.0 0.0	15 min at 300°C - 500°C +30 min at 950°C
95% Fe 3% Cu 2% Sn	0.5 0.5 0.5	6.70) 7.00)6.81 6.75)	145) 181)162 159)	1.0 1.5 1.0	15 min at 300°C - 500°C +30 min at 950°C

4.4.2. Mechanical properties of compacts sintered in pure H_2.

Zinc stearate addition, 0.5%
Compaction pressure, 463 MN/m^2
5% addition of elemental or pre-alloyed Cu and Sn powders to iron.

Table 28.

Cu:Sn ratio	sinter temperature, °C	UTS MN/m^2	elongation %
3:2 elemental	1100	201	3.0
	"	275 } 249	3.0 } 3.0
	"	272	3.0
3:2 elemental	950	273	2.0
	"	272 } 268	2.0 } 2.0
	"	260	2.0
6:2 elemental	1100	264	6.0
	"	279 } 273	6.0 } 6.3
	"	275	7.0
6:2 elemental	950	247	6.0
	"	247 } 267	6.0 } 6.0
	"	306	6.0
8:2 elemental	1100	253	7.0
	"	256 } 252	9.0 } 8.0
	"	247	8.0
8:2 elemental	950	261	7.0
	"	261 } 256	7.0 } 7.0
	"	246	7.0
3:2 pre-alloyed	1100	290	2.0
	"	283 } 285	2.0 } 2.0
	"	283	2.0
3:2 pre-alloyed	950	281	2.0
	"	303 } 297	2.5 } 2.2
	"	306	2.0

4.5. Diffusion Experiments

4.5.1. The reaction between 60% Cu 40% Sn alloy and 0.8% C steel at 1100°C for 60 minutes.

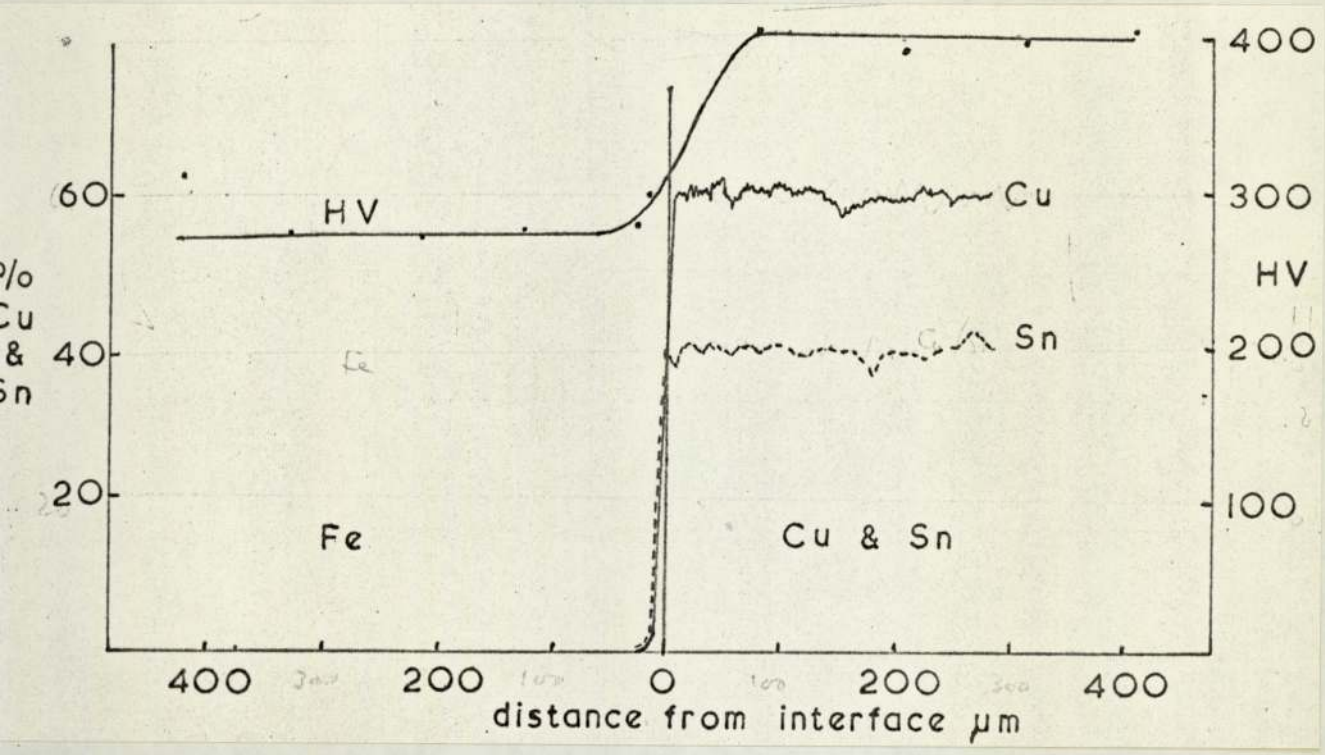

Fig. 34

4.5.2. The reaction between 60% Cu 40% Sn alloy with a fully pearlitic iron powder matrix.

Fig. 35

4.5.3. Electron microprobe analysis of the reactions between various Cu:Sn ratio alloys and iron at 1100°C.

Cu only

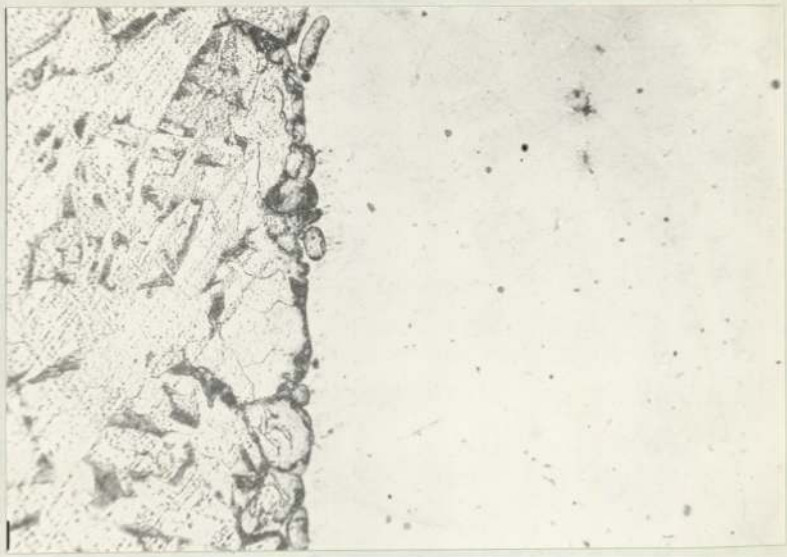

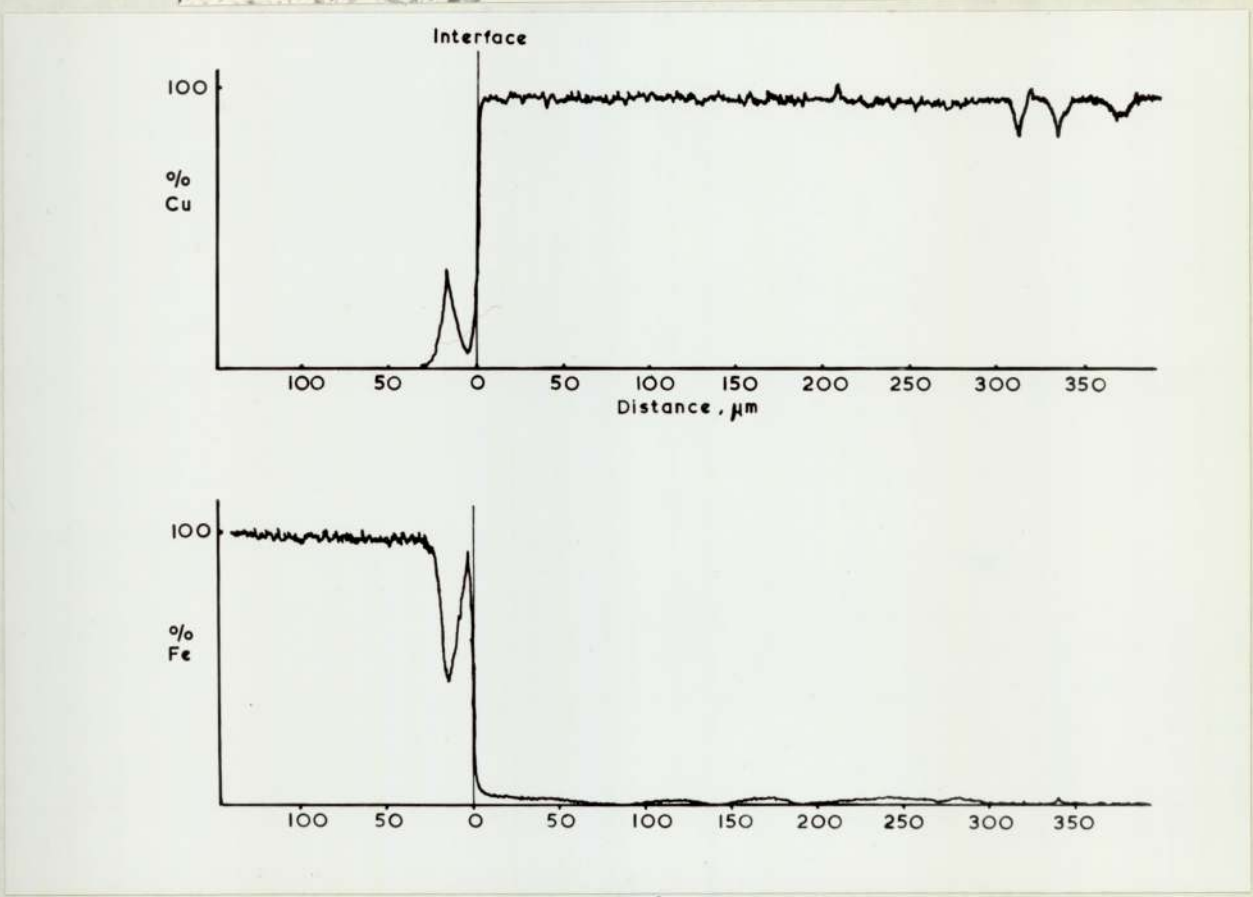

Fig. 36

60% Cu 40% Sn

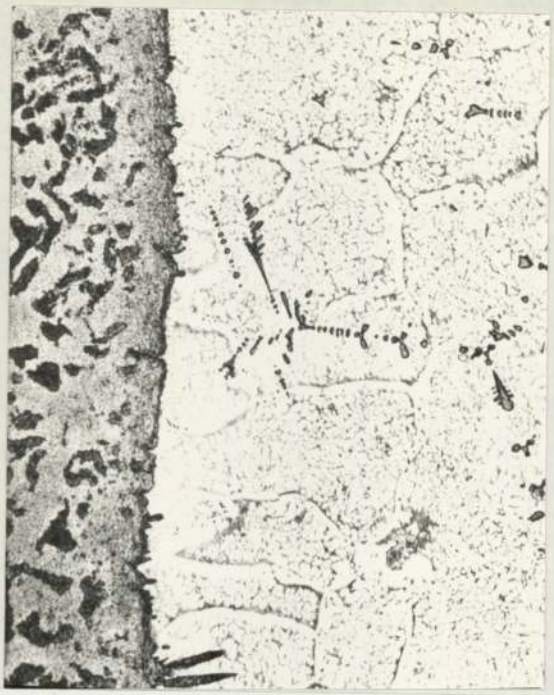

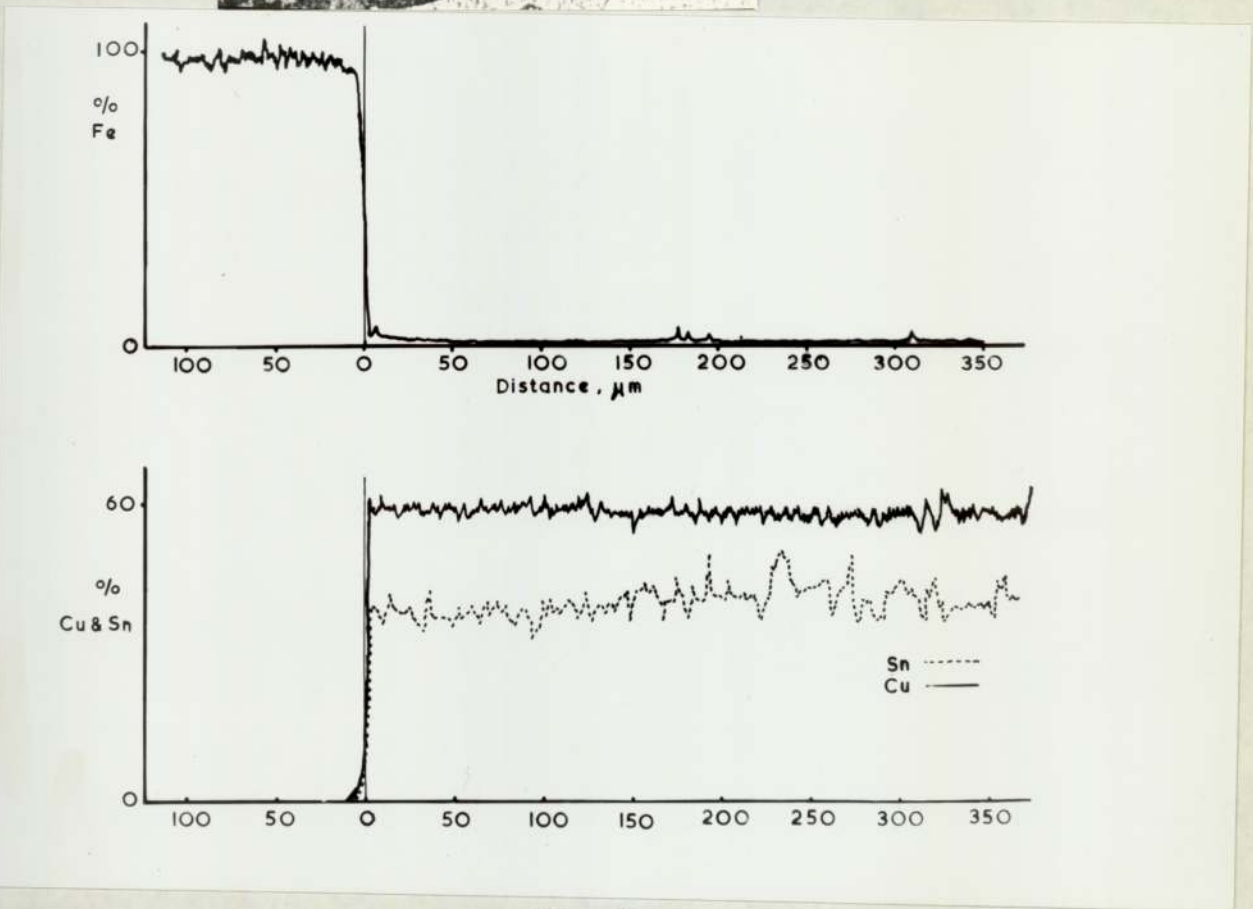

Fig. 37

60% Sn 40% Cu

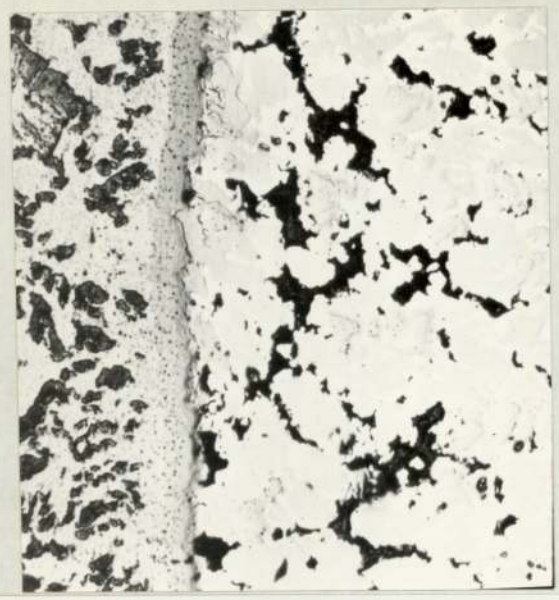

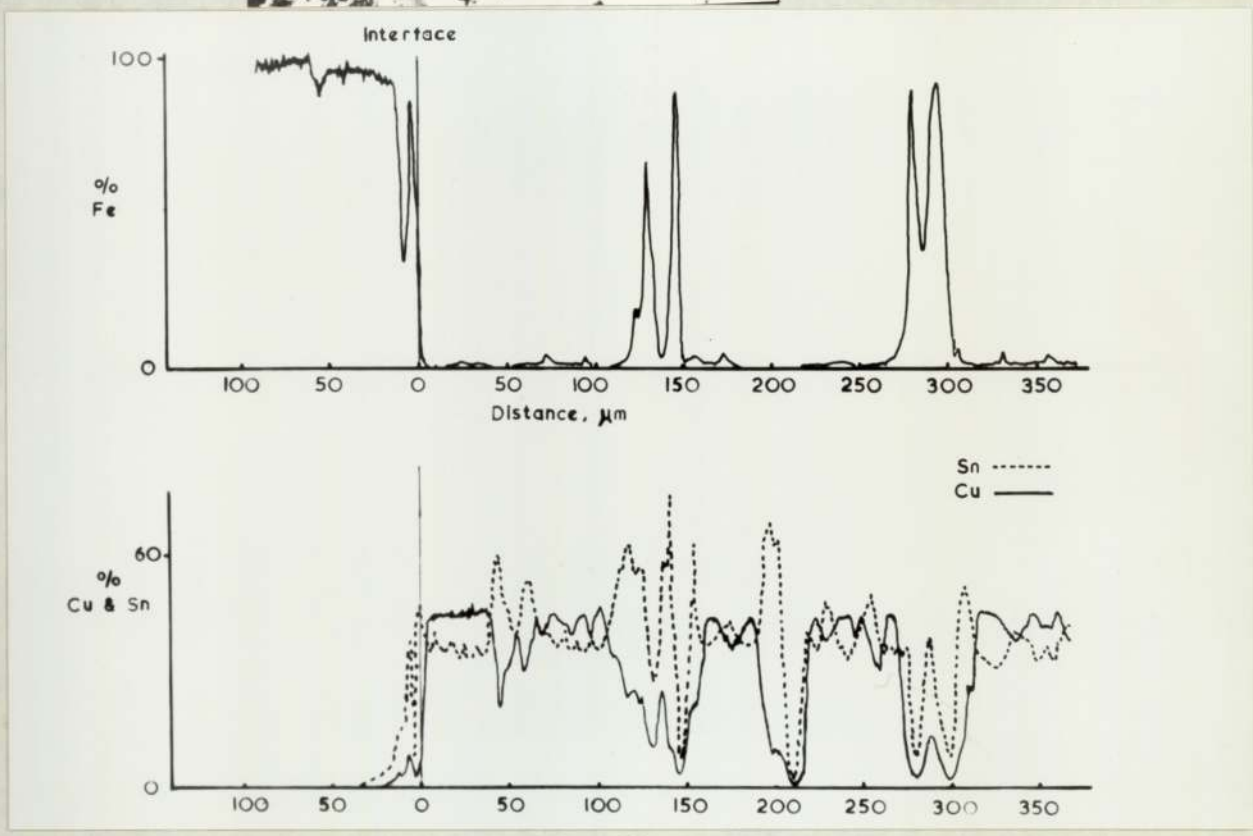

Fig. 38

Sn only

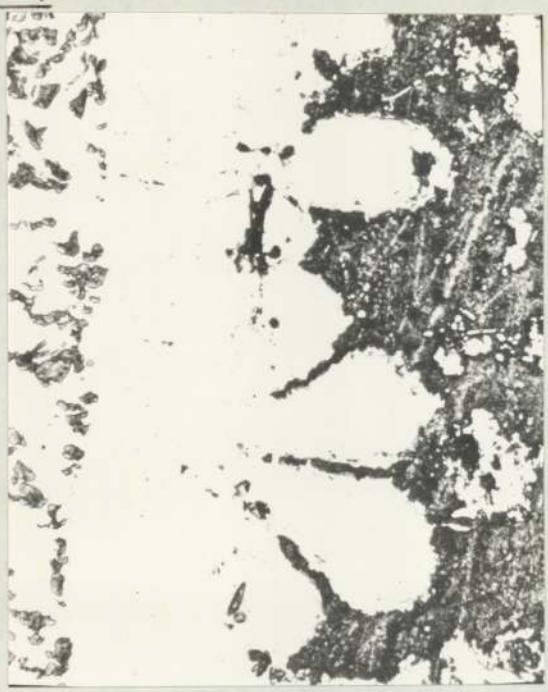

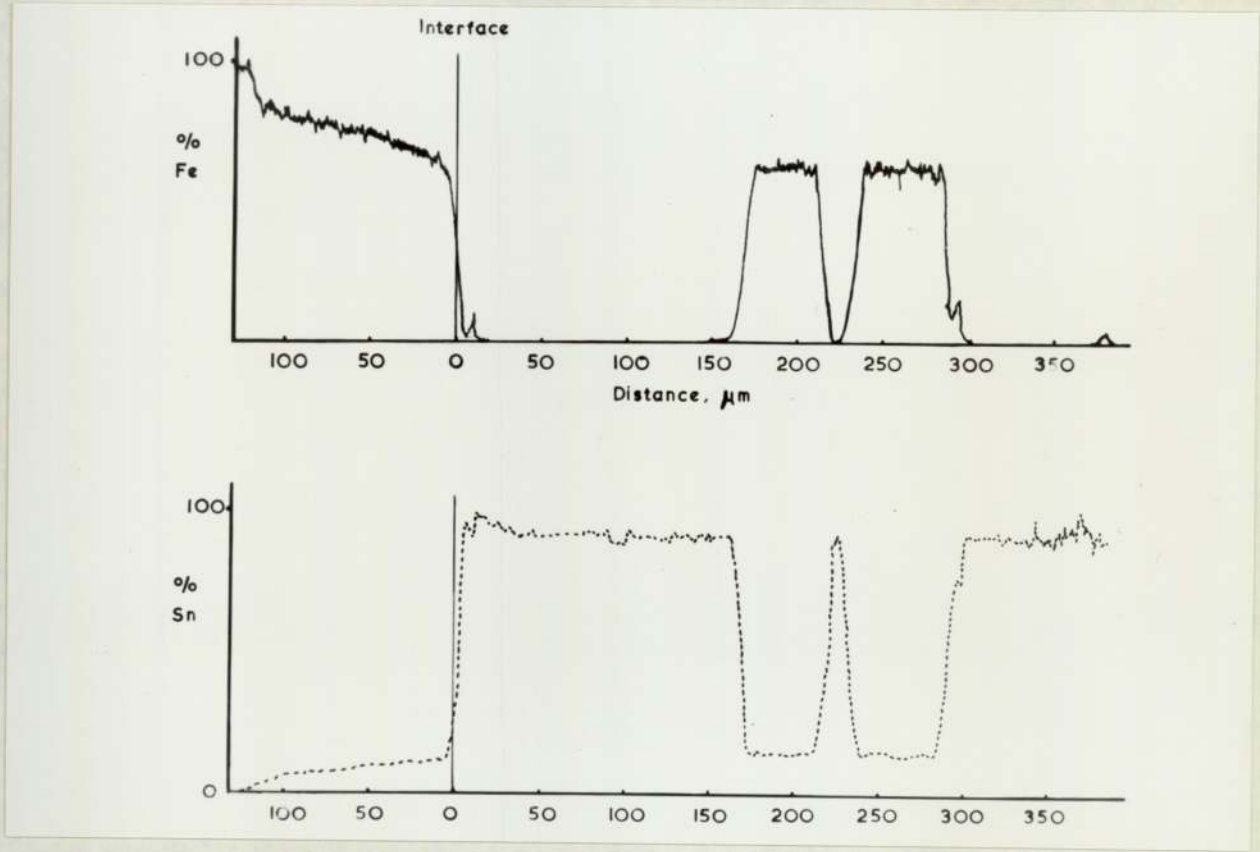

Fig. 39

Electron
Image

50μ

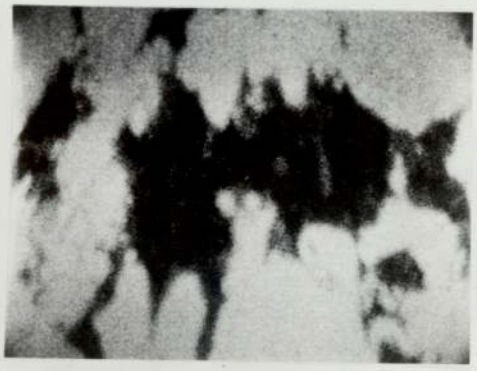

Fe X ray
Image

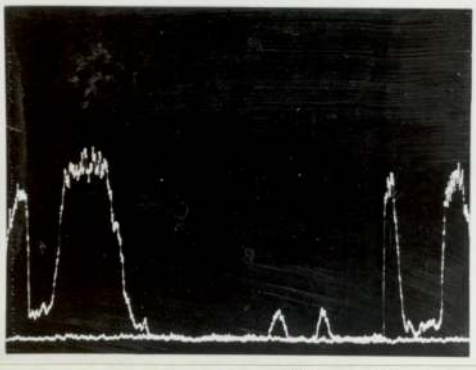

Fe X ray
Scan

Fig. 40

4.6. Thermal analysis

The following figures show the cooling curves for 100 g samples of 60% Cu 40% Sn alloy containing up to 15% iron.

4.6.1. The cooling curve and microstructure of 60% Cu 40% Sn alloy

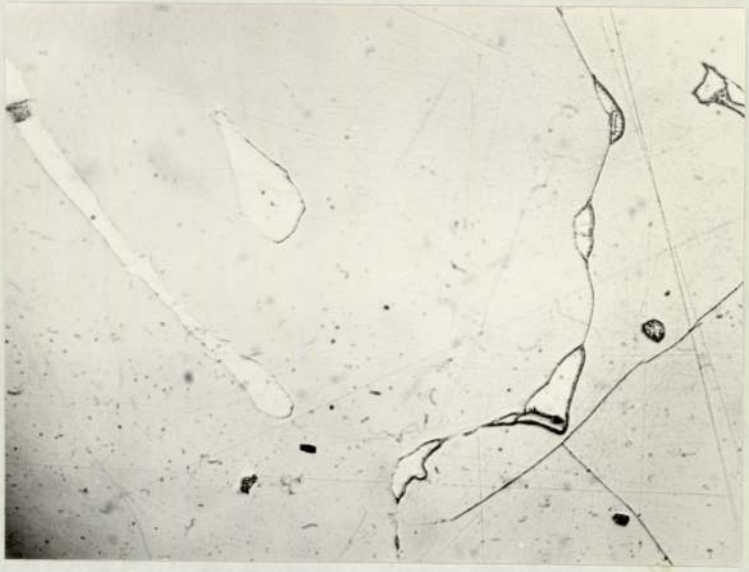

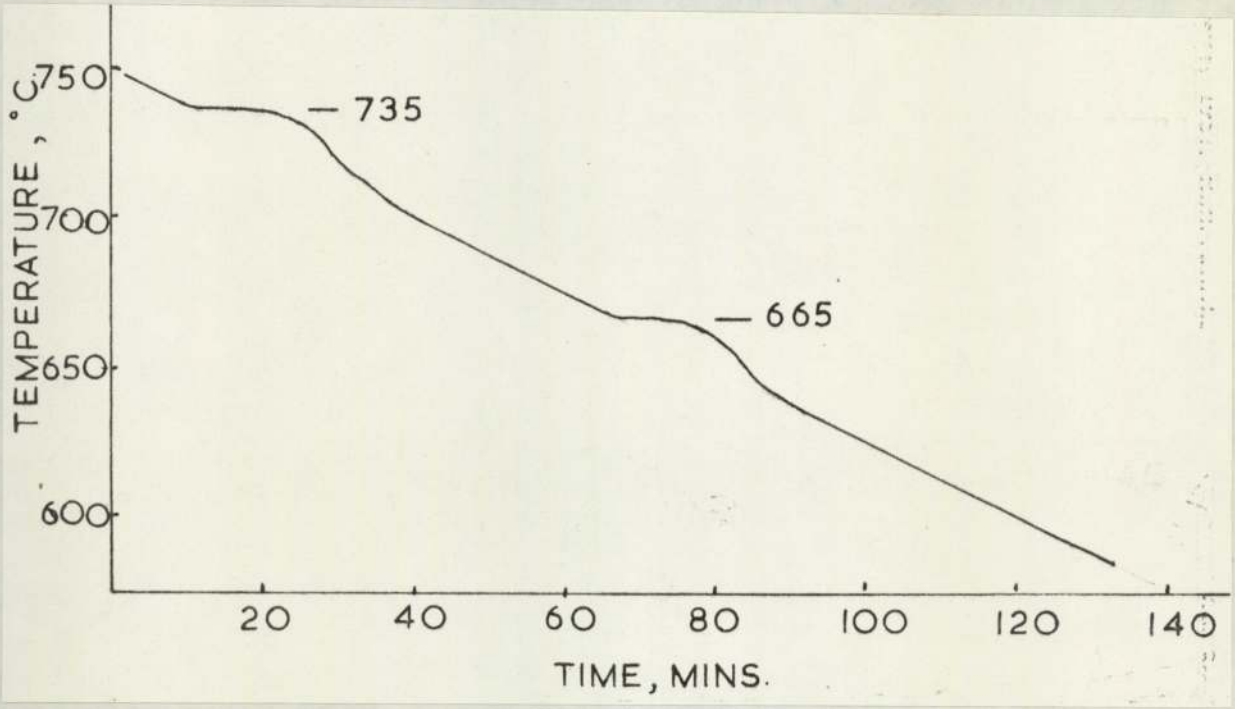

Fig. 41

4.6.2. The cooling curve and microstructure of 3:2 Cu:Sn ratio alloy containing 5% iron

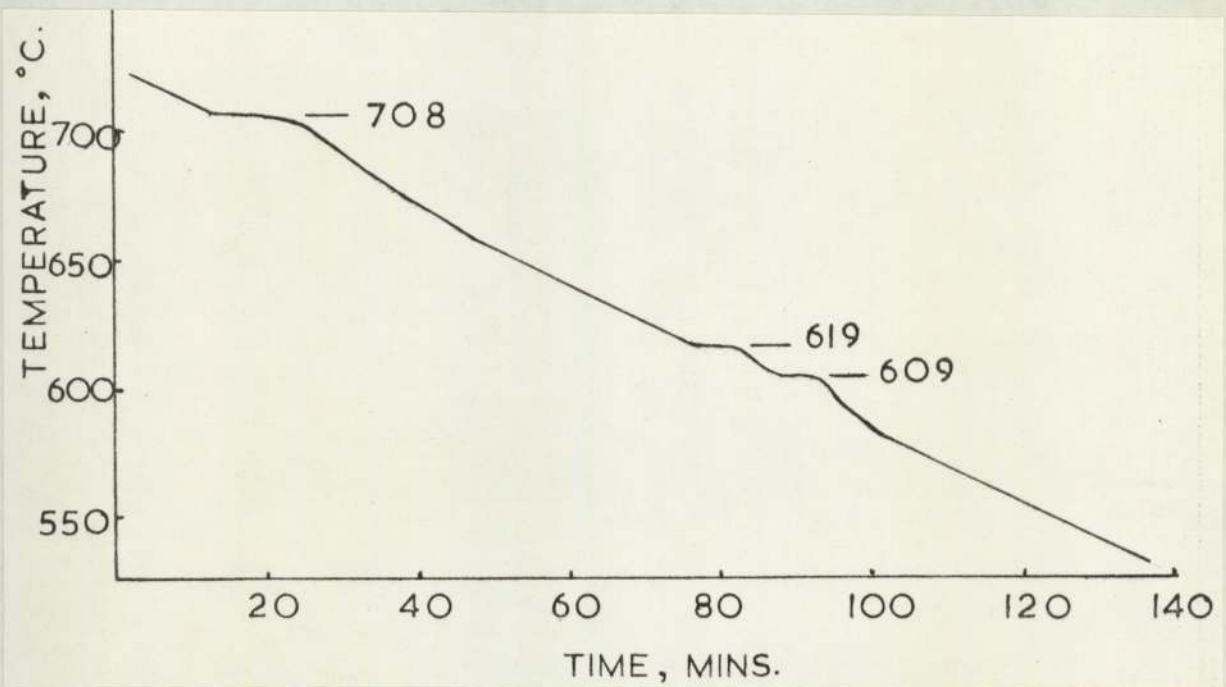

Fig. 42

4.6.3. The cooling curve and microstructure of 3:2 Cu:Sn ratio alloy containing 10% iron

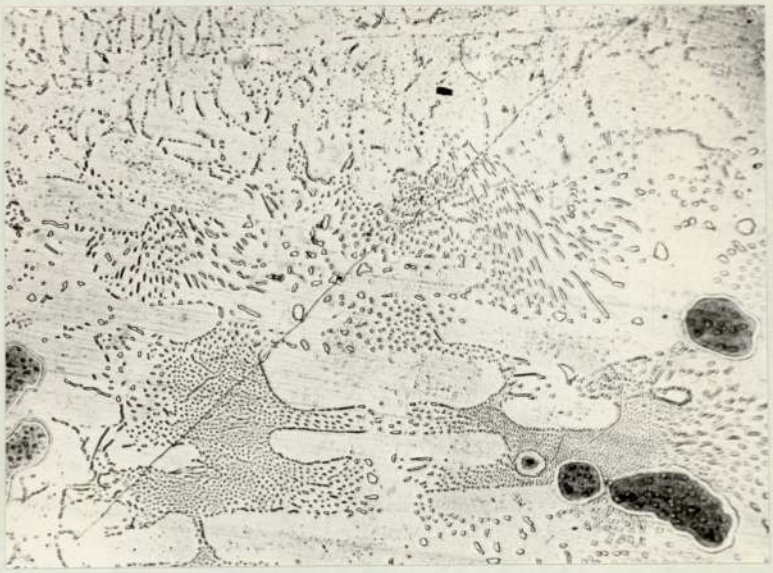

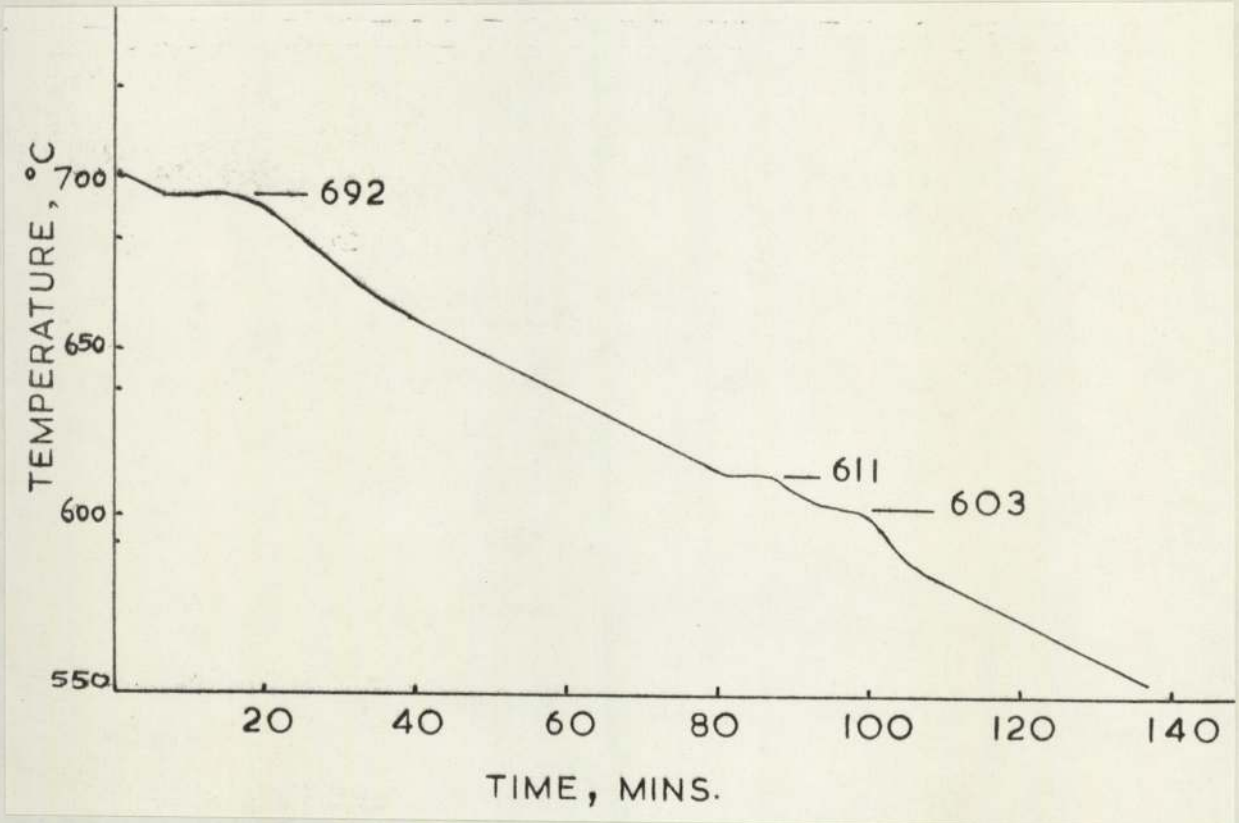

Fig. 43

4.6.4. <u>The cooling curve and microstructure of 3:2 Cu:Sn ratio alloy containing 15% iron</u>

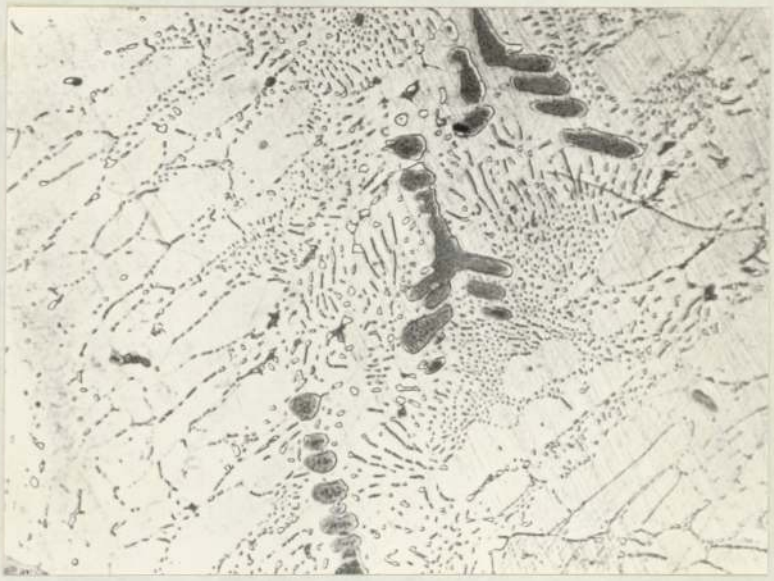

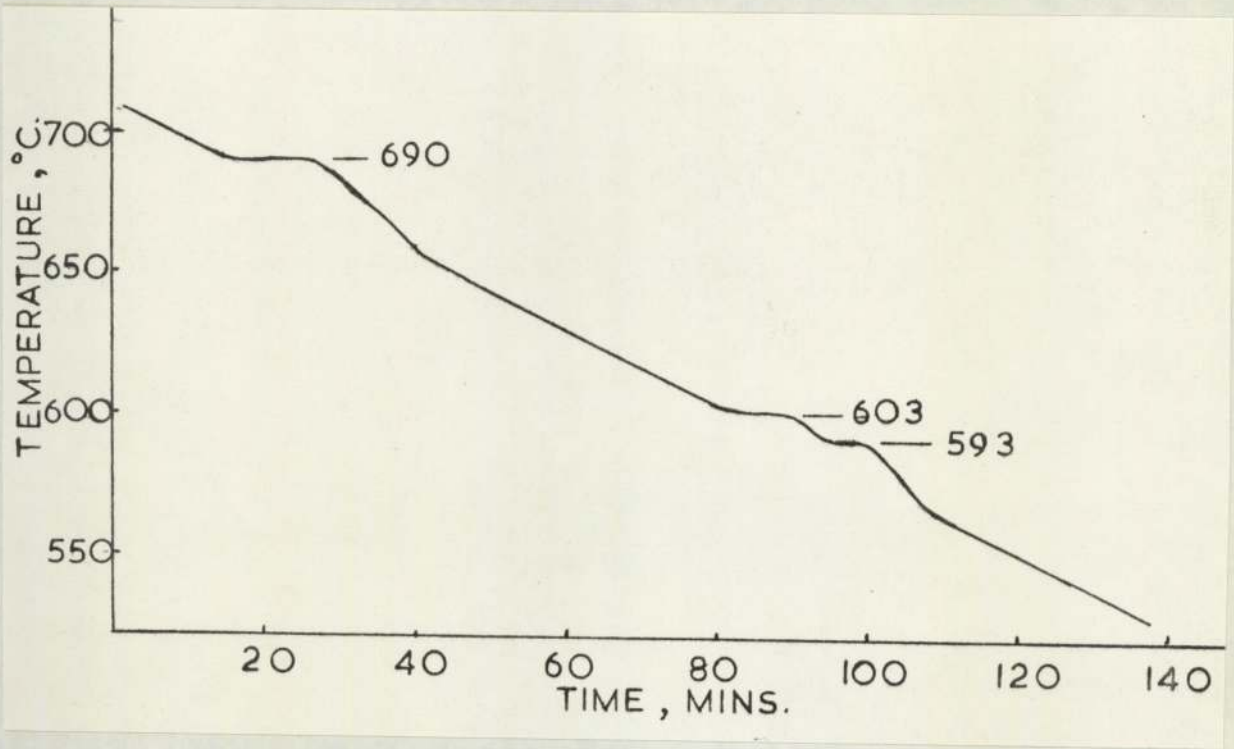

Fig. 44

4.7. The results of electron microprobe analysis of 95% Fe, 3% Cu, 2% Sn compacts sintered for 5 minutes at various temperatures

400°C

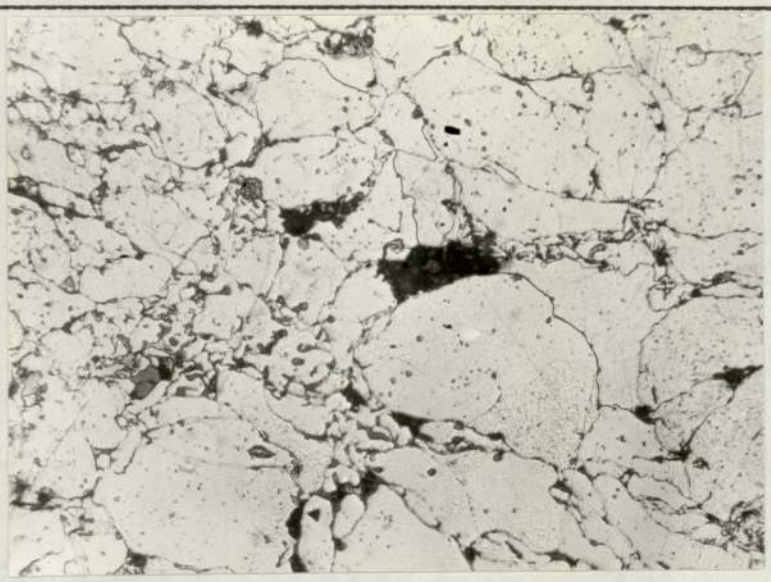

X 200

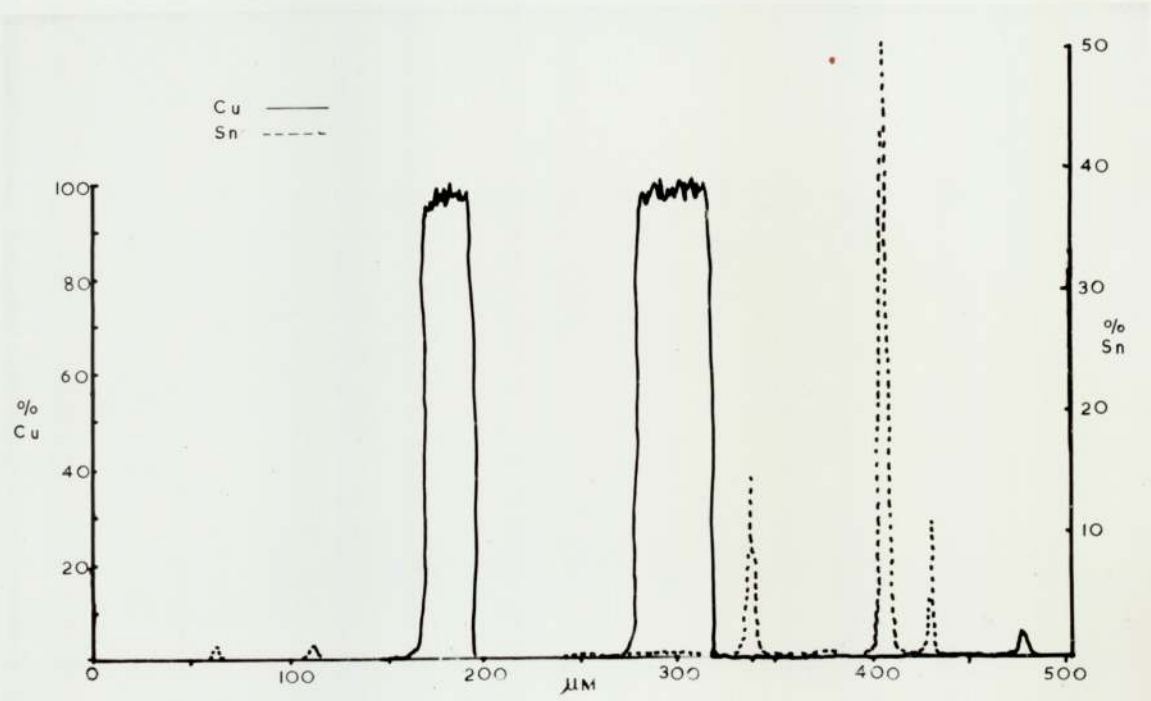

Fig. 45

4.7.2. Sinter temperature 500°C

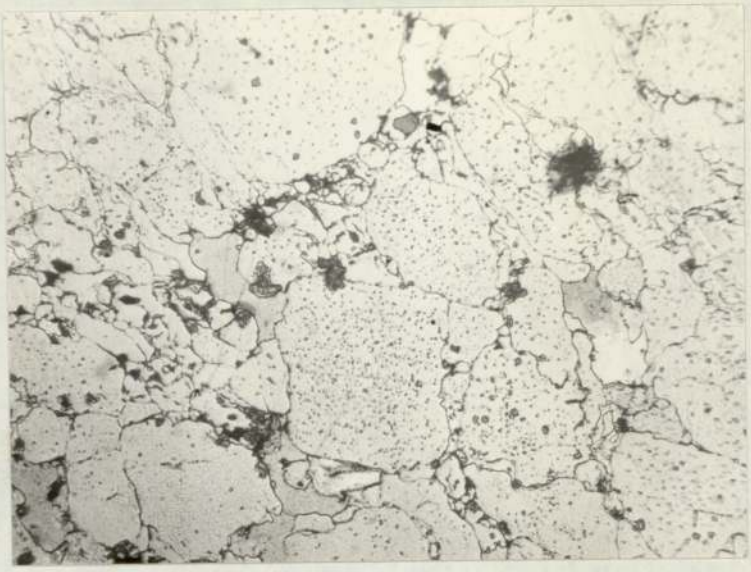

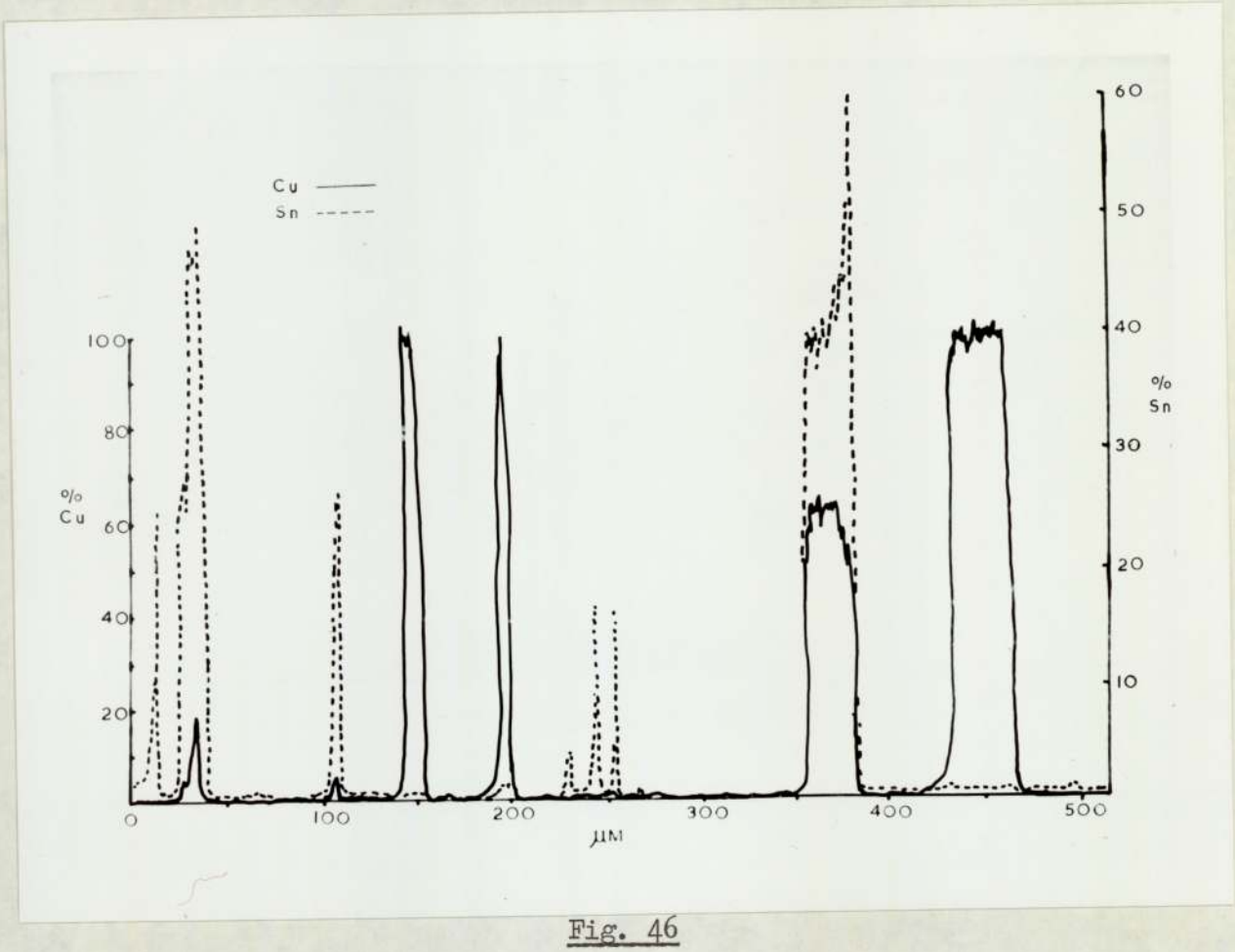

Fig. 46

4.7.3. Sinter temperature 600°C

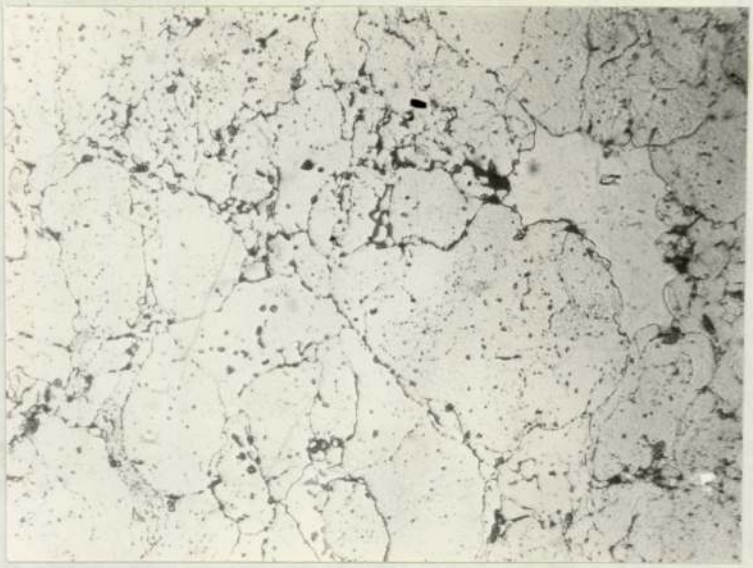

X200

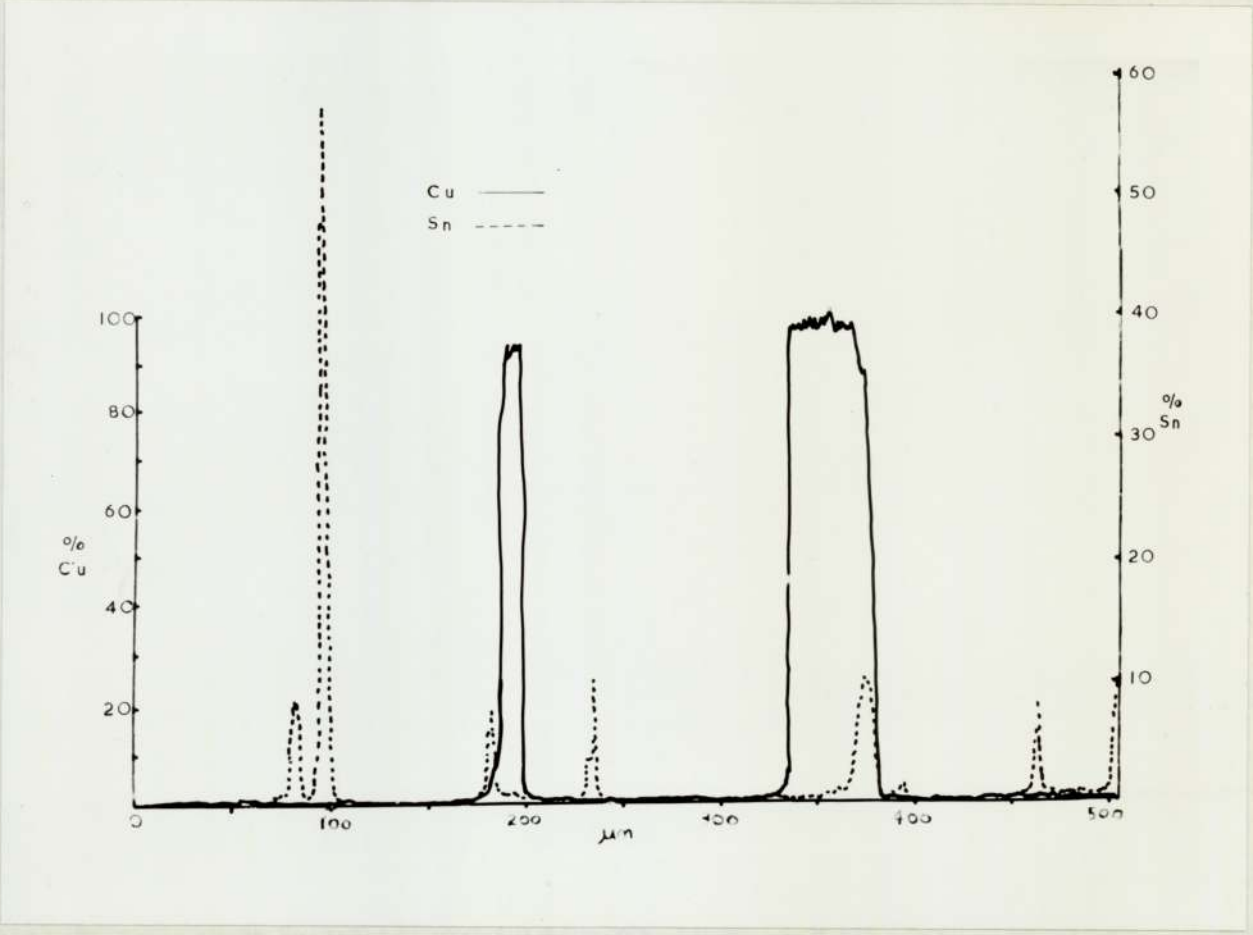

Fig. 47

4.7.4. Sinter temperature 700°C

X 200

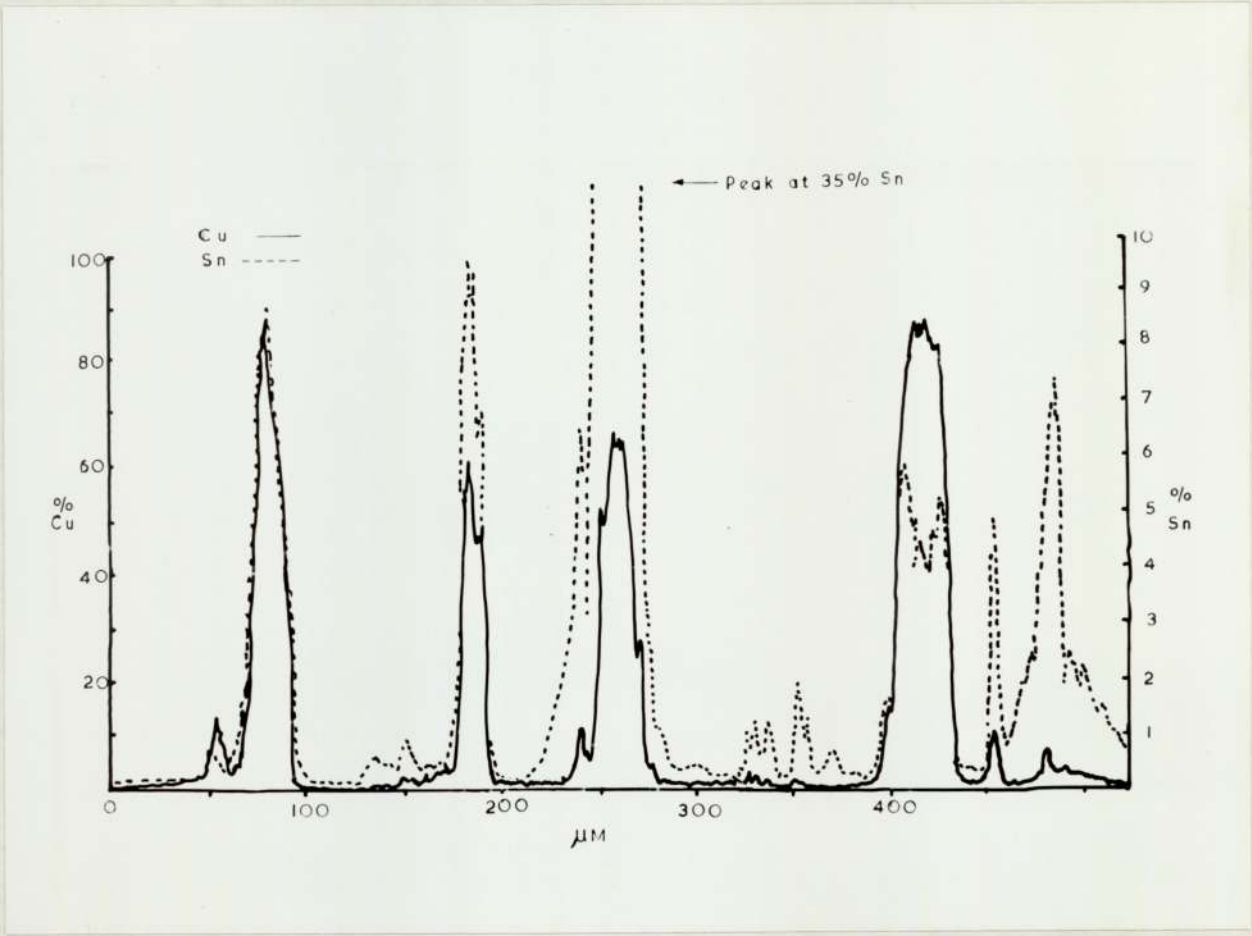

Fig. 48

4.7.5. Sinter temperature 800°C

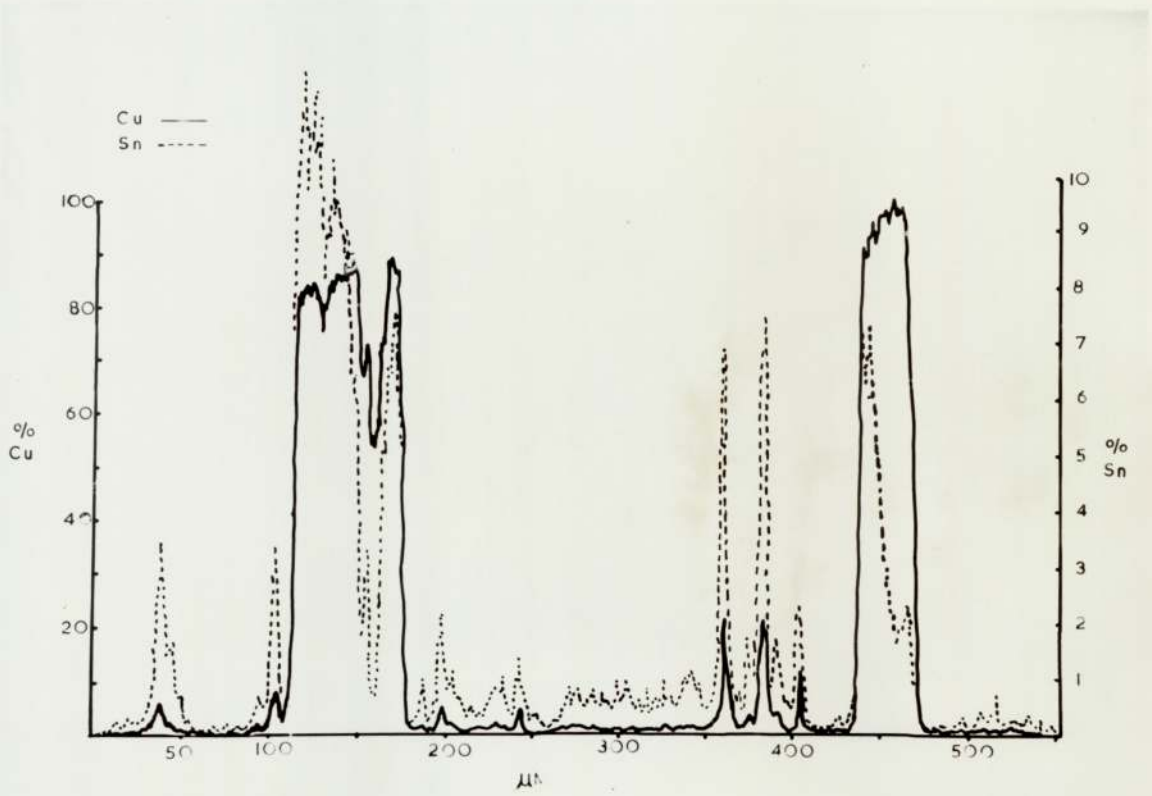

Fig. 49

4.7.6. Sinter temperature 900°C

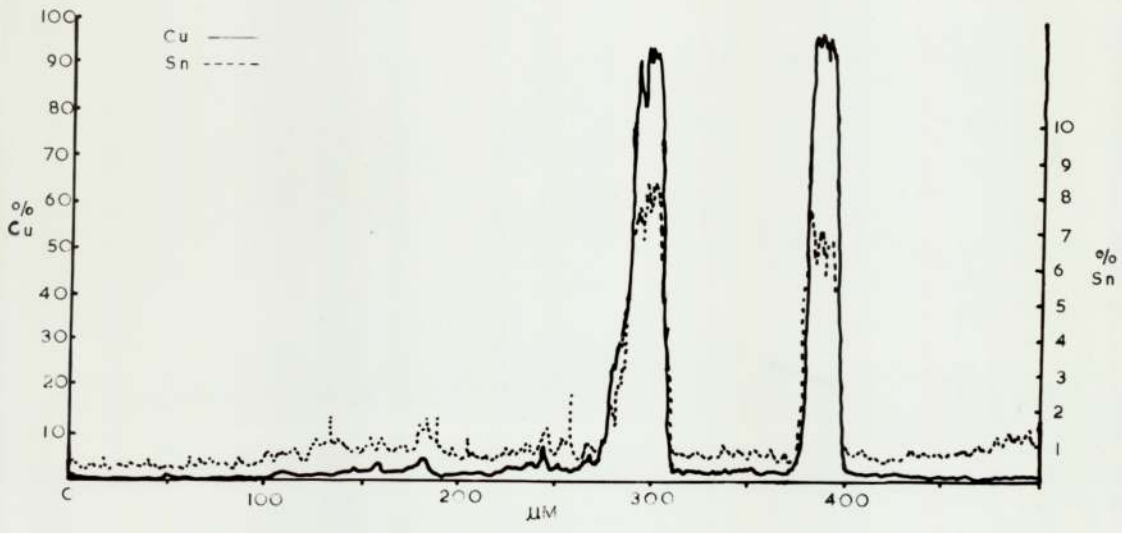

Fig. 50

4.8. The results of adding 5% of pre-alloyed 60% Cu 40% Sn powder to iron powder compacts

The mechanical test results shown in Table 28 illustrate that the results of using pre-alloyed Cu-Sn powders rather than elemental additions to iron is to give mechanical properties superior to those obtained in the latter case.

4.9. Wire spool experiments

The results of measurements made on wire spool models infiltrated with either 3:2 or 15:2 Cu:Sn ratio liquid are shown in Table 29. Fig. 51 shows that the value of the exponent 'n' which governs the mechanism of neck growth is indeterminate, due to the lack of enough contact areas for measurement.

Table 29.

sinter time minutes	Cu:Sn ratio	interface width mm	$\frac{x}{a}$ x 10^{-2}	$\log_{10}$ time minutes	$\log_{10} \frac{x}{a}$
5	3:2	0.1775	8.876	0.6990	-1.0518
5	15:2	0.1300	5.058	0.6990	-1.2960
60	3:2	0.1650	6.247	1.7782	-1.2043
60	15:2	0.1225	4.647	1.7782	-1.3328
120	3:2	0.1750	6.606	2.0792	-1.1802
120	15:2	0.2000	7.548	2.0792	-1.1222
300	3:2	0.1750	6.554	2.4771	-1.1835
300	15:2	0.1800	6.742	2.4771	-1.1712

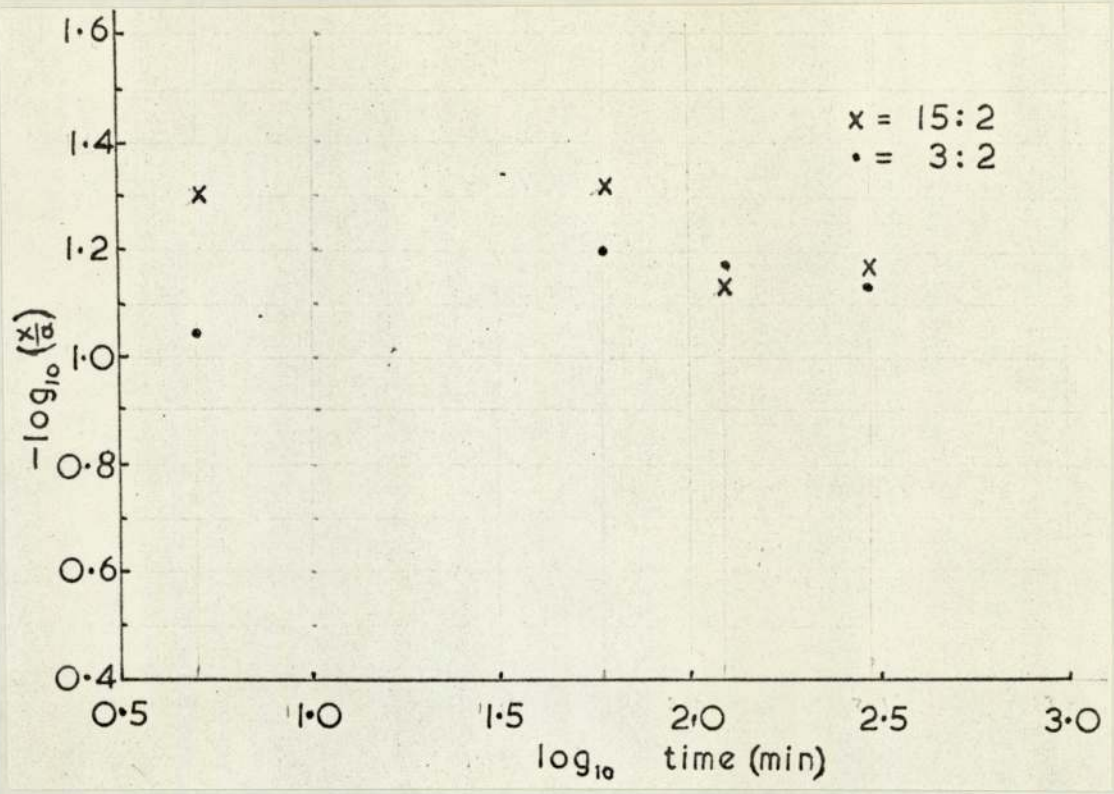

Fig. 51

4.10. Furnace atmosphere and carbon additions

4.10.1. The effect of furnace atmosphere upon the porosity of various Fe-Cu-Sn-C compacts.

Table 30.

Cu:Sn ratio	atmosphere	% added carbon	total porosity %	interconnected porosity %	closed porosity %
3:2	argon	0.8 1.2	17.79 18.24	17.36 17.72	0.43 0.52
"	carbon monoxide	0.8 1.2	17.99 18.43	17.56 17.81	0.43 0.62
"	90%$N_2$10%H_2	0.8 1.2	17.64 18.01	16.79 17.16	0.85 0.85
"	H_2	0.8 1.2	19.13 17.68	17.58 15.04	1.54 2.64
15:2	argon	0.8 1.2	17.55 18.62	17.37 18.33	0.18 0.29
"	carbon monoxide	0.8 1.2	18.80 17.58	18.04 16.79	0.75 0.78
"	90%$N_2$10%H_2	0.8 1.2	18.34 18.59	17.99 16.05	0.35 2.53
"	H_2	0.8 1.2	18.52 18.88	17.46 16.01	1.06 2.87

4.10.2. The effect of furnace atmosphere upon the mechanical properties of various Fe-Cu-Sn-C compacts

4.10.2.1. Compacts containing a 5% addition of Cu + Sn in the ratio of 3:2, sintered at 950°C for 30 minutes

Table 31.

% Carbon addition	Atmosphere	Rockwell 'A'		Elongation %		UTS_2 MN/m^2	
0.2	90%N_2 10%H_2	55.0		1		214	
0.2		59.0	56.0	1	1	99	167
0.2		54.0		1		188	
0.6		49.3		2		263	
0.6	"	52.0	50.0	2	2	263	262
0.6		48.0		2		261	
0.8		54.0		1		223	
0.8	"	56.0	54.0	2	1.5	202	220
0.8		53.0		2		234	
1.2		54.6		1		247	
1.2	"	61.0	57.7	2	1.5	300	270
1.2		57.8		2		262	
0.2	H_2	60.0		1		181	
0.2		55.0	58.3	1	1	237	178
0.2		60.0		1		115	
0.6		51.3		2		228	
0.6	"	48.3	49.3	1.5	1.5	241	237
0.6		48.3		1.5		243	
0.8		57.0		1		261	
0.8	"	59.0	58.3	1	1	232	248
0.8		59.0		1		250	
1.2		51.7		2		243	
1.2	"	47.0	46.1	2	2	242	237
1.2		45.7		2		226	

Table 31 cont.

% Carbon addition	Atmosphere	Rockwell 'A'	Elongation %	UTS MN/m^2
0.2	Argon	53.0)	1)	193)
0.3		49.0)53.0	1) 1	180)189
0.2		57.0)	1)	195)
0.6		50.0)	1)	230)
0.6	"	55.0)53.0	1) 1	228)221
0.6		53.0)	1)	206)
0.8		67.0)	1)	256)
0.8	"	69.0)68.3	1) 1	255)256
0.8		69.0)	1)	256)
1.2		63.3)	1)	290)
1.2	"	81.0)75.4	1) 1	292)297
1.2		82.0)	1)	308)
0.2	CO	63.0)	2)	247)
0.2		52.0)55.9	2) 2	252)244
0.2		52.6)	2)	233)
0.6		60.3)	1)	273)
0.6	"	56.0)60.3	1.5)1.5	269)275
0.6		64.6)	1.5)	284)
0.8		80.0)	1)	292)
0.8	"	74.3)76.1	1) 1	267)274
0.8		74.0)	1)	265)
1.2		73.0)	1)	321)
1.2	"	79.0)78.3	1) 1	338)326
1.2		83.0)	1)	319)

4.10.2.2. Compacts containing a 5% addition of Cu + Sn in the ratio of 15:2, sintered at 950°C for 30 minutes

Table 32.

% Carbon addition	Atmosphere	Rockwell 'A'		Elongation %		UTS MN/m^2	
0.2	90%N_2 10%H_2	40.6		6		231	
0.2		38.0	39.3	4	5.3	201	219
0.2		39.3		6		224	
0.6		36.0		4		213	
0.6	"	35.3	36.1	5	4.7	204	210
0.6		37.0		5		213	
0.8		39.0		4		213	
0.8	"	39.3	41.3	4	3.7	196	201
0.8		45.7		3		195	
1.2		42.0		4		189	
1.2	"	39.3	40.7	4	3.7	173	192
1.2		40.7		3		214	
0.2	H_2	40.0		4		213	
0.2		40.6	39.5	4	4.3	215	212
0.2		38.0		5		209	
0.6		37.3		4		213	
0.6	"	36.0	37.2	5	4.3	209	210
0.6		38.0		4		207	
0.8		37.0		4		157	
0.8	"	40.0	38.0	6	5.0	198	177
0.8		37.0		5		177	
1.2		39.0		6		196	
1.2	"	42.0	40.0	4	4.7	202	195
1.2		39.0		4		187	
0.2	Argon	40.0		3		201	
0.2		39.5	40.7	5	4.3	213	214
0.2		42.6		5		228	
0.6		61.0		3		323	
0.6	"	56.0	58.1	3	3.0	281	296
0.6		57.3		3		284	
0.8		64.7		2		336	
0.8	"	70.0	70.5	2	2.3	357	344
0.8		76.7		3		338	
1.2		80.0		2		395	
1.2	"	78.3	78.9	2	2.0	397	391
1.2		78.3		2		381	

Table 32 cont.

% Carbon addition	Atmosphere	Rockwell 'A'	Elongation %	UTS MN/m^2
0.2	CO	50.6)	2)	247)
0.2		50.6)51.4	2)2	275)260
0.2		53.0)	2)	259)
0.6		64.3)	2)	325)
0.6	"	62.0)66.0	2)2	333)333
0.6		71.6)	2)	340)
0.8		76.0)	2)	375)
0.8	"	82.0)76.6	2)2	383)375
0.8		71.7)	2)	368)
1.2		77.0)	1)	398)
1.2	"	81.0)79.1	1)	393)391
1.2		79.3)	1)	382)

4.11. Oxygen contents of powders and compacts

4.11.1. Oxygen content of powders as received:

ROSPA MP32 iron powder, oxygen = 0.28% by weight.

Atomised tin powder, = 0.096% "

Atomised copper powder, = 0.222%

TRI Hoganas iron powder, = 0.47%

TRI atomised tin powder, = 0.14%

4.11.2. Oxygen analysis of sintered compacts

Table 33.

Cu:Sn ratio	Oxygen, wt %			
	Sintered in N_2H_2 at		Sintered in pure H_2 at	
	950°C	1150°C	950°C	1150°C
3:2 5% addition	0.199	0.22	0.135	0.076
15:2 5% addition	0.196	0.231	0.132	0.074

4.11.3. Oxygen analysis of samples sintered in an industrial furnace using cracked ammonia

The sintering temperature employed was 1130°C for a time of 40 minutes. Samples were made with 5% additions of Cu + Sn in the ratios 3:2 and 15:2, using both the authors' powders, and the TRI powders.

Table 34.

Material	TRI powders	Authors' powders
Fe	0.38	0.17
Fe + 3:2 Cu:Sn	0.31	0.14
Fe + 15:2 Cu:Sn	0.35	0.13

4.11.4. The reduction of SnO by H_2 and 90% N_2 10% H_2 atmospheres at 950°C

The powdered oxide was reduced in an alumina crucible at 950°C for 30 minutes in the required atmosphere. The extent of reduction was calculated from weight loss measurements.

Reduction by H_2

Weight of crucible	= 24.84671 g
Weight of crucible + SnO	= 28.23326 g
Weight of oxide	= 3.38655 g
Weight of crucible + residue after reduction	= 27.78390 g
Weight of residual	= 2.93719 g
Weight of oxygen removed	= 0.44936 g

$$\% \text{ loss in weight of SnO} = \frac{3.38655 - 2.93719}{3.38655} \times 100\%$$

$$= 13.27\% \qquad (1)$$

% oxygen by weight in pure SnO_2

$$= \frac{16}{134.7} \times 100\%$$

$$= 11.88\% \qquad (2)$$

The result (1) could be larger than (2) because the purity of the SnO_2 used was quoted as only 80% minimum by the manufacturers. If the remainder was SnO_2, then the total available oxygen for reduction becomes

$$80 \times \frac{16}{134.7} + 20 \times \frac{32}{150.7} \%$$

= 13.75% maximum for the lower level of purity.

Reduction of SnO by 90% N_2 10% H_2

Weight of oxide = 2.43970 g

Weight of residual after reduction = 2.14810 g

$$\% \text{ loss in weight} = \frac{2.43970 - 2.14810}{2.43970} \times 100\%$$

= 12%

Within the purity limits of the SnO powder, all of the SnO was reduced in 30 minutes at 950°C in either H_2 or 90% N_2 10% H_2.

4.11.5. The reduction of SnO_2 by H_2 and 90% N_2 10% H_2 atmospheres at 950°C

Reduction by H_2

Weight of oxide = 2.17107 g

Weight of residue after reduction = 1.70605 g

$$\% \text{ less in weight} = \frac{2.17107 - 1.70605}{2.17107} \times 100\%$$

$$= 21.40\%$$

The theoretical weight loss for the complete reduction of pure SnO_2 is:

$$\frac{32}{150.7} \times 100\%$$

$$= 21.23\%$$

This result indicates that all of the oxygen has been removed by this treatment. The appearance of the residue after reduction was a singular metallic globule.

Reduction by 90% N_2 10% H_2

Weight of oxide = 2.60778 g

Weight of residue after reduction = 2.18456 g

$$\% \text{ loss in weight} = \frac{2.60778 - 2.18456}{2.60778} \times 100\%$$

$$= 16.23\%$$

The % of oxide reduced

$$= \frac{21.23 - 16.23}{21.23} \times 100\%$$

$$= 76.7\%$$

Therefore, one quarter of the SnO_2 is unreduced by heating in a crucible at 950°C for 30 minutes in 90% N_2 10% H_2. The residue in this case was not a singular metallic globule, but many globules surrounded by SnO_2 powder.

The micrographs illustrated in Fig. 52 show that additions of SnO_2 instead of Sn to compacts of composition 95% Fe 3% Cu 2% Sn still contain SnO_2 after sintering in 90% N_2 10% H_2 at 950°C for 30 minutes.

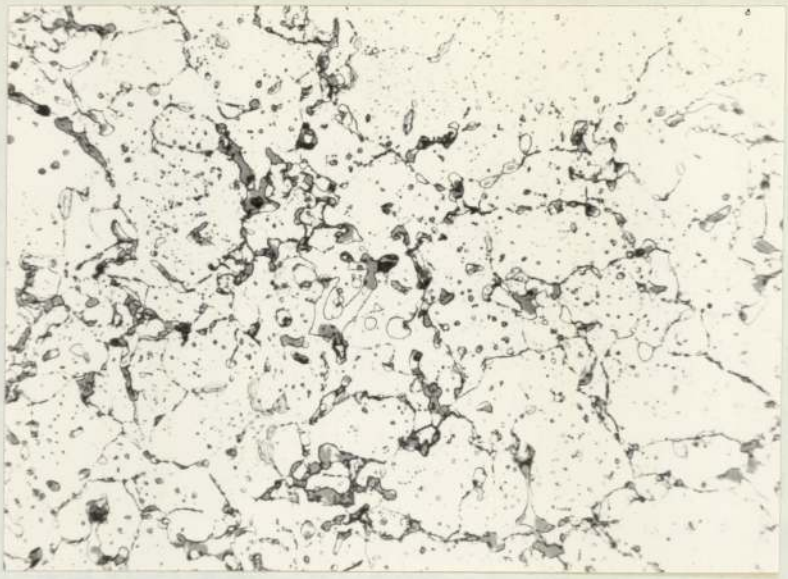

Fig. 52

95% Fe 3% Cu 2% Sn (added as SnO_2) sintered at 950°C for 30 min in N_2/H_2 mixture. The lack of complete reduction can be seen as oxide globules are present.

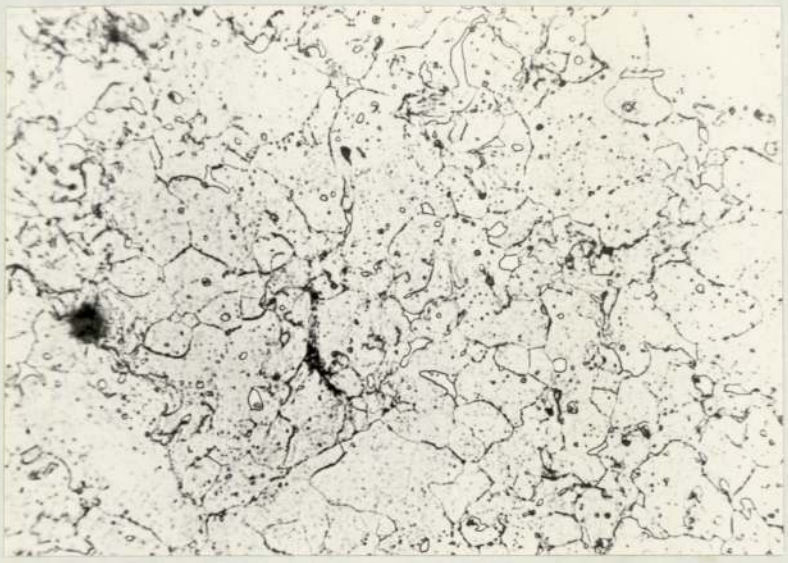

Fig. 53

The same composition as above, sintered in H_2 for 30 minutes at 950°C. All of the SnO_2 is reduced.

4.11.6. The mechanical properties of compacts containing SnO and SnO_2 instead of metallic tin.

The Cu:Sn ratios used were 3:2 and 15:2 with a 5% total addition to iron. Compacting pressure was 463 MN/m^2 with no lubricant addition.

Table 35.

SnO additions sintered in H_2 at 950°C

Cu:Sn ratio	UTS MN/m^2	Elongation %
3:2	247	1.5
"	258	1.0
"	220	1.0
	242	1.0
15:2	217	6.0
"	228	5.0
"	225	6.0
	223	5.3

Table 36.

SnO additions sintered in 90% N_2 10% H_2 at 950°C

Cu:Sn ratio	UTS MN/m^2	Elongation %
3:2	126	1
"	78	1
"	110	1
	105	1
15:2	207	5.5
"	212	6.0
"	214	5.5
	211	5.7

Table 37.

SnO_2 additions sintered in pure H_2 at 950°C

Cu:Sn ratio	UTS MN/m^2	Elongation %
3:2	184	1
"	220 } 202	1 } 1
"	202	1
15:2	214	6
"	224 } 222	5 } 5.3
"	228	5

Table 38.

SnO_2 additions sintered in 90% N_2 10% H_2 at 950°C

Cu:Sn ratio	UTS MN/m^2	Elongation %
3:2	104	1
"	67 } 85	1 } 1
"	85	1
15:2	213	5.0
"	207 } 208	6.0 } 5.3
"	205	5.0

4.11.7. The influence of sintering atmosphere on the UTS of compacts already sintered for 30 minutes at 950°C in pure H_2.

Twelve samples containing 95% Fe 3% Cu and 2% Sn were sintered at 950°C for 30 minutes in H_2. They were then re-sintered for a further 30 minutes in one of four atmospheres; H_2, 90% N_2 10% H_2, CO, or argon.

Table 39.

Treatment after initial sinter	UTS$_2$ MN/m^2
30 min in H_2	173)
"	222)199
"	202)
30 min in Ar	81)
"	147)113
"	110)
30 min in N_2H_2	157)
"	123)120
"	80)
30 min in CO	287)
"	284)288
"	292)

4.12. Heat treatment of Fe-Cu-Sn and Fe-Cu-Sn-C compacts

4.12.1. Fe-Cu-Sn compacts

Samples were made with either 5% of 3:2 or 15:2 Cu:Sn additions. These were compacted at 463 MN/m^2 pressure and sintered at 950°C for 30 minutes prior to quenching in water or oil. The mechanical properties are shown in the following table:

Table 40.

Cu:Sn ratio	Quench medium	Hardness Rockwell 'A'		Anneal	UTS MN/m^2		Elongation %	
3:2	Water	47.5	48.1	None	167	167	1	1
"	"	48.8		"	167		1	
"	"	39.5	40.0	30 min at 700°C	66	88.5	1	1
"	"	40.5		"	111		1	
"	"	51.2	47.9	30 min at 800°C	88	72.4	1	1
"	"	44.5		"	56.7		1	
15:2	Water	50.0	52.0	None	246	261	3.5	3.0
"	"	54.0		"	276		2.5	
"	"	42.0	42.1	30 min at 700°C	214	204	4.0	3.2
"	"	42.2		"	194		2.5	
"	"	40.2	41.8	30 min at 800°C	185	194	3.0	3.5
"	"	43.5		"	202		4.0	
3:2	Oil	61.2	54.7	None	80	174	1	1
"	"	52.5		"	224		1	
"	"	50.2		"	218		1	
15:2	Oil	51.2	53.3	None	261	285	3.5	2.7
"	"	56.2		"	298		2.0	
"	"	52.5		"	297		2.5	

4.12.2. Fe-Cu-Sn-C compacts

Table 41.

Cu:Sn ratio	Quench medium	Hardness Rockwell 'A'	Anneal	UTS MN/m^2	Elongation %
3:2+0.4C	H_2O	56.0, 46.5 — 51.25	None	214, 205 — 208	1, 1 — 1
"	"	62.7, 64.2 — 63.45	"	- , - — too brittle	1, 1 — 1
3:2+1.2C	"	63.2, 65.0 — 64.1	"	- , - — "	1, 1 — 1
15:2+0.4C	H_2O	52.5, 41.5 — 47.0	None	154, 203 — 179	1, 1
"	"	58.8, 66.0 — 62.4	"	- , -	- , -
15:2+0.8C	"	63.0, 64.0 — 63.5	"	- , -	- , -
15:2+1.2C	"				
3:2+0.4C	H_2O		30 min at 500°C	79, 140 — 110	1, 1
"	"		"	171, 134 — 152	1, 1
3:2+0.8C	"		"	59, 56 — 57.5	1, 1
"	"		"		
3:2+1.2C	"				
"					
15:2+0.4C	H_2O		30 min at 500°C	288, 341 — 315	1, 1 — 1.0
"	"		"	286, 298 — 292	1, 2 — 1.5
15:2+0.8C	"		"	299, 349 — 324	2, 2 — 2
"			"		
15:2+1.2C	"				
"					

Section V Discussion of Results

5.1. Determination of the variables to be studied.

5.1.1. Initial results.

In the preceding section, it was noted that a study of the most important variables to be considered in the sintering of the Fe-Cu-Sn alloys was undertaken. Additions of both copper and tin to iron powder have the effect of activating the sintering process so that compacts of good mechanical properties can be obtained using sintering temperatures markedly below those usually used for iron-based compacts; in the region of 950°C instead of 1150°C. The usual sintering temperature for iron-copper compacts containing up to 10% copper is 1100-1150°C, and the saving in furnace heating element life, together with a reduction in the time of sintering to approximately 20 minutes which can be obtained using Fe-Cu-Sn powder compacts containing up to five percent of Cu+Sn, is economically important. The results of initial work by the author and C. Fletcher[28] are illustrated in Figs. 22-33. A detailed study of these results show marked differences from published work.

Fig. 22 shows that increasing additions of tin to compacts sintered at 950°C and 1100°C produced a rapid decline in UTS. All samples were very brittle and elongations were not measurable. Duckett and Robins[21], however, obtained the results illustrated in Fig. 54.

This diagram shows that 2% tin additions to iron powder increased the UTS to about 247 MN/m^2 (16 tsi) when sintered at 1000°C for 60 minutes in pure H_2. 0.5% stearic acid was added as a binder.

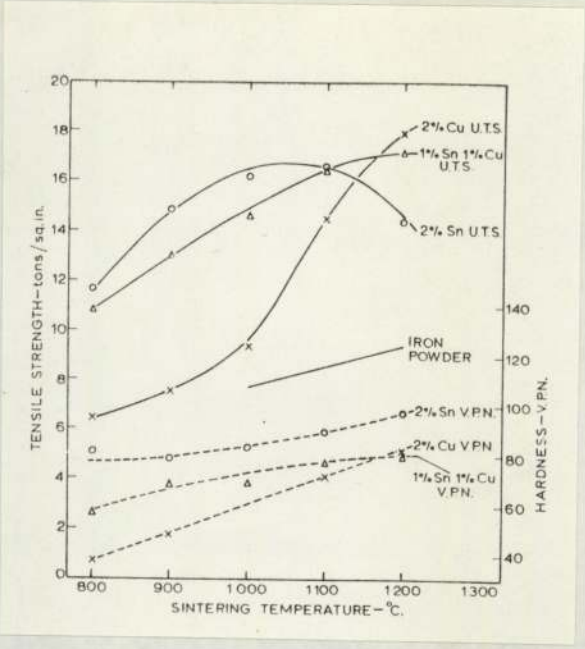

Fig. 54

Because the authors' initial results were showing consistently low strength measurements with even small tin additions of 1% when sintered in an atmosphere of 90% N_2 10% H_2 mixture, it was decided to use the same conditions as prescribed by Duckett and Robins. The results of these experiments are shown as a dotted line in Fig. 22 and indicate that under certain conditions only, will tin improve the sintered properties of iron. These conditions include the use of a pure H_2 atmosphere, and 0.5% stearic acid as a powder lubricant. It can be concluded from these results that either the sintering atmosphere employed, or the use of a pre-treatment to burn off the binder prior to sintering had a profound effect upon the sintered properties when tin additions were made to iron powder. No explanation

for the apparent disastrous effect of tin additions to iron powder sintered in 90% N_2 10% H_2 atmosphere can be given from these results alone, although the suggestion made by Esper et. al.[26] that it may be due to the precipitation of an Fe-Sn compound during cooling cannot be accepted unless this precipitation were controlled by the sintering atmosphere employed. In addition, no Fe-Sn compounds could be detected metallographically within the low tin content samples exhibiting this brittle behaviour.

5.1.2. Additions of copper and tin separately.

The addition of copper only to iron compacts sintered at 1100°C (Fig. 22) produced an increase in strength because the sintering rate was increased by the presence of a liquid phase and also because of the solid solution strengthening effect of copper in iron. The finer copper powder addition produced a greater strengthening effect than the coarse copper powder owing to its greater dissemination and therefore improved effectiveness. The very slight improvement in strength of compacts containing -152 μm Cu sintered at 900°C, at which temperature the mechanism is solid-state sintering, was due to the solid solution strengthening of the small amount of copper that was able to diffuse into the iron at this temperature.

5.1.3. Simultaneous additions of copper and tin.

The increase in strength produced by the addition of tin to the copper (Figs. 24-28) was due to the increased sintering rate associated with the liquation of tin at low temperatures. As will be shown in a further section, tin wets the iron particles at a relatively low temperature, thus assisting the copper-tin alloy to flow around the iron grains as soon as it becomes molten. The rapid fall-off in

strength at low copper:tin ratios was probably due to the high tin content and to the operation of the embrittling mechanisms associated with Fe-Sn and Cu compounds.

All the work illustrated in these graphs demonstrates that optimum mechanical properties were obtained with a copper:tin ratio of 15:2 when using a gas atmosphere of 90% N_2 10% H_2. This copper: tin ratio was much higher than that suggested by the Tin Research Institute (3:2) for compacts sintered in an atmosphere of pure hydrogen. This also differs substantially from the ratios recommended by Esper, Freize and Zeller who showed that the Cu:Sn ratio varied according to sintering temperature from pure tin to 7:2 Cu:Sn. The effect of furnace atmosphere upon powder mixtures is further illustrated in the following table:

Table 42.

Sintering temp °C	Atmosphere	UTS N/mm^2			
		Cu/Sn ratios			
		1:1	3:2	10:2	15:2
950	10% H_2N_2	15.9	65	199	202
	pure H_2	105	226	218	206
1150	10% H_2N_2	-	161	-	268
	pure H_2	-	241	-	288

These results agree well within experimental error with the other reported work and suggest that some correlation may exist between the mechanical properties and the final oxidation state of the powders used in the experimental work. This aspect will be discussed more fully later.

The conclusions which may be drawn at this stage are as follows:

1) Significantly higher strengths may be obtained by using a

copper:tin ratio of 15:2 than by using either pure iron or iron-copper compacts sintered at the same temperature in an atmosphere of 90% N_2 10% H_2.

2) A considerably lower sintering temperature can be used to achieve similar properties. For example, iron with a ten percent addition of 15:2 Cu:Sn sintered at 900°C will produce higher strengths than will iron with 10% copper sintered at 1100°C.

3) Elongations are generally of the same order as those expected with normally sintered iron-copper alloy compacts.

4) Dimensional control is better than with iron-copper compositions.

5) Copper particle size seems to have little effect upon dimensional control.

6) Lower sintering temperatures bring economies not only from reduced heating costs but also from longer furnace-belt life and lower maintenance costs.

5.1.4. Regression analysis of TRI and U/A results.

The above results showed that both the atmosphere used for sintering (pure H_2 or 90% N_2 10% H_2) and the copper:tin ratio were two factors which control the final mechanical properties of Fe-Cu-Sn sintered compacts. The results of experiments carried out by the author and by the Tin Research Institute workers were subjected to a statistical analysis to determine those variables of major importance. (See Appendix 'B').

The regression equation obtained in this manner was as follows:

$$UTS_{(Kg/mm^2)} = 23.1249 + 9.0648\ (mix/press) - 29.073\ (atmosphere) - 9.5098\ (Cu:Sn\ ratio) - 3.1725\ (mix \times sinter) + 4.6413\ (sinter \times ratio) + 3.8022\ (gas \times ratio) + 0.0175\ (gas \times temperature)$$

In order to show the effect of each variable upon the strength of the sintered compacts, known values for the independent variables can be substituted in the regression set. Thus for samples prepared and sintered at TRI using their own powders and a hydrogen atmosphere, the following results are obtained:

$UTS_{(Kg/mm^2)}$ = 15.5 for the 3:2 ratio at 950°C

and $UTS_{(Kg/mm^2)}$ = 19.0 " " " " " 1150°C

Changing the furnace atmosphere to 90% N_2 10% H_2 then has the following predicted effect upon the UTS:

$UTS_{(Kg/mm^2)}$ = 6.857 for the 3:2 ratio at 950°C

and $UTS_{(Kg/mm^2)}$ = 13.857 " " " " " 1150°C

Performing a similar set of calculations as above, but considering the 15:2 Cu:Sn ratio, we obtain:

$UTS_{(Kg/mm^2)}$ = 14.44 for the 15:2 ratio at 950°C in H_2

and $UTS_{(Kg/mm^2)}$ = 17.94 " " " " " 1150°C in H_2

Changing the furnace atmosphere to 90% N_2 10% H_2 and holding all the other variables the same, we obtain:

$UTS_{(Kg/mm^2)}$ = 9.6 for the 15:2 ratio at 950°C in N_2H_2

and $UTS_{(Kg/mm^2)}$ = 16.6 " " " " " 1150°C in N_2H_2

The use of the final regression equation in this way indicates the relative importance of the variables in the regression set. Taking the first order variables first, it is found that the mixing and pressing procedure carried out at Aston to be superior to that carried out at TRI in terms of the increase in the value of the UTS.

The second term, gas atmosphere, is always negative, and a hydrogen atmosphere yields better properties in all situations.

This statement is not surprising; most carbon-free iron base powder component producers would agree, but due to cost considerations a pure H_2 atmosphere is not to be recommended for these alloys. The logical progression from here is to determine which alloy of Fe-Cu-Sn responds to sintering in a leaner atmosphere the best.

The Cu:Sn ratio term is negative, which means generally the 15:2 ratio will be inferior to the 3:2 ratio.

These first order variables set the trend for prediction of the important variables, but the second order variables can have the effect of cancelling out the first order ones in certain situations. For instance, the statement that the 3:2 ratio is superior to the 15:2 ratio because of the first order term:

.... -9.5098 (ratios)

only applies when the two second order terms

.... + (sinter x ratio) and + (gas x ratio)

are minimum, as when using the pure H_2 atmosphere and the University of Aston sintering procedure. By using an atmosphere of 90% N_2 10% H_2 it is found that in fact the 15:2 ratio is superior.

The term

.... -29.073 (gas atmosphere)

can in no situation be nullified by the second order positive terms

.... +3.8 (gas x ratio) + 0.0175 (gas x temperature)

Although the value of the gas atmosphere coefficient is the highest (-29), it must be remembered that the temperature is in units of deg. Centigrade, so that the (gas x temperature) second order

coefficient is in fact quite large, approximately equal to + 17 (gas atmosphere).

In conclusion, the above discussion of the regression equation leads to these observations:

1) The gas atmosphere used in sintering Fe-Cu-Sn compacts is of prime importance in controlling the mechanical properties.

2) The copper:tin ratio employed is of equal importance, and for maximum strength levels in the final compact, the Cu:Sn ratio must be tailored to the sintering atmosphere, or vice versa.

3) The UTS rises with increasing sintering temperature more so in the case of the 15:2 Cu:Sn ratio than the 3:2 Cu:Sn ratio.

4) The variables rejected from the regression set have little importance in determining the final strength levels of these compacts. These include:

The powders used (within the experimental limits), the temperature (as a first order variable which can act on its own without any other parameter change) and the sintering furnace employed.

This means that the major strengthening effect of the copper and tin additions to iron, and hence the sintering process itself does not depend upon the powders used, or the sintering furnace and procedure, at least within the limits of the experimental conditions described.

5.2. Zinc stearate additions.

Although a study of the mechanical properties and microstructures of sintered compacts give many indications of the effectiveness of the sintering process, it is necessary to avoid those variables with an indeterminate effect when studying the sintering mechanisms involved. For this reason it was decided to dispense with lubricant additions in

the Fe-Cu-Sn compacts used in these studies. A preliminary survey of the effect of admixed zinc stearate upon mechanical properties was carried out, however, because much of the published data concerning the Fe-Cu-Sn powder system included such additions.

Meyer, Pillot and Pastor[30] stated that the effect of admixed lubricants is to slightly increase the compactibility of the powder, reduce tool wear and ejection pressure, and to eliminate physical defects within the compact. Their results indicated that in the green density range of 5.5 to 7.0 g/cm^3, additions of 0.25 - 1.0% of a lubricant to iron powder would increase the green density by about 0.5 g/cm^3. With zinc stearate additions, these authors stated that solid residues equal to 18% of the lubricant weight remained within the compact as ZnO even at 750°C. In comparison with a lubricant which left no residue, the mechanical properties of zinc stearate-lubricated compacts were lower.

These results indicated that any increase in mechanical properties in samples containing zinc stearate additions was due to the enhanced green density of these compacts for a given compaction load, and consequently greater surface area of metal/metal contacts within the compacts, rather than to any effect of the residue left after the sintering operation.

The results in table 27 show an average green density of 6.60 g/cm^3 for samples pressed at 386 MN/m^2 (25 tsi) without lubricant, and 6.81 g/cm^3 for those containing 0.5% zinc stearate. The corresponding UTS and elongation measurements show that the addition of this amount of lubricant increases the ductility by one percent, and the UTS by about 250% while a 15 minute burn off period without the addition of

lubricant prior to sintering has the effect of raising the UTS by about 50% under these conditions. The zinc stearate addition has a significant effect upon the mechanical properties, and the gases evolved on burn-off could affect the distribution of the liquid phases present during heating up.

Table 28 shows the results of mechanical tests carried out on samples containing 0.5% zinc stearate at various copper/tin ratios to compare with the published work. The mechanical properties are similar to those reported by Esper, Freise and Zeller[26], and Robins et. al.[22] for pure H_2 sintering atmospheres.

Having confirmed that this system gave comparable results to those reported when all of the parameters were the same, zinc stearate additions to the Fe-Cu-Sn powders were discontinued due to their unknown effect upon the sintering mechanisms, and their obvious effect upon mechanical properties. Consequently it will be reasonable to assume that the measured mechanical properties of the sintered compacts reflect the sintering process.

5.3. Sintering mechanisms.

The study of the sintering mechanisms operating in the Fe-Cu-Sn sytem was based upon diffusion experiments with and without a powder matrix; low temperature experiments to assess reactions as they occur on heating; thermal analysis to determine whether the liquid phase formed on sintering remains in this state during the sintering process; and additions of pre-alloyed Cu-Sn powder to iron powder in order to remove the intermediate reactions which occur upon heating up of the compacts. The results of mechanical tests at various stages have been used in the discussion of sintering mechanisms.

5.3.1. Diffusion Experiments.

5.3.1.1. The reaction between 60% Cu 40% Sn alloy with steel of varying carbon content.

The reaction between a liquid alloy of 60% Cu 40% Sn at 1100°C with steel of various carbon contents is illustrated in Fig. 34. This figure refers to the 0.8% carbon steel only, because no difference either metallographically or by microprobe analysis was detected with the other carbon steels, so that the illustrated results are fully representative. Both the microprobe scan and the microhardness traverse indicate a depth of penetration of the copper or tin into the iron of $< 50\ \mu m$. The reason for the choice of a fully pearlitic structure was that if $> 3\%$ of tin diffused into the steel at any point, the α-phase would be stabilised with a consequent change of microstructure as the carbon was precipitated from solution. No α-phase stabilisation was observed at any time indicating that penetration of the tin into the steel under these conditions was small. The theory that it is mainly α-phase stabilisation which promotes sintering as proposed by the TRI workers (loc. cit.) is not substantiated by these results unless it is entirely a surface phenomenon. The photomicrograph in Fig. 35 shows that the fully pearlitic structure is retained under the conditions of a powder matrix sintered under the same conditions.

5.3.1.2. The effect of Cu:Sn ratio on the amount of iron dissolved in the Cu/Sn alloy at 1100°C.

The results of these experiments are shown in Figs. 36-39 which illustrate the microstructures at the interface between solid steel containing 0.1% carbon and the copper-tin alloys after heating for 30 minutes at 1100°C. Electron scans showing the changes in

composition across the interface are reproduced beneath each photomicrograph.

Fig. 36 shows some grain boundary diffusion of copper into the iron, although the extent is very limited due to the low level of superheat in the liquid copper at the experimental temperature, 1100°C. The electron scans also show that little iron has dissolved into the copper. The peak in the copper scan within the iron layer is caused by the electron beam cutting across a copper-rich grain boundary. This data verifies the presence of grain boundary diffusion of copper into the iron.

The composition of the copper-tin alloy analysed in Fig. 37 was 60% Cu 40% Sn, i.e. the 3:2 Cu:Sn ratio. Iron has dissolved into the liquid at 1100°C, as shown by the primary dendrites within the Cu/Sn matrix which analyse 95% iron and 5% copper and tin. The traces show no significant diffusion of either copper or tin into the iron, and the copper/tin matrix is uniform ε-phase, Cu_3Sn. Near the interface a zone of apparent precipitation from the iron can be seen as was noted by Esper et. al. [24] within the grains of their sample sintered at 1050°C. However, this 'precipitation'was not noticeable in unetched specimens in the present work, and it is believed that it is an electrochemical effect produced by etching two dissimilar metals in 2% Nital solution.

From the electron scan in Fig. 38 it can be seen that much more iron was dissolved in the copper-tin liquid, although no dendrites were etched up in the photomicrograph. Porosity in the copper-tin-rich phase was due to the unavoidable break-up of the very brittle constituents during polishing. The electron-scan traces also showed a diffusion

gradient of copper and tin within the iron but only to a distance of ~30 μm. In the copper-tin matrix two intermetallic phases were present: ε-Cu_3Sn and η-Cu_6Sn_5, as well as the iron-rich constituent.

Fig. 39 shows the result of an experiment in which pure tin was held in contact with iron for 30 minutes at 1100°C. Extensive reaction occurred. As well as the tin diffusing into the iron over a considerable distance (~120 μm), iron had dissolved into the tin to give dendrites of an iron-tin compound in the tin matrix. This experiment emphasises that two-way solution occurs between the metallic phases. Note also that tin has pushed the small amount of carbon in the iron ahead of its diffusion front.

These diffusion experiments confirm the finding of other workers that both copper and tin individually will diffuse into iron. At 1100°C the diffusion of tin is considerable, but with copper, diffusion is limited mainly to grain boundaries as the level of superheat in the molten copper is very low.

As tin is added to iron/copper mixes, diffusion of copper into the iron decreases to an almost undetectable level at the sintering temperature, while the solubility of iron in the liquid copper-tin increases. At high tin levels, tin diffusion into the solid iron becomes noticeable simultaneously with increasing solubility of iron in the liquid. This restriction by tin on the copper diffusion and by copper on tin diffusion confirms the work of Robins et. al. [31] and of Esper et. al. [24] and helps to keep the copper-tin additions molten at the sintering temperatures, consequently aiding the sintering process. Intermediate copper-tin alloys seem to react with iron mainly by dissolving it rather than by diffusion into it to a significant

extent. Dissolution of iron at the interface would tend also to remove any solid diffusion gradient that might be set up within the iron. According to Long and Robins [31] this would be disadvantageous to the sintering process, but the present work does not seem to substantiate this theory.

In all the present investigations, it was found that a copper:tin ratio of 3:2 was the lowest that could be used before excessive brittleness began to affect the final mechanical properties. It was also found that only tin diffused significantly into the iron at lower copper:tin ratios. Long and Robins suggested that this was the major factor in improving the sintering characteristics of Fe-Cu-Sn sintered compacts by increasing the self-diffusion rate of iron by stabilising the α phase at the sintering temperature. Evidence for this theory was cited in the sintering behaviour of Fe-Cu-Sn compacts containing carbon[25]. The tensile strength of these compacts was decreased by increasing the carbon content, although a liquid phase was always present. It was suggested that because carbon is a strong γ stabiliser at the sintering temperature of 1000°C, its presence overruled α-stabilisation by tin, and consequently poorer sintering ensued together with lower final mechanical properties.

It has already been emphasised that the composition of the atmosphere is a major factor in controlling the sintering characteristics of Fe-Cu-Sn compacts, and that when carbon is associated with these elements in an attempt to improve final mechanical properties it is very important to control the dew-point of the sintering gases. Fairbank and Palethorpe[32] showed that the dew-point must be 270-256K (-3--17°C) for a steel containing 0.8% carbon potential at

900–1100°C when using an endothermic gas. The following table shows that very different values of tensile strength can be obtained in Fe-Cu-Sn compacts (3:2 and 15:2 ratios) sintered at 950°C according to whether the furnace atmosphere is hydrogen or carbon monoxide.

Table 43.

Effect of Sintering Atmosphere on the UTS of Fe–Cu–Sn–C Compacts*

Copper : Tin Ratio (5% addition)	Added Carbon %	UTS kgf/mm²	UTS N/mm²	Sintering Atmosphere
3:2	0·2	18·1	178	H_2
,,	0·6	24·3	238	,,
,,	0·8	25·2	247	,,
,,	1·2	24·3	238	,,
3:2	0·2	24·9	244	CO
,,	0·6	28·0	275	,,
,,	0·8	28·0	275	,,
,,	1·2	33·2	326	,,
15:2	0·2	21·7	213	H_2
,,	0·6	21·4	210	,,
,,	0·8	18·1	178	,,
,,	1·2	19·8	195	,,
15:2	0·2	26·6	261	CO
,,	0·6	34·0	334	,,
,,	0·8	38·3	375	,,
,,	1·2	40·0	392	,,

* Sintered at 950°C. Compacting pressure 386 N/mm² (25 tonf/in²).

These results will be discussed more fully with regard to furnace atmospheres, but for the present, they illustrate that in certain cases, the mechanical properties are increased by carbon additions, so that it is unlikely that carbon under these conditions has a detrimental effect upon the sintering process.

The results for 3:2 copper:tin compacts agree reasonably well with those of Barua and Thwaites[25], determined on compacts sintered for 60 minutes at 1000°C in pure H_2. They showed a decrease in final

strength with increasing carbon. This suggested that there is no increased strengthening of the matrix by carbon solution, possibly, they explained, because the extent of sintering is decreased by high carbon content. This cannot be the full explanation, as the results for carbon monoxide sintering show (especially in the case of 15:2 Cu:Sn ratio) that the UTS is raised considerably above that of compacts containing no carbon.

Esper and Zeller[24] could not detect any tin in the iron at copper:tin ratios of 3:1 - 5:1, but the UTS with the 4:1 Cu:Sn ratio was very similar to that obtained with the 3:2 ratio. Therefore it is suggested that α-phase stabilisation by solution of tin in the iron matrix is not the major factor controlling the sintering process. Only at very low Cu:Sn ratios can phase stabilisation occur to any significant extent, and at these tin levels, the brittleness of the tin rich phases nullifies any increase in sintering due to the greater self-diffusion rates of iron in the phase. The results of the low temperature experiment, Fig. 40, show that tin reacts very rapidly with iron particles even at 400°C. With copper present, this wetting of the iron enables the tin to move around the grains of iron more quickly to react with the copper. At 950°C after a short period of time, all of the tin is in the liquid phase with the copper. It is postulated that this interaction of tin with iron and copper delays its diffusion into the iron until complete liquid saturation occurs. Hence a liquid phase with a high iron solubility exists during sintering, and the very much greater rate of mass transfer of iron through the liquid due to this solubility is the major reason for the fast sintering rates associated with this system.

5.3.2. Thermal analysis.

The increased sintering rate associated with the formation of a liquid phase at the sintering temperature depends upon how long the liquid phase remains during the sintering cycle. For a liquid phase to be in equilibrium with the solid phase during sintering then the rate of solution of the solid phase in the liquid must equal the rate of precipitation from the liquid onto the solid. Cases of this type can be found in most metallic systems in which there is a solidus and a liquidus. At some constant temperature between the two, a solid phase can be maintained in equilibrium with a liquid phase.

In the case of the Fe-Cu-Sn ternary system, no data at all was available concerning the phase equilibria. The thermal analysis experiments were designed to determine whether the liquid Cu/Sn phase present during the sintering of these Fe-Cu-Sn compacts remained liquid throughout the sintering process. If the effect of iron solution in the liquid Cu/Sn phase during sintering was to cause solidification of this phase at the sintering temperature, then the sintering process itself would be retarded. Electron probe microanalysis of the Cu/Sn phase present in these compacts showed an iron content never exceeding 15% with Cu:Sn ratios between 3:2 and 15:2. Therefore, the cooling curves of alloys with a Cu:Sn ratio of 3:2 containing up to 15% of iron were studied to determine the effect of the iron additions upon the solidification temperatures. Fig. 41 shows that the cooling of a 60% Cu 40% Sn alloy from 1100°C to room temperature is consistent with what would be expected from the relevant equilibrium diagram. Additions of up to 15% of iron to this system tend to form a ternary eutectic structure which has a melting point even lower than that of the Cu_3Sn

phase. The areas under the cooling curves where they deviate from linearity are proportional to the amount of latent heat evolved, and hence to the amount of liquid present at any given temperature. Because the range of temperature within which this latent heat evolution occurs varies very little with up to 15% of iron present, it may be expected that the liquid produced during heating up of the compacts will remain liquid for the normal sintering times.

5.3.3. Low temperature experiments.

The reactions which occur during the heating up of Fe-Cu-Sn compacts were studied because of their obvious bearing upon the sintering mechanisms involved. A comprehensive study by Esper et. al.(loc. cit.) listed all of the reactions occuring during heating up of Fe-Cu-Sn compacts. The study carried out by the author was to determine the physical effect on liquid distribution of these low temperature reactions, because the sintering process itself depends upon how well disseminated is the liquid phase throughout the iron matrix. With an addition of only 5% Cu+Sn, and porosity levels around 17-18%, there are obviously regions within the compact devoid of direct contact between the iron and the Cu+Sn additions.

Fig. 45 shows that at 400°C, after 5 minutes at temperature, the Cu and Sn are still separate from each other. The copper areas are large, and the tin areas small as shown by the flat plateaus in the electron scans in the former case, and the spikey scans in the latter case. The tin scan does not reach above 50% tin because the size of the tin areas are too small to give an accurate quantitative reading.

At 500°C, some interaction between Cu and Sn occurs shown by the juxtaposition of the two scans, but the reactions do not reach

completion as the relative amounts are not in the added ratio of 60% Cu 40% Sn.

At 600°C, the results are similar after five minutes, but at 700°C it can be seen that tin and copper are associated with each other. The copper trace shows areas which are definitely Cu-rich (60-90% Cu) whereas the tin trace shows no similar tin-rich regions.

The association between Cu and Sn increases at 800°C and 900°C (Figs. 49-50). At 900°C no areas with only one of these constituents present were seen. It is interesting to note that in Fig. 50 (900°C) areas were seen which contained 90% Cu, 7% Sn. This is far removed from the added ratio of 60% Cu 40% Sn. It is also known that after sintering at 950°C for 30 minutes, the intermetallic lakes have a composition close to 60% Cu 40% Sn[31].

The low-temperature experiment illustrated in Fig. 40 gives some indication of why this may be so. Here, 10% tin was added to iron powder and heated to 400°C for 15 minutes. The tin flowed around the iron and considerable reaction had occurred between the iron and the molten tin, causing precipitation of an iron-tin compound as reported by Esper et. al.[24]. The electron scan showed iron within the tin lake. Therefore, if tin reacted with iron to form a solid Fe-Sn compound coating the iron grains, as well as reacting with the copper present in the compacts, then it will take some time at 900°C for the liquid to attain the ratio of 60% Cu 40% Sn because some of the tin is 'locked up' in the surface of the iron grains. Thus, after 5 minutes at 900°C, the lakes analysed at about 90% Cu, 7% Sn, whereas after a maximum of 30 minutes at 950°C, the added ratio of 60% Cu 40% Sn was restored. In conclusion, the tin reaction with iron at

400°C illustrates the wetting effect of tin on iron even at this temperature, enabling the tin to permeate around the grains of the compact. As the temperature rises, the tin reacts more readily with the copper than with the iron until at the sintering temperature, the added Cu:Sn ratio is obtained within the liquid lakes. This further illustrates that no tin enters solution in the iron, and that any tin-iron compounds formed dissolve into the liquid rather than diffuse into the iron.

5.3.4. Additions of pre-alloyed 60% Cu 40% Sn to iron compacts.

Mechanical tests carried out upon compacts containing pre-alloyed Cu/Sn powder showed that equivalent strength levels could be obtained using pre-alloyed material as by using elemental Cu and Sn powders (table 28). These results showed that the initial reactions which occurred upon heating of the compacts had no effect upon the final mechanical properties, and because these properties were indicative of the sintering process itself, it appeared that this was unaffected by the reactions occurring during the heating up period. The high degree of wetting of the iron by the Cu/Sn liquid was undoubtedly responsible for these results.

5.3.5. Wire spool experiments.

The final study of the sintering mechanisms involved was by the use of wire spool models. In this way it was hoped that quantitative information about the sintering process could be obtained. According to Kuczynski[10] a time law for neck growth should be obtained with the exponent n=5 for volume diffusion, or n=7 for surface diffusion if the sintering mechanism was due to α-phase stabilisation, which is a solid-state phenomenon. If, however, the mechanism is that of

dissolution and reprecipitation of iron due to the enhanced solubility of iron in the liquid, then an exponent of n=3 would be expected because this process is directly comparable to that of evaporation and recondensation. Fig. 51 shows that in fact the exponent was indeterminate due to a lack of neck growth at 950°C even after 5 hours. This lack of neck growth may have been due to the effects of iron solution by the liquid copper-tin alloy. If the initial neck contacts formed by winding the iron wire onto the spools were removed by iron solution into the liquid, there would be no re-precipitation in preferred areas to assist in neck growth because of the absence of concave areas of reduced chemical potential for solution.

5.4. Furnace atmospheres and carbon additions.

The regression analysis and early mechanical test results showed that the furnace atmosphere had a critical effect upon the mechanical properties of sintered Fe-Cu-Sn compacts. This could be due to some sintering effect, or due to the higher oxide contents in samples sintered in leaner atmospheres. If the atmosphere affected the sintering rate, it could do so only by affecting the distribution of the liquid phase within the compacts. If, for instance, some leaner atmospheres caused the liquid to de-wet from the iron, then bad mechanical properties would be expected, because sintering would be retarded. The results of porosity measurements on samples sintered in four different atmospheres (table 30) showed that in all cases the majority of the porosity was open, or interconnected. Also, the maximum closed porosity occurred when a pure H_2 sintering atmosphere was used. The worst closed porosity figures were obtained with argon, which has no reducing properties at all.

Porosity levels tended to stay constant whichever atmosphere was used. In fact, one of the advantages of Fe-Cu-Sn sintered compacts is their lack of shrinkage or expansion on sintering (Fig. 29). Shrinkage would be expected if the sintering mechanism was due to iron self-diffusion as proposed by the TRI workers, but not if the mechanism of iron solution and reprecipitation proposed earlier was operative.

The effect of furnace atmosphere upon the mechanical properties illustrated in Table 31 suggests that there may be some correlation between the final oxidation state of the powders used in the experimental work and the mechanical properties. This is confirmed by the oxygen analyses shown below:

Table 44.

Material	Oxygen wt %				
	Untreated	Sint in N_2H_2 at		Sintered in pure H_2 at	
		950°C	1150°C	950°C	1150°C
Powders: Iron (mp 32)	0.28	-	-	-	-
Copper	0.226	-	-	-	-
tin	0.096	-	-	-	-
Compacts:					
Cu:Sn ratio 3:2	-	0.199	0.22	0.135	0.076
Cu:Sn ratio 15:2	-	0.196	0.237	0.132	0.074

It would seem that the 10% H_2 atmosphere is not sufficiently reducing to SnO_2, even at 1150°C, and leaves behind oxide particles that cause a deterioration in the properties of the final sintered compact. Hence the compositions leaner in tin (15:2 Cu:Sn ratio) give better results in the low-hydrogen atmosphere, and the higher tin compositions (3:2 Cu:Sn ratio) better results in pure hydrogen.

5.4.1. SnO and SnO_2 reduction.

The results in Section 4.11.4-5. show that SnO and SnO_2 were completely reduced at 950°C by hydrogen after 30 minutes whereas SnO_2 was not completely reduced by 90% N_2 10% H_2 gas under the same conditions. The associated photomicrographs illustrate the point that SnO_2 can remain within the sintered compact when using an atmosphere of 90% N_2 10% H_2.

The effect of adding either SnO or SnO_2 instead of metallic tin to the compacts prior to sintering was to give mechanical properties directly comparable to those obtained using metallic tin additions, and also the mechanical properties were representative of the last sintering operation to be carried out. For example, Table 39 shows the ultimate tensile strength measured after sintering 3:2 Cu:Sn ratio 95% Fe compacts in pure H_2 for 30 minutes. Re-sintering in various atmospheres gave results characteristic of those atmospheres. This means that the mechanical properties were controlled by the final sintering atmosphere rather than by the initial optimum sintering operation in pure hydrogen.

5.4.2. Mechanical properties of carbon-bearing compacts.

The results in Table 31 are shown graphically in Fig. 55 for the 3:2 and 15:2 Cu:Sn ratio compacts.

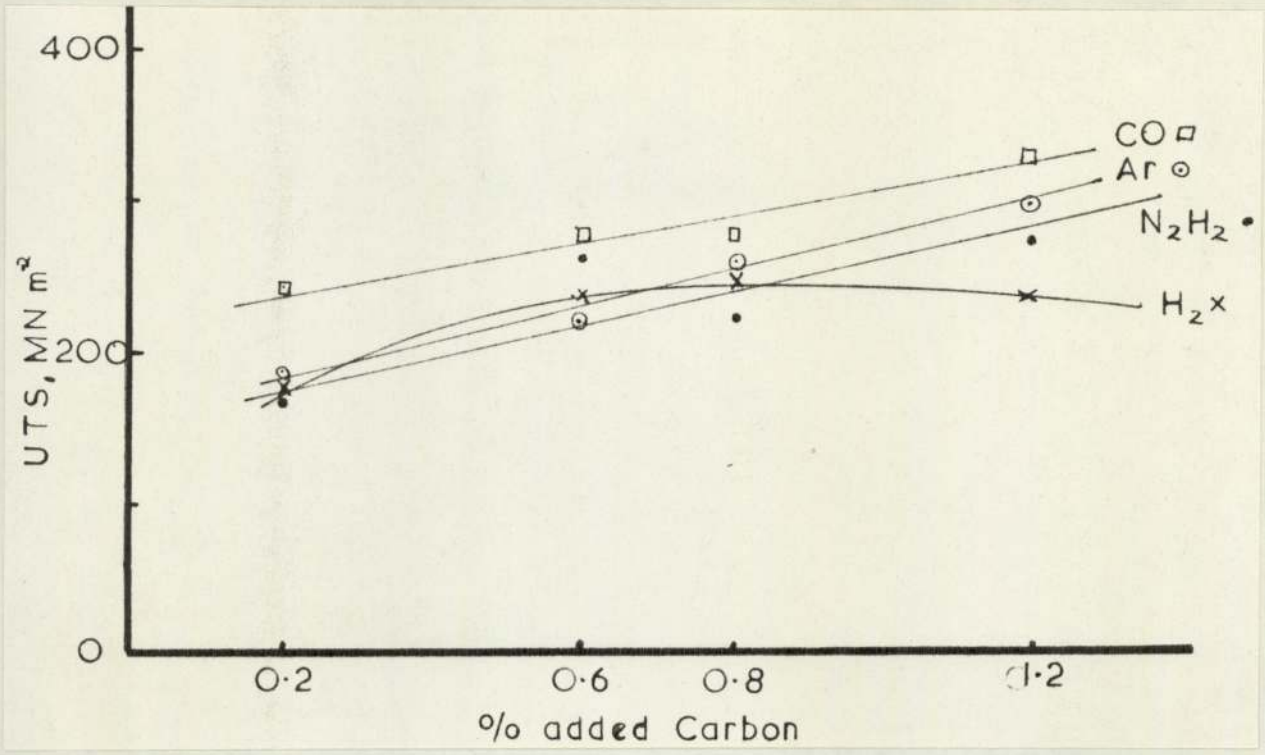
400
200
0
UTS, MN m⁻²
CO
Ar
N₂H₂
H₂
0·2
0·6
0·8
1·2
% added Carbon

Fig. 55

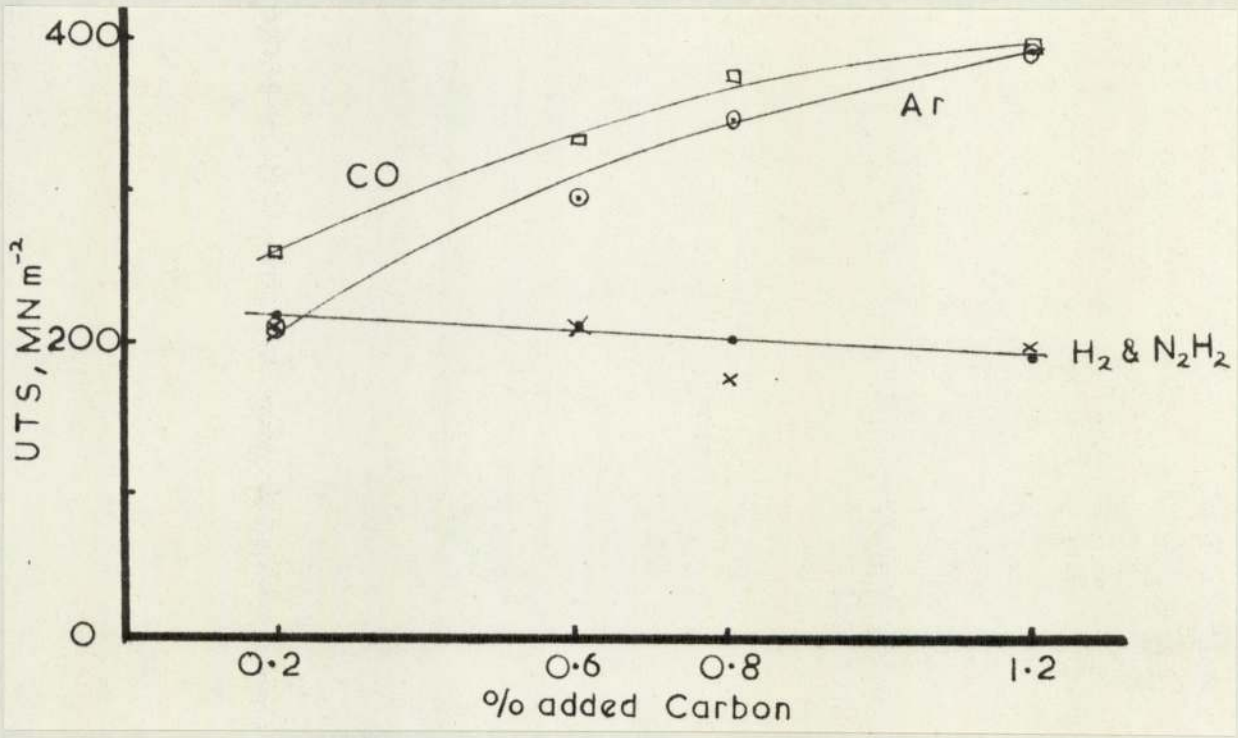
400
200
0
UTS, MN m⁻²
CO
Ar
H₂ & N₂H₂
0·2
0·6
0·8
1·2
% added Carbon

Fig. 56

The results for 3:2 Cu:Sn ratio compacts sintered in H_2 agreed reasonably well with those of Barua and Thwaites(loc. cit.) which showed a decrease in final strength with increasing carbon. These results can be explained with reference to the final oxidation states, and the final carbon levels.

In the case of hydrogen sintering, the strength levels are high due to the efficient removal of all oxides within the compact. Additions of carbon then have little effect upon the strength which is controlled by the embrittling effect of the Cu Sn lakes within the compacts.

In the case of sintering in a 90% N_2 10% H_2 atmosphere where the final oxidation state was higher than the former case, additions of carbon improve the properties because the presence of carbon can reduce any oxides present still further.

The higher strengths of compacts sintered in argon and CO result from the enhanced reducing effect of the carbon present, but also from the higher final carbon contents of these compacts. The graph illustrated below indicates how the final carbon content depends upon the atmosphere employed and the time of sintering:

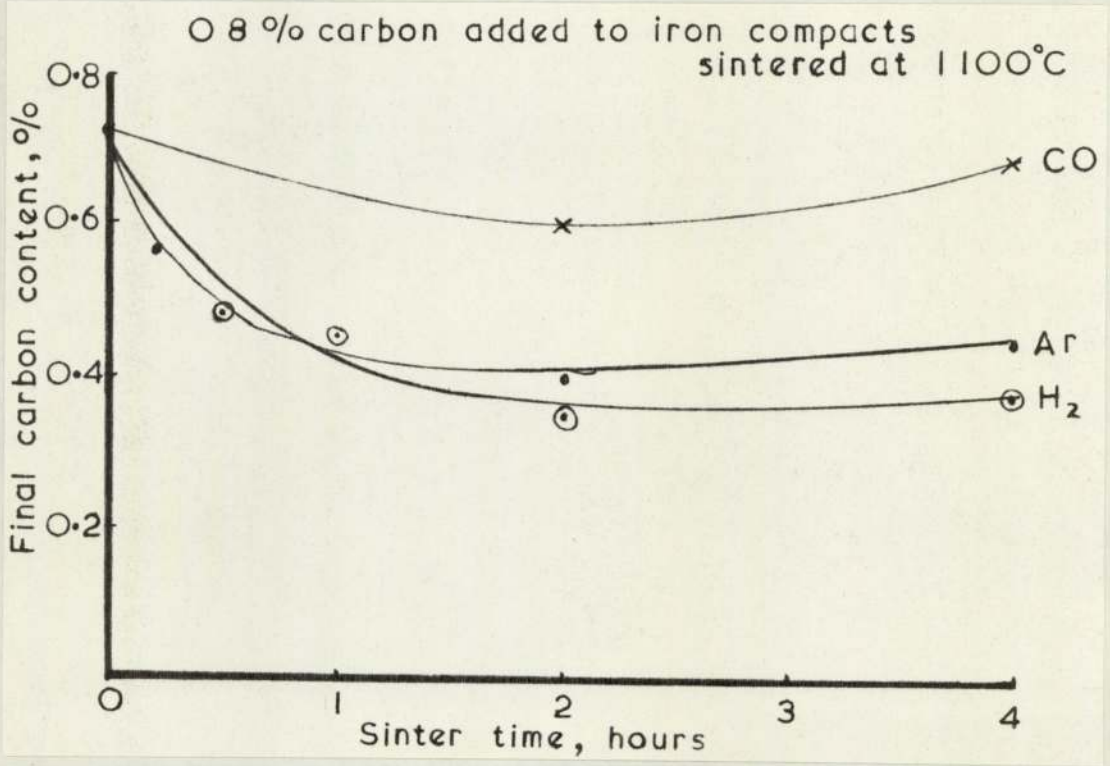

Fig. 57

Hence the compacts sintered in H_2 or N_2H_2 lose their carbon at a greater rate than do those sintered in CO or argon, and high strength levels resulting from the presence of carbon, and its additional reducing effect upon SnO_2 can result only when these atmospheres are used.

5.5. Heat treatment of Fe-Cu-Sn and Fe-Cu-Sn-C compacts.

The short series of experiments concerned with heat treatment of these compacts was designed to assess the effect upon the mechanical properties of quenching and tempering operations. Work carried out by Esper and Zeller(loc. cit.) indicated that a slow cool of $< 10^{\circ}C$/minute after sintering could improve the properties of compacts containing 3% Cu and 2% Sn. Alternatively, tempering treatments of ten hours at $650^{\circ}C$ were necessary to improve the strength to ≥ 30 Kg/mm^2 (294 MN/m^2) and the elongation to $\geq 6\%$. When it is remembered that the two major reasons why the Fe-Cu-Sn powder system is so attractive commercially are

1) A reduction in sintering time to 20 minutes or less

2) A reduction in sintering temperature,

then any prolonged after treatment reduces the advantage of this system over the commonly used alternatives. Therefore it is only reasonable to heat treat these Fe-Cu-Sn alloys if the treatment is short and simple, or if dramatic improvements in the mechanical properties can be obtained.

Esper and Zeller failed to improve the tensile strength of Fe-3% Cu-2% Sn compacts by heat treatment, but managed to raise the ductility to 6% from an 'as-sintered' level of 2% by the treatment described earlier. An alloy of 95% Fe 4% Cu 1% Sn responded slightly better to heat treatment, and quenching from $650^{\circ}C$ caused the elongation to rise from the 'as-sintered' value of 7% to as much as 12%, although the higher ductility results in lower strength.

From these results, it is plain that no significant improvement in mechanical properties was obtained by heat treatment. Increased ductility can be obtained more easily and cheaply by using a 15:2 Cu:Sn ratio 5% addition, and increased strength can be obtained by the addition of carbon, as shown in Tables 31 and 32.

The effect of quenching from the sintering temperature followed by annealing is shown in Table 40 for Fe-Cu-Sn compacts. Maximum strength was obtained using an oil quench with no annealing treatment afterwards. The effect of annealing after the quenching operation was to reduce the UTS and hardness. This was true of both the 15:2 and the 3:2 Cu:Sn ratios. No strength increase above the 'as-sintered' strength levels normally obtained from the Fe-Cu-Sn compacts was obtained.

The results shown in Table 41 for Fe-Cu-Sn-C compacts containing up to 1.2% added carbon show that after quenching the samples are too brittle to yield any reproducible results. The annealing treatment of 500°C for 30 minutes failed to give strength levels in excess of those to be expected in the 'as-sintered' state.

The failure of these simple heat treatment processes to improve the mechanical properties of Fe-Cu-Sn or Fe-Cu-Sn-C compacts is due to the controlling influence of the brittle Cu/Sn phases present upon the fracture of the specimens. If these phases can be made more ductile, then the influence of the hardened iron matrix will become apparent. The 15:2 Cu:Sn ratio compacts are more ductile, and do in fact respond in some cases to heat treatment better than do compacts containing 3% Cu and 2% Sn. Indeed, Esper and Zeller stated that all Fe-Cu-Sn compositions with a Cu:Sn ratio of 3:1 to 9:1 can be carbo-nitrided with some gain in tensile strength.

In conclusion, it was found that heat treatment of Fe-Cu-Sn and Fe-Cu-Sn-C compositions did not improve the mechanical properties of the compacts over the 'as-sintered' properties. In contrast to the heat treatment approach, the use of carbon has been shown to give strength increases in the case of samples sintered in atmospheres other than pure hydrogen of up to 200% without any heat treatment. Therefore the advantages of the Fe-Cu-Sn system, such as short sintering time; reduced sintering temperature; and low alloy addition (25%) can be fully retained by using carbon additions and an atmosphere of the correct carbon potential to maintain the carbon at its added level, rather than by using heat treatment to obtain high strength levels after sintering.

5.6. Suggestions for further work.

The practical value and theoretical significance of the present work would be increased by investigation of the following topics:-

1) Further work on the application of sintering models to this system. If a cold weld of known dimensions instead of point contact could be introduced in the wire spool configuration, then the dissolution effect of the liquid copper/tin alloy would not remove the contacts in the same way as occurs when only point contacts are present. Then the kinetics of neck growth could be studied in a range of furnace atmospheres.

2) The manufacture of specific components using Fe-Cu-Sn and Fe-Cu-Sn-C compacts, and their use in the designed application is really the best way to assess their performance. The use of mechanical tests on tensile specimens, although very useful in the development stage, does not predict accurately the performance of a differently shaped component stressed in a more complex way.

3) Various other alloy systems could be investigated. Using the basis of the iron-copper powder system, and the knowledge that it is the

iron solution rate into the liquid phase during sintering which activates the sintering process, then it may be possible to discover other alloying elements which achieve this end, and also produce an alloy with the copper which has a lower melting point than the copper, and perhaps better ductility than the Cu/Sn alloys.

4) The regression analysis described in this thesis could be carried out more fully to include carbon additions and various other sintering atmospheres. This would make it easier to choose the correct combination of variables to give the desired properties.

Section VI. Conclusions.

6.1. Additions of small amounts of tin to iron-copper compacts reduce the effective sintering temperature and time. Iron with a ten percent addition of Cu + Sn in the ratio of 15:2 sintered at 900°C will produce equivalent strength to iron +10 percent copper sintered at 1100°C.

6.2. Small additions of less than 6% tin to iron compacts improve the sintered properties only when admixed lubricant is added, and the sintering atmosphere is pure hydrogen. The use of 90% N_2 10% H_2 atmosphere and no admixed lubricant causes these tin additions to be detrimental to the mechanical properties of iron compacts.

6.3. The dimensional change of Fe-Cu-Sn compacts upon sintering is less than that of Fe-Cu compacts.

6.4. Tin reacts with iron even at 400°C, and this reaction helps the tin wet the iron, and so come into contact with the copper particles during the heating up of the compacts. During heating, the tin reacts mainly with the iron at low temperatures, but forms a liquid phase with the copper at sintering temperatures.

6.5. The intermediate reactions which occur upon heating Fe-Cu-Sn compacts have little effect upon the final mechanical properties.

6.6. Both copper and tin separately will diffuse into iron at normal sintering temperatures. When they are added together to iron, however, their diffusion into the iron is limited.

6.7. The solubility of iron in the liquid Cu-rich phase during sintering increases with the tin content of that liquid phase, enabling a higher rate of mass transfer of iron through the liquid phase.

6.8. No evidence of stabilisation of the α-phase during sintering of

Fe-Cu-Sn compacts has been detected except in the case of tin-rich Cu:Sn ratio additions, and pure tin additions. Cu:Sn ratios of 3:2 and 15:2 do not exhibit any signs of α-phase stabilisation when sintered at 900-1100°C.

6.9. The major reason for the increased sintering rates observed in the Fe-Cu-Sn system is the presence of a low melting point liquid phase with a greater solubility for iron than has copper on its own. The rapid process of dissolution, and re-precipitation of iron in regions of lower chemical potential can then occur.

6.10. The liquid phase formed during sintering remains liquid during normal sintering times.

6.11. The lower sintering temperatures bring economies not only from reduced heating costs but also from longer furnace-belt life and lower maintenance costs.

6.12. The elongations obtained with 15:2 Cu:Sn ratio additions to iron compacts are generally of the same order as those expected with sintered iron-copper alloy compacts.

6.13. Additions of zinc stearate as an admixed lubricant improve the mechanical properties of Fe-Cu-Sn compacts by increasing the green density for a given compaction load, and hence the number of iron-to-iron contacts established during compaction.

6.14. The choice of sintering atmosphere is of the utmost importance in controlling the sintered properties of Fe-Cu-Sn compacts, and there is a correlation between the final oxidation states of the compacts and the final mechanical properties.

6.15. The choice of Cu:Sn ratio employed is of equal importance as the above in controlling the mechanical properties of Fe-Cu-Sn compacts. High tin ratios respond best to highly reducing atmospheres, whereas lower tin ratios respond best to the leaner atmospheres, or inert

atmospheres.

6.16. The addition of carbon increases the strength of Fe-Cu-Sn compacts when sintered in atmospheres which do not react with the carbon.

6.17. Quenching and tempering operations carried out upon Fe-Cu-Sn and Fe-Cu-Sn-C sintered compacts do not improve the mechanical properties over the 'as-sintered' properties due to the brittleness of the Cu/Sn compound present within the compacts which controls the fracture mechanisms involved.

6.18. The mechanical properties required from Fe-Cu-Sn or Fe-Cu-Sn-C compacts can be controlled to a large degree by judicious choice of Cu:Sn ratio, sintering atmosphere, and carbon addition, whilst retaining the advantages of short sintering time, lowered sintering temperature, and closer dimensional tolerances.

Appendix 'A'

Phase Equilibrium Diagrams

Fe-Sn

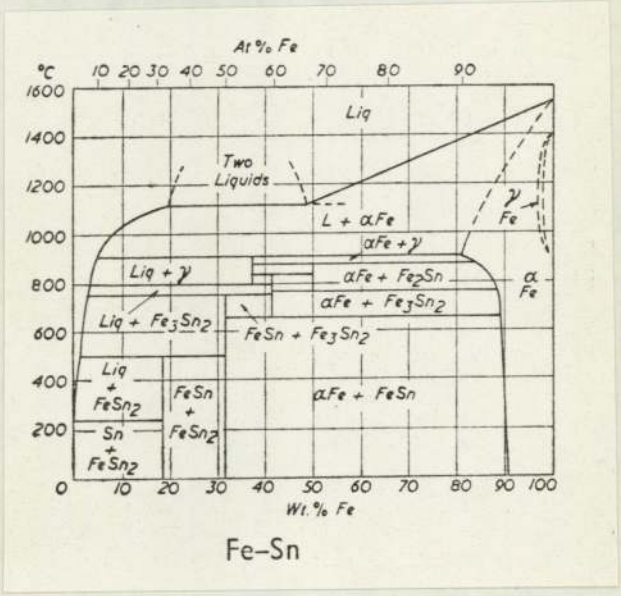

Fe-Sn

Fe-Cu

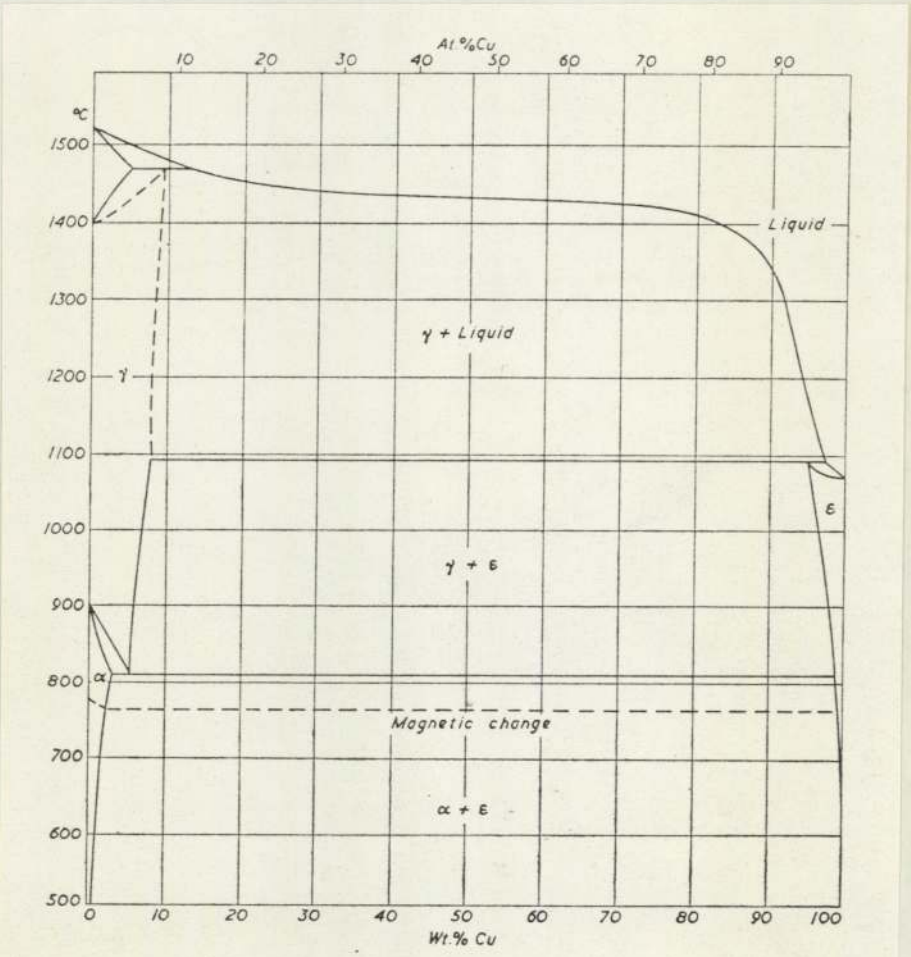

Cu-Fe

Cu-Sn

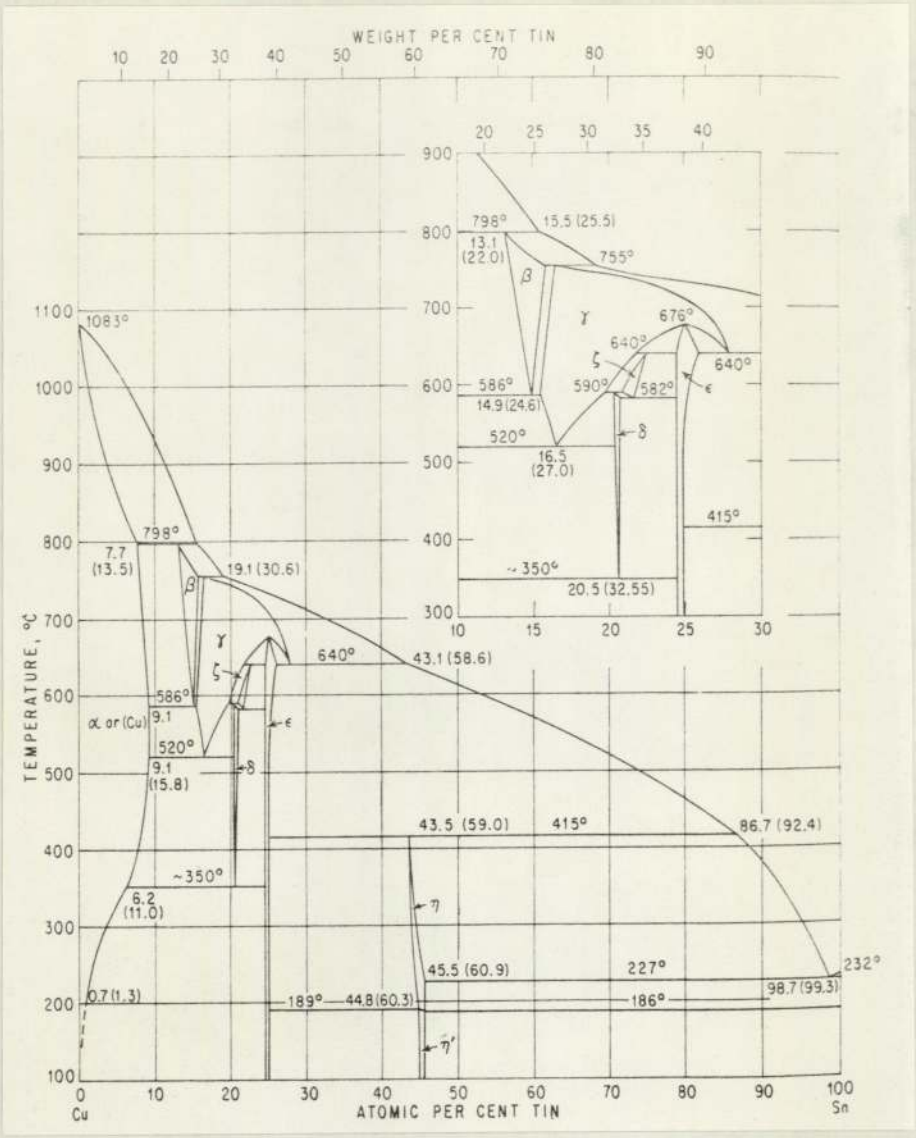
WEIGHT PER CENT TIN
10 20 30 40 50 60 70 80 90
20 25 30 35 40
900
800
700
600
500
400
300
1100
1000
900
800
700
600
500
400
300
200
100
1083°
798°
7.7
(13.5)
19.1 (30.6)
β
γ
ζ
640°
43.1 (58.6)
586°
9.1
α or (Cu)
520°
9.1
(15.8)
δ
ε
43.5 (59.0)
415°
86.7 (92.4)
~350°
6.2
(11.0)
η
45.5 (60.9)
227°
232°
0.7 (1.3)
189°
44.8 (60.3)
186°
98.7 (99.3)
η'
798°
15.5 (25.5)
13.1
(22.0)
755°
676°
640°
640°
590°
582°
586°
14.9 (24.6)
520°
16.5
(27.0)
δ
415°
~350°
20.5 (32.55)
TEMPERATURE, °C
0 10 20 30 40 50 60 70 80 90 100
Cu
ATOMIC PER CENT TIN
Sn

Appendix 'B'

Manipulation of the data for regression analysis

In multiple regression, it is assumed that we have a 'dependent' variable Y which is 'dependent' upon p 'independent' variables X_1, X_2, ... X_p such that each Y value, Y_i can be expressed as follows:

$$Y_i = \alpha + \beta_1 x_{1i} + \beta_2 x_{2i} + \cdots \beta_p x_{pi} + \epsilon_i$$

where $\alpha, \beta_1, \beta_2 \cdots \beta_p$ are parameters and the $x_{1i}, x_{2i}, \cdots x_{pi}$ are known. The ϵ_i are observations on a random variable, independent of the X's, and takes the form of factors not otherwise accounted for. This equation is linear such that Y is a sum of products of parameters, known functions of the X's, and an error. The partial regression coefficients β_1, β_2, ... β_p show how much influence each X variable has on Y in units of the original data.

The results were put into the following form for the computer:

The Tin Research Institute procedure or powder was indicated by the numeral 1, and the University of Aston procedure or powder by the numeral 2, so that the following table was obtained.

The dependent variable was chosen to be the ultimate tensile strength. The independent variables were then the powders used, the mixing and pressing technique, the sintering procedures, the two gas atmospheres, the Cu:Sn ratios, the sintering temperature, and finally the second order variables obtained by multiplying any two of the above together The number of degrees of freedom was 36. The variables in the regression set were as follows:

Mixing and pressing	regression coefficient = + 9.0647
Gas atmosphere	= -29.0728

Cu:Sn ratio	= -9.5098
(Mixing and pressing) x (sinter)	= -3.1724
(Sinter) x (Cu:Sn ratio)	= +4.6413
(Gas atmosphere) x (temperature)	= +0.0175

All other variables were rejected from the set. The intercept term was 23.1249.

Then for the general equation:

$$Y = \alpha + \beta_1 x_1 + \beta_2 x_2 + \cdots \beta_p x_p$$

the X's can have the value of 1 or 2 as set out in the table. The only exception is for the variable containing the temperature term, which is retained in units of deg Centigrade

	Powder	Mix/ Press	Sinter	Gas Atm.	Cu:Sn ratio	Temp °C	UTS
TRI:	1	1	1	$H_2 \equiv 1$	3:2 ≡ 1	950	Kg/mm^2
U/A:	2	2	2	$N_2H_2 \equiv 2$	15:2 ≡ 2	1150	
	1	1	1	1	1	950	22.30
	1	1	1	1	1	1150	20.30
	1	1	1	1	2	950	15.90
	1	1	1	1	2	1150	20.10
	1	1	2	2	1	950	10.75
	1	1	2	2	1	1150	15.00
	1	1	2	2	2	950	16.00
	1	1	2	2	2	1150	21.60
	1	2	2	2	1	950	10.10
	1	2	2	2	1	1150	16.10
	1	2	2	2	2	950	17.90
	1	2	2	2	2	1150	26.10
	2	2	2	2	1	950	6.60
	2	2	2	2	1	1150	16.40
	2	2	2	2	2	950	20.60
	2	2	2	2	2	1150	27.30
	2	2	1	1	1	950	23.00
	2	2	1	1	1	1150	24.30
	2	2	1	1	2	950	23.30
	2	2	1	1	2	1150	26.00
	2	1	1	1	1	950	10.70
	2	1	1	1	1	1150	12.20
	2	1	1	1	2	950	15.20
	2	1	1	1	2	1150	18.20
	2	2	2	1	1	950	23.00
	2	2	2	1	1	1150	24.60
	2	2	2	1	2	950	21.00
	2	2	2	1	2	1150	29.10
	2	1	2	1	1	950	17.75
	2	1	2	1	1	1150	19.23
	2	1	2	1	2	950	17.80
	2	1	2	1	2	1150	24.18
	2	1	2	2	1	950	8.22
	2	1	2	2	1	1150	18.00
	2	1	2	2	2	950	14.58
	2	1	2	2	2	1150	22.98
	1	2	1	1	1	950	20.08
	1	2	1	1	1	1150	24.05
	1	2	1	1	2	950	16.00
	1	2	1	1	2	1150	22.40
	1	2	1	2	1	950	15.30
	1	2	1	2	1	1150	21.50
	1	2	1	2	2	950	13.90
	1	2	1	2	2	1150	21.50

Acknowledgements

The author wishes to thank his supervisor, Dr. J.C. Billington, for all the encouragement and helpful advice given during the course of this work.

Thanks are also due to Dr. D.A. Robins and Mr. P.A. Ainsworth for the helpful discussions and experiments carried out within their organisation.

Grateful acknowledgements are made to all members of the academic and technical staff of the Metallurgy Department for their advice throughout the duration of the experimental work.

References

1. F. Sauerwald, Kolloid Z., 1943, 104, 144.
2. J. Frenkel, J. Physics (U.S.S.R.), 1945, 9, 385.
3. Pines, Zhur, Tekhn. Fiziki, 1956, 26, 2,100.
4. F. Thummler, Planseeber. Pulvermet., 1958, 6, 2.
5. W.D. Kingery, 'Kinetics of High-Temperature Processes', p. 187, 1959: New York and London (John Wiley).
6. W.D. Kingery, J. Appl. Physics, 1959, 30, 301.
7. W.D. Kingery and M.D. Narasimhan, ibid., 1959, 30, 307.
8. W.D. Kingery, E. Niki and M.D. Narasimhan, J. Amer. Ceram. Soc., 1961, 44, 29.
9. G.C. Kuczynski, Trans. Amer. Inst. Min. Met. Eng., 1949, 185, 169.
10. G.C. Kuczynski, 'Powder Metallurgy' (edited by W. Leszynski). 1961: New York and London (Interscrience Publishers).
11. F. Thummler and W. Thomma, Metallurgical Reviews no. 115. vol. 12, 1967, p. 69.
12. F. Eisenkolb and I. Kalning, Wiss. Z. tech. Hochschule Dresden, 1956-57, 6, (1), 125-134.
13. G. Matsumura, Int. J. Powder Met., 5, (2), 1969.
14. G.A. Geach and F.O. Jones, 'Metallographic Study of the Sintering Process', Research 2, 493-4, (1949).
15. B.H. Alexander and R.W. Balluffi, Acta Met., 1957, 5, (11), 666-77.
16. H.F. Fischmeister and R. Zahn, 'Modern Dev. in Powder Metallurgy" vol. 2, ed. H. Hausner, p. 12. Plenum Press N.Y. 1966.
17. J. Bacmann and G. Cizeron, Int. J. Powder Met., 5, (2), 1969, p.55.
18. Coult and Munro, Powder Met., 1970, vol. 13, no. 26.
19. M. Eudier, 'Symposium on Powder Met., 1954', (Special report no. 58), p. 59, 1956, London (ISI).

20. A.D. Shelmerdine and D.A. Robins. JISI, 1965, 205, (1) 40.

21. R. Duckett and D.A. Robins, Metallurgia, 1966, 74, 163.

22. S.K. Barua, P.A. Ainsworth, and D.A. Robins. Metallurgia, 1969, 80, 87.

23. B.F. Dyson, Trans. AIME, 1963, 227, 1098.

24. F.J. Esper, K.H. Friese and R. Zeller. Int. J. of Powder Met., 1969, 5, (3), 19.

25. S.K. Barua and C.J. Thwaites, Metall, 1970, 24, (5), 460.

26. F.J. Esper and R. Zeller, Powder Metallurgy, 1971, 311.

27. F.J. Esper and R. Zeller, Powder Metallurgy International, 1972, 4, 1.

28. J.C. Billington, C. Fletcher and P. Smith, Powder Metallurgy, 1973, vol. 16, no. 32, 327.

29. P. Smith, Undergraduate thesis, 1971.

30. I.M. Coult and A.J. Munro, Powder Met., 1970, 13, No. 26, 295.

31. J.B. Long and D.A. Robins, 'Mod. Dev. in Powder Met.', vol. 4, 303, 1971: New York (Plenum Press).

32. L.H. Fairbank and L.G.W. Palethorpe, 'Heat Treatment of Metals', (Special Rep. no. 95), p. 57, 1966: London (Iron & Steel Inst.).

Ph.D. 1974

IRON–COPPER–TIN SINTERED COMPACTS*

J. C. Billington,† C. Fletcher,† and P. Smith†

A wide range of copper and tin powder additions to iron powder sintered compacts has been studied. From mechanical-property tests it has been shown that when using sintering temperatures of 900–1100°C in nitrogen/10% hydrogen atmospheres there is an optimum copper:tin ratio of 15:2. The mechanical properties obtained from compacts pressed from iron mixed with 4% copper+tin in this ratio and sintered at 900°C were similar to those obtained from iron–10% copper powder compacts sintered at 1100°C. Moreover, the iron–copper–tin components showed improved dimensional accuracy.

In a further series of experiments, it was shown that tin additions to iron–copper alloy compacts increased the solubility of iron in the liquid phase at the sintering temperature and simultaneously decreased the rate of diffusion of copper into the iron particles. At the same time, tin improved the wettability of the liquid, reducing its surface tension and allowing it to disperse more completely throughout the matrix. The mechanical properties of compacts containing larger amounts of tin were decreased by the presence of brittle compounds, although the sintering rate was increased. It is concluded that the optimum properties of iron–copper–tin compacts are obtained by making correct additions of copper and tin to the iron powder and giving careful consideration to the sintering atmosphere.

THIS work was put in hand to confirm and extend the results obtained by Robins *et al.*[1,2] and Esper *et al.*[3,4]. It was shown by these workers that improved mechanical properties could be obtained with much lower sintering temperatures by the addition of tin to iron and iron–copper powder compacts. It was suggested by Barua, Ainsworth, and Robins[2] that an addition to iron of 5% of mixed powders having a copper–tin ratio of 3:2 gave the maximum strength in compacts sintered at 950°C. Esper and his co-workers agreed with these general conclusions but suggested that a higher copper to tin ratio (4:1) could be almost as effective. This is industrially very significant when the relative prices of tin and copper are considered (~£1735 and £675/tonne respectively). It was the aim of the present work to examine a much wider range of copper:tin ratios and total additions and to make a theoretical study of some of the mechanisms involved in the sintering processes.

* Manuscript received 7 May 1973. Contribution to a Symposium on 'PM Alloys and Properties', to be held in Eastbourne on 19–21 November 1973.

† Department of Metallurgy, University of Aston in Birmingham.

I. Some Physical Properties of Fe–Cu–Sn Sintered Compacts

Experimental Procedure

The powders used were −100 mesh (~152 μm) MP 32 iron powder, −100 mesh and −300 mesh (~53 μm) atomized copper powder, and −300 mesh tin powder.

Mixing was carried out either in glass jars for small quantities of powder (<500 g), or in a double-cone mixer for larger quantities. No lubricant was added to the powder during mixing.

Samples weighing ~20g were pressed in a BS 2590 die at 470 N/mm² (30 tonf/in²). The die was lubricated with a 2% solution of stearic acid in ether. The density of the green compacts produced was ~6·8 g/cm³.

Sintering was carried out in a horizontal tube furnace of 80 mm dia., one end of the tube being water-cooled to increase the cooling rate of the compacts after sintering. The temperature was controlled to ±5 deg.C. Compacted samples were pulled into the hot zone directly without the pretreatment needed for powder lubricated with stearic acid.

The furnace atmosphere was a 90/10 nitrogen–hydrogen mixture, approximating to an industrial type of atmosphere. Before the gas entered the furnace it was passed over a catalyst, which caused any oxygen present to react with the hydrogen to form water vapour. This was then removed by silica gel and magnesium perchlorate. The dew-point of the gas entering the furnace was always <244 K (−29°C).

Results

Fig. 1 shows that increasing additions of tin to compacts sintered at 900 and 1100°C produced a rapid decline in UTS. All samples were very brittle and elongations were not measurable. These results are valid only for the experimental conditions described but, as will be shown in the discussion, later work has demonstrated that the properties of sintered compacts containing 2 and 6% tin can be considerably improved by including stearic acid as a powder lubricant.

Additions of −100 mesh copper (~152 μm) produced only a marginal increase in UTS when sintering at 900°C, but after the temperature was raised to 1100°C a marked increase was found. When −300 mesh copper (~50 μm) was used a further increase of up to 40 N/mm² was observed in the UTS at 1100°C.

Fig. 2 shows that at 900°C copper additions had very little effect on the dimensional change while at 1100°C they produced a large expansion. Additions of −300 mesh tin caused expansion of compacts sintered both at 900 and 1100°C. The degree of expansion was always less than half that produced in compacts containing an equivalent addition of copper.

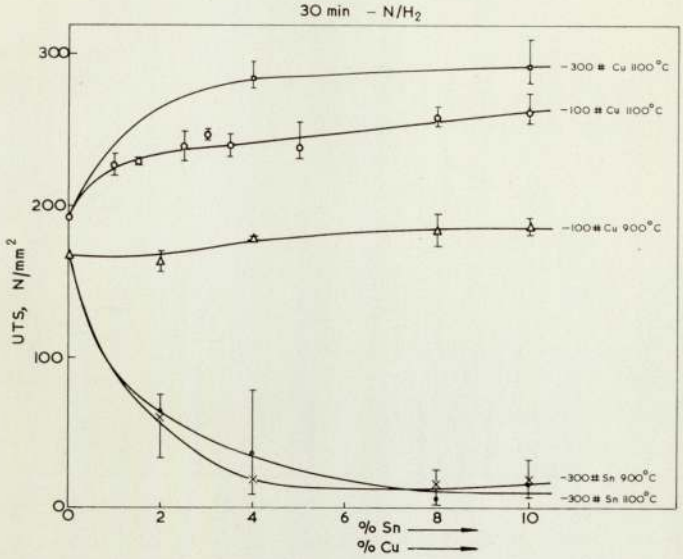

FIG. 1. UTS vs. individual copper and tin additions for samples sintered for ½ h.

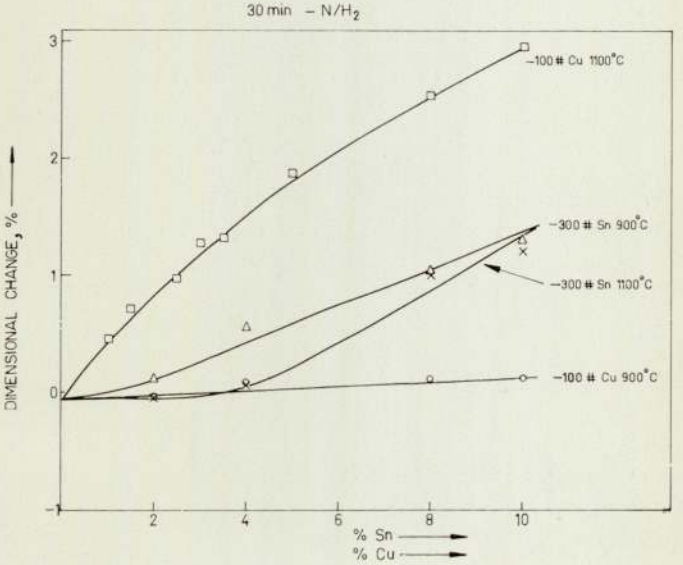

FIG. 2. Dimensional change vs. individual copper and tin additions for samples sintered for ½ h.

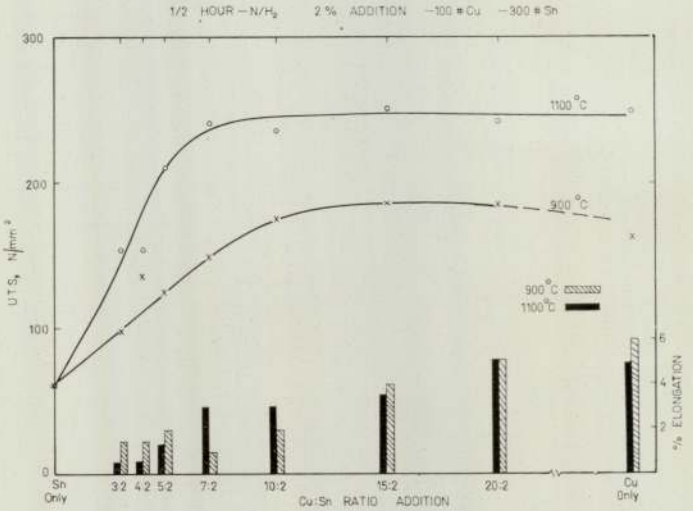

FIG. 3. UTS and elongation % vs. Cu:Sn ratio for 2% alloy addition of −100 mesh Cu and −300 mesh Sn powder after sintering for ½ h at 900 and 1100°C.

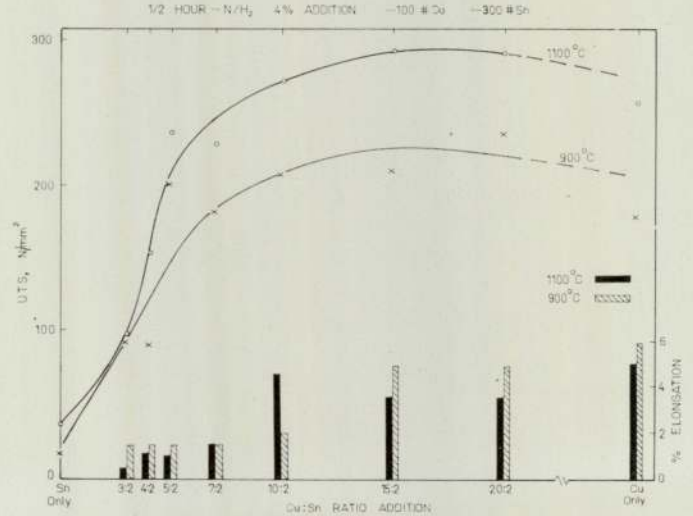

FIG. 4. UTS and elongation % vs. Cu:Sn ratio for 4% alloy addition of −100 mesh Cu and −300 mesh Sn powder after sintering for ½ h at 900 and 1100°C.

The effects of adding copper and tin together when sintering at 900 and 1100°C are shown in Figs. 3–6 for 2, 4, 8, and 10% total additions. With 2% addition no increase is seen in the UTS when the Cu:Sn ratio exceeds 10:2. For the 4, 8, and 10% additions, a maximum UTS was obtained at a Cu:Sn ratio of 15:2. The difference in the maximum UTS found with additions of 4 and 10% is only ~10 N/mm² at 1100°C. There is also no sudden decrease in UTS on either side of the optimum ratio. At 900°C there was, however, a significant difference in the maximum UTS obtained for different total alloy additions (187–270 N/mm²).

Iron powder with no copper or tin additions when sintered at 1100°C for ½ h had a UTS of 195 N/mm², while with an addition of 4% of 15:2 copper–tin it developed a UTS of 300 N/mm², an improvement of 54%. At 900°C, iron powder with no additions gave a UTS of 167 N/mm² and the maximum UTS produced by adding 10% of 15:2 copper–tin was 270 N/mm², an increase of >65%.

All samples having a copper–tin ratio of <7:2 behaved in a brittle manner, which was reflected in the low elongation results and the wide scatter shown in the UTS results. Iron without any additions showed elongations of 4 and 6% at 900 and 1100°C, respectively.

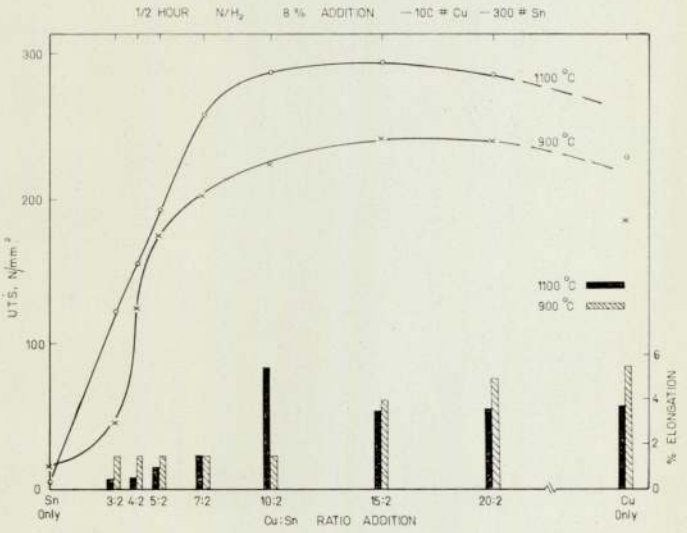

FIG. 5. UTS and elongation % vs. Cu:Sn ratio for 8% alloy addition of —100 mesh Cu and —300 mesh Sn powder after sintering for ½ h at 900 and 1100°C.

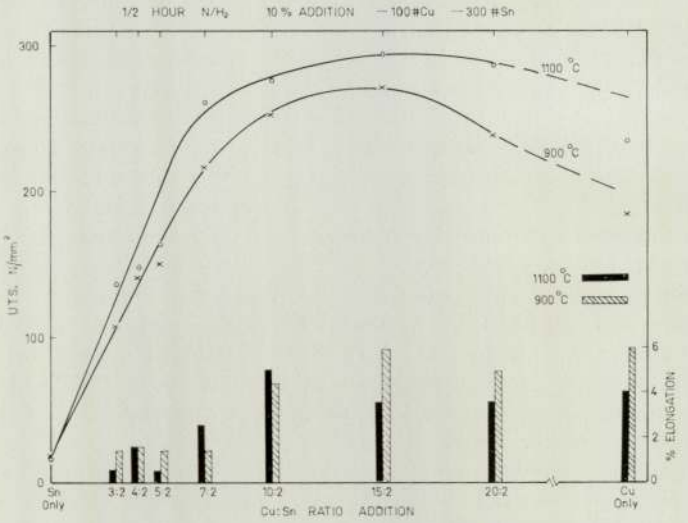

FIG. 6. UTS and elongation % vs. Cu:Sn ratio for 10% alloy addition of −100 mesh Cu and −300 mesh Sn powder after sintering for ½ h at 900 and 1100°C.

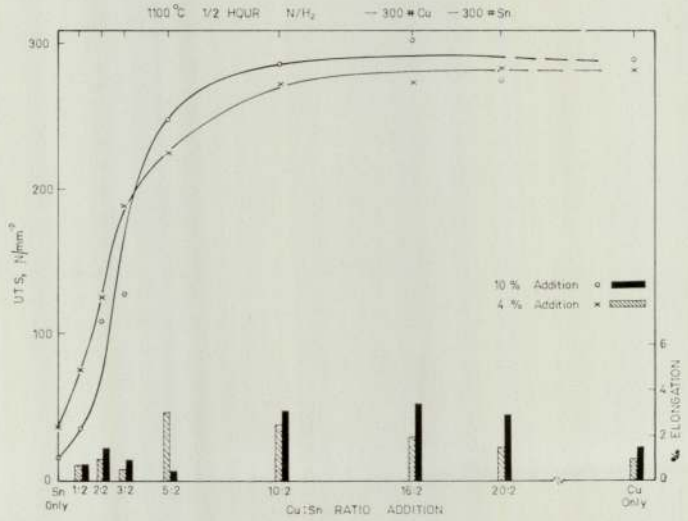

FIG. 7. UTS and elongation % vs. Cu:Sn ratio for 4% and 10% alloy additions of −300 mesh Cu and −300 mesh Sn powder after sintering for ½ h at 1100°C.

The effect of reducing the particle size of the copper to that of the tin (−300 mesh) is shown in Fig. 7. The same maximum value of UTS (within the limits of experimental error) was obtained at a copper–tin ratio of 15:2. The curves follow each other quite closely in shape but the use of −300 mesh copper appears to offset the marked decrease in UTS seen at low copper–tin ratios.

Elongation results followed a similar pattern except that the addition of −300 mesh copper powder alone produced lower elongations than the corresponding −100 mesh additions.

The effects of copper–tin additions on the dimensional accuracy are shown in Figs. 8–10. For the 8 and 10% total alloy additions a minimum growth is observed at 3:2 and 7:2 copper:tin ratios sintered at 900 and 1100°C, respectively. The size of the copper powder used had no appreciable effect on the dimensional change as can be seen from the 4 and 10% curves for −300 mesh copper and tin; these follow very closely the curves for −100 mesh copper and −300 mesh tin.

Fig. 11 shows the effect of sintering temperature on the UTS in the range 800–1150°C for a 15:2 copper–tin ratio. At temperatures above 1050°C there is no significant difference in UTS between the 4 and 10% alloy additions confirming the results shown in Figs. 4 and 6. The corresponding dimensional changes are shown in Fig. 12.

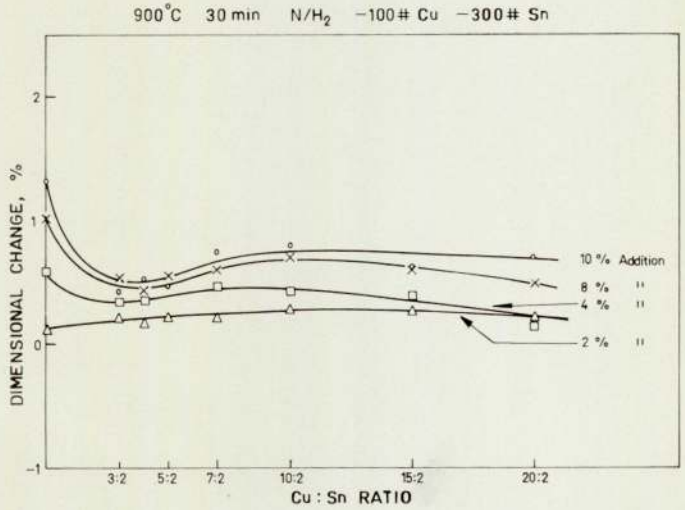

FIG. 8. Dimensional change vs. Cu:Sn ratio for 2, 4, 8, and 10% alloy additions of −100 mesh Cu and −300 mesh Sn powder after sintering for $\frac{1}{2}$ h at 900°C.

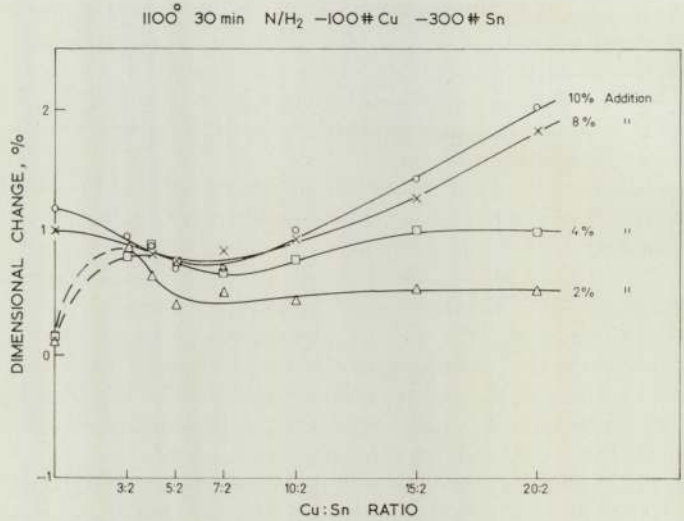

FIG. 9 Dimensional change vs. Cu:Sn ratio for 2, 4, 8, and 10% alloy additions of −100 mesh Cu and −300 mesh Sn powders after sintering for ½ h at 1100°C.

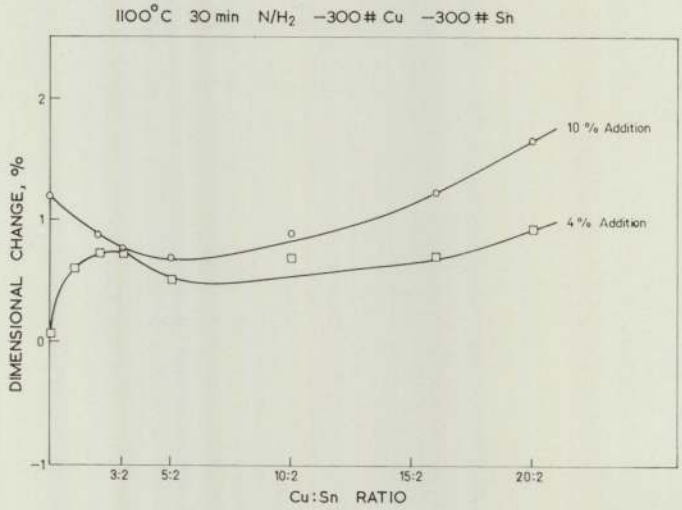

FIG. 10. Dimensional change vs. Cu:Sn ratio for 4 and 10% alloy additions of −300 mesh Cu and −300 mesh Sn powders after sintering for ½ h at 1100°C.

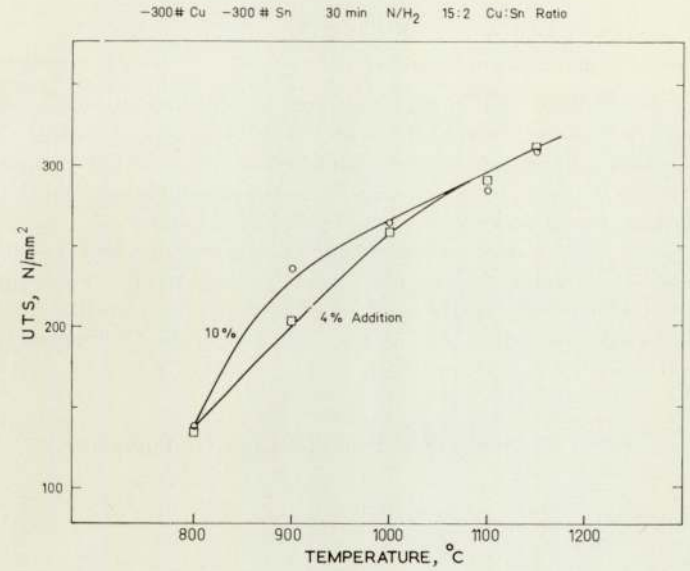

FIG. 11. UTS vs. temperature for 4 and 10% alloy additions of 15:2 Cu:Sn (−300 mesh Cu, −300 mesh Sn) powder after sintering for ½ h.

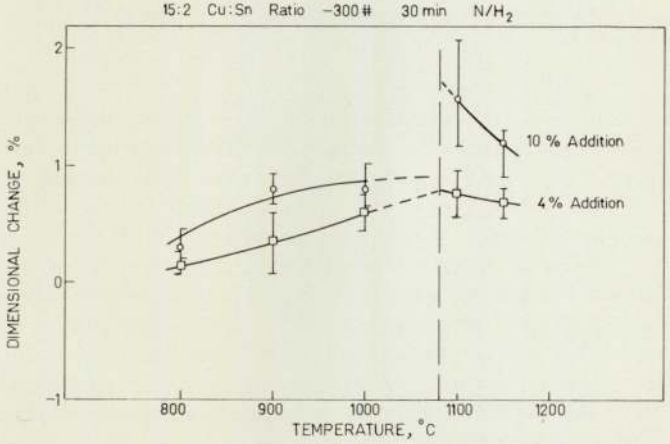

FIG. 12. Dimensional change vs. temperature for 4 and 10% alloy additions of 15:2 Cu:Sn (−300 mesh Cu, −300 mesh Sn) powders after sintering for ½ h.

Discussion

Addition of Copper and Tin Separately

The results illustrated in Fig. 1 for pure tin additions are at complete variance with those obtained by Robins *et al.*[1,2] and Esper *et al.*[3,4] No explanation for the apparent disastrous effect of tin added separately to iron can be given, but it may be due to the precipitation of an Fe–Sn compound during cooling, as suggested by Esper *et al.*[3] No metallographic evidence of iron–tin intermetallic compounds has however, been observed in samples sintered for $\frac{1}{2}$ h at 900 or 1100°C. Subsequent work, in which 0·5% stearic acid in ether was added at the powder mixing stage, has given the results shown in Table I, (compacting pressure 386 N/mm^2 (25 tonf/in^2)).

TABLE I. **Strength of Iron and Iron–Tin Compacts**

Compact Composition	Sintering Atmosphere*	UTS, N/mm^2
Fe only	N_2+10% H_2	164, 175
Fe+2% Sn	,,	124, 187
Fe+6% Sn	,,	63·8, 67·3
Fe only	Pure H_2	170, 164
Fe+2% Sn	,,	269, 267
Fe+6% Sn	,,	137, 102

* Sintered for $\frac{1}{2}$ h at 1000°C after burn-off for 10 min at 400°C.

These results confirm that tin under certain conditions does improve the strength of iron sintered compacts as previously reported by Robins and Esper. They also illustrate the effects both of stearic acid additions and of gas atmosphere on the final properties.

The addition of copper to compacts sintered at 1100°C (Fig. 1) produced an increase in strength because the sintering rate was increased by the presence of a liquid phase and also because of the solid-solution-strengthening effect of copper in iron. The finer copper powder addition produced a greater strengthening effect than the coarse copper owing to its greater dissemination and therefore improved effectiveness.

The very slight improvement in strength of compacts containing −100 mesh Cu sintered at 900°C, at which temperature the mechanism is solid-phase sintering, is due to the solid-solution-strengthening of the small amount of copper that was able to diffuse into the iron.

Simultaneous Additions of Copper and Tin

The increase in strength produced by the addition of tin to the copper (Figs. 3–7) is probably the result of increased sintering rate. As will be shown in Part II, tin wets the iron particles at a relatively low temperature, thus assisting the copper–tin alloy to flow around the iron grains as soon as it becomes molten. The rapid fall-off in strength at low copper:tin ratios is probably due to the high tin content and to the operation of the embrittling mechanisms described earlier.

The absence of any increase in maximum UTS when the total addition is increased beyond 4% when sintering at 1100°C (Figs. 4–6) would indicate that this addition produces the optimum volume of liquid required to aid sintering.

At 900°C, however, not all the copper is dissolved by the tin (Figs. 3–6) and the volume of liquid present at the sintering temperature is thus only a fraction of the total alloy addition. Consequently it is suggested that with larger total alloy additions more liquid phase will be present and this will lead to increased strength.

The results, which show no major changes in UTS when the copper particle size is changed, at about the optimum Cu:Sn ratio (Fig. 7), indicate that when the copper becomes molten it flows easily and alloys with the tin present. For samples with low Cu:Sn ratios the use of finer copper particles tended to push the curve towards the left. Since there is then considerably more tin present, there is less chance of tin particles being left unalloyed or incompletely alloyed.

All the work reported demonstrates that optimum mechanical properties were obtained with a Cu:Sn ratio of 15:2, using a gas atmosphere of nitrogen/10% hydrogen for sintering. This Cu:Sn ratio was much higher than that suggested by the Tin Research Institute (3:2) for compacts made in a sintering atmosphere of pure hydrogen. This also differs substantially from the ratios recommended by Esper, Friese, and Zeller who showed that they varied, according to sintering temperature, from pure tin to 7:2 Cu:Sn. This effect of atmosphere is further illustrated in Table II where the two atmospheres are compared for unlubricated powder mixtures compacted at 386 N/mm^2 (25 tonf/in^2).

These results agree well within experimental error with the other reported work and suggest that some correlation may exist between the mechanical properties and the final oxidation state of the powders used in the experimental work. This is confirmed by the oxygen analyses reported in Table III.

It would seem that the 10% hydrogen atmosphere is not sufficiently reducing to SnO_2, even at 1150°C, and leaves behind oxide particles that cause a deterioration in the properties of the final sintered compact.

TABLE II. **Ultimate Tensile Stress (N/mm²) of Fe–Cu–Sn Powder Compacts Sintered for ½ h with No Low-Temperature Burn-Off Period**

Sintering Temperature, °C	Atmosphere	UTS, N/mm²			
		Cu:Sn Ratio			
		1:1	3:2	10:2	15:2
950	10% H_2/N_2	15·9	65	199	202
	Pure H_2	105	226	218	206
1150	10% H_2/N_2	—	161	—	268
	Pure H_2	—	241	—	288

TABLE III. **Oxygen Analyses of Powders and Sintered Compacts**

Material	Oxygen, wt.-%				
	Untreated	Sintered in N_2/10% H_2 at		Sintered in pure H_2 at	
		950°C	1150°C	950°C	1150°C
Powders: Iron (M.P. 32)	0·28	—	—	—	—
Copper	0·226	—	—	—	—
Tin	0·096	—	—	—	—
Compacts: Cu:Sn ratio 3:2	—	0·199	0·22	0·135	0·076
Cu:Sn ratio 15:2	—	0·196	0·237	0·132	0·074

The use of stearate lubrication by Esper *et al.* could be contributory to subsequent reduction in producing a deposition of carbon by its breakdown during the burn-off period.

Co-operative work with the Tin Research Institute on gas-atmosphere effects is currently in progress.

Dimensional Change with Pure Copper and Pure Tin Additions

The shape of the curves relating dimensional change with metal addition (Fig. 2) is thought to result from the following two opposing mechanisms: (1) the expansion caused by diffusion of the solute (copper or tin) into the iron lattice; and (2) the contraction caused by the increase in sintering rate due to the presence of a liquid phase. The observed dimensional changes due to copper and tin additions can be qualitatively explained in terms of the difference in their melting points (1083 and 232°C). Greater liquid-phase sintering activity follows when tin is used at the higher temperature of 1100°C.

Dimensional Change with Simultaneous Additions of Copper and Tin

The minima shown in Figs. 8–10 for additions of copper and tin at different Cu:Sn ratios at sintering temperatures of 900 and 1100°C are a consequence of the increase in sintering rate that follows when tin is added to the copper. Also, expansion is reduced by a decrease in the rates of diffusion of tin and copper into iron, as will be shown in Part II.

When compacts containing additions having a Cu–Sn ratio >9:2 were sintered at 900°C no increase in dimensional change was observed since insufficient tin was present to melt the copper completely.

The curves relating dimensional changes with sintering temperature for compacts containing copper and tin at various ratios are similar in shape whether finer (Fig. 10) or coarser (Fig. 9) copper powder is used. Copper particle size evidently has little effect on dimensional accuracy.

The curve of dimensional change vs. sintering temperature for a 15:2 Cu:Sn ratio (Fig. 12) showed a marked growth for the 10% total addition which was not seen in the 4% sample. Metallographic examination of samples sintered for ½ h at 1000°C revealed that some copper remained undissolved by the tin in compacts containing 10% additions, while no undissolved copper was observed in the 4% addition samples. At its melting point the undissolved copper would diffuse into the iron, producing the rapid growth seen in the 10% samples. At temperatures >1083°C the growth is reduced as there is no more copper available for the diffusion into the iron and also the general sintering reactions are accelerated.

Conclusions

(1) Significantly higher strengths can be obtained by using a copper: tin ratio of 15:2 than by using either pure iron or iron–copper compacts sintered at the same temperature in an atmosphere of nitrogen containing 10% of hydrogen.

(2) A considerably lower sintering temperature can be used to achieve similar properties. For example, iron with a 10% addition of 15:2 copper:tin sintered at 900°C will produce higher strengths than will iron with 10% copper sintered at 1100°C.

(3) Elongations are generally of the same order as those expected with sintered iron–copper alloy compacts.

(4) Dimensional accuracy control is better than with iron–copper compositions.

(5) Copper particle size seems to have little effect on dimensional accuracy.

(6) Lower sintering temperatures bring economies not only from reduced heating costs but also from longer furnace-belt life and lower maintenance costs.

II. Sintering Mechanisms in the System Fe–Cu–Sn

Literature Survey

The Tin Research Institute[1] initiated the use of tin additions to iron powder to improve its sintering characteristics. They reported that the incorporation of tin powder increased the tensile strength of iron compacts sintered at temperatures below those normally employed, but that addition of $> 2\%$ tin caused undesirable embrittlement and a lowering of mechanical properties. By adding copper as well as tin this excessive brittleness was prevented. They thus concluded that only a part of the copper should be replaced by tin. It was also suggested that the increased mechanical properties were due to some effect of tin in solid solution in the iron, such as a modification of the surface energy of the iron particles, or α-phase stabilization at the sintering temperatures employed (~ 950–1100°C).

In further work they aimed to determine the optimum copper–tin ratio, the correct addition, and the sintering parameters of this system. Barua, Ainsworth, and Robins[2] found the optimum ratio to be 3:2 copper:tin (within the investigated range from pure tin to 70:30 copper:tin) and the best level of addition 5% when sintering in pure dry hydrogen. They found that near-maximum strengths were obtained with a sintering temperature of 950°C, which was a substantial reduction from the usual sintering temperature of 1100–1150°C for iron–copper compacts. Again, the mechanism of sintering was thought to be due to the effect of tin in solid solution in the iron at low copper:tin ratios. Copper was considered to have little effect upon the rate at which tin went into solution. At a copper:tin ratio of 3:2, significant amounts of Cu_3Sn are formed and with higher ratios there is a loss of strength due to the embrittling effect of this phase.

Esper, Friese, and Zeller[3] used a dilatometric technique to study the sintering reactions occurring in Fe–Sn and Fe–Cu–Sn sintered compacts. They postulated many reactions occurring at various temperatures up to the sintering temperature, but these facts have limited use as it was shown that pre-alloyed copper–tin powder gives very similar results to elemental powder additions, without the possibility of all the intermediate reactions.

In a further paper, Esper and Zeller[4] examined other compositions in an attempt to obtain better ductility. They obtained maximum ductility with a 4:1 copper:tin addition, which gave an ultimate tensile strength only $\sim 6\%$ lower than that obtained with a copper:tin ratio of 3:2, and therefore not significant. They found no evidence of tin in solid solution at ratios of 3:1–5:1, and a high dilation due to the $\alpha \rightarrow \gamma$ phase transformation. At a ratio of 3:2 they detected some tin in

solution, with a corresponding lowering of the dilatation due to the smaller amount of $\alpha \rightarrow \gamma$ transformation.

To investigate the sintering mechanisms more closely, it was necessary to design diffusion experiments on a macroscale so that accurate analysis of any reactions occurring could be carried out. In conventional powder compacts the intergranular lakes were ~ 10 μm in dia., making investigation difficult even with an electron microprobe analyser (resolution 3–5 μm).

Experimental Procedure

Copper and tin powders of composition ranging from pure copper through various alloys to pure tin were placed in 3·2 mm ($\frac{1}{8}$ in.)-dia. holes drilled into a block of vacuum-cast 0·1% carbon steel. This was heated for $\frac{1}{2}$ h at 1100°C in an atmosphere of dry 90% nitrogen/10% hydrogen. The block was then sectioned and studied metallographically and by electron-microprobe analysis.

A second series of experiments was performed to investigate the reaction of tin with iron at low temperature. -100 mesh (-152 μm) MP 32 iron powder and -300 mesh (-53 μm) tin powder were used with no lubricant addition. The composition of the powder mix was 90% Fe/10% Sn and it was compacted at a pressure of 470 N/mm^2 (30 tonf/in^2) to a density of $\sim 6{\cdot}8$ g/cm^3. It was sintered at 400°C for 15 min in dry 90% nitrogen/10% hydrogen. The compact was then sectioned and studied metallographically and by electron-microprobe analysis.

Results

The results of the diffusion experiments are shown in Figs. 13–18, which illustrate the microstructures at the interface between solid steel and the copper–tin alloys after heating for $\frac{1}{2}$ h at 1100°C. Electron scans showing the changes in composition across the interface are reproduced beneath each photomicrograph.

Fig. 13 shows some grain-boundary diffusion of copper into the iron, although the extent is very limited due to the low level of superheat in the liquid copper at the experimental temperature, 1100°C. The electron scans show that little iron has diffused into the copper. The peak in the copper scan within the iron layer is caused by the electron beam cutting across a copper-rich grain boundary. It verifies the presence of grain-boundary diffusion of copper in the iron.

The composition of the copper–tin alloy analysed in Fig. 14 was 60% copper–40% tin, i.e. 3:2 copper:tin ratio. Iron has dissolved into the liquid at 1100°C, as shown by the primary dendrites within the copper–tin matrix which analyse 95% iron, the remainder copper and tin.

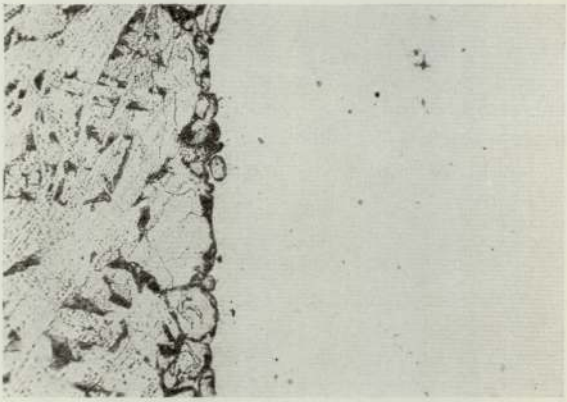

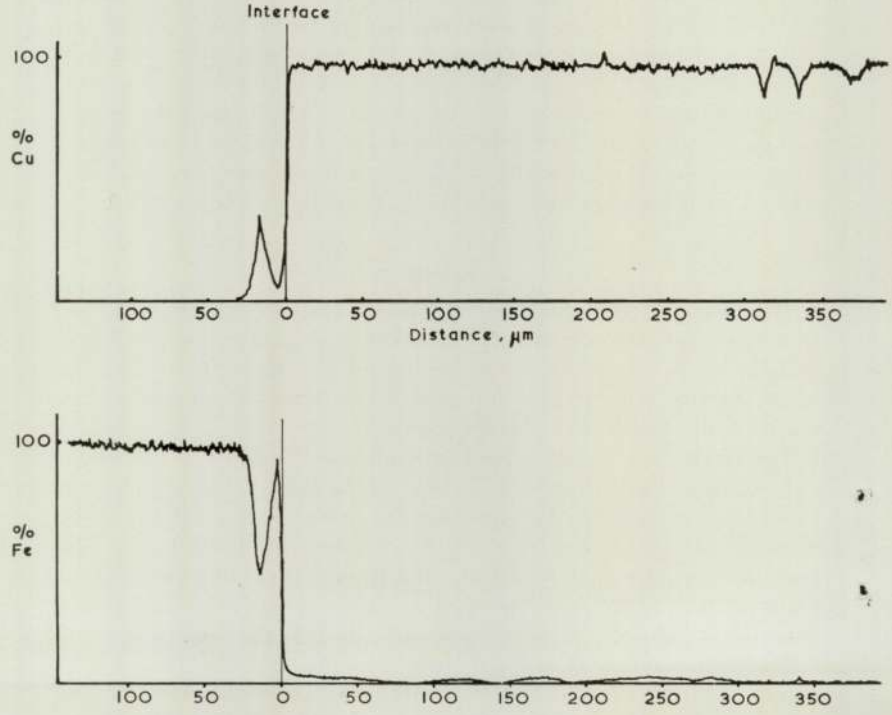

FIG. 13. Microstructure and electron-probe scan of section of the interface between Fe and Cu after diffusion.

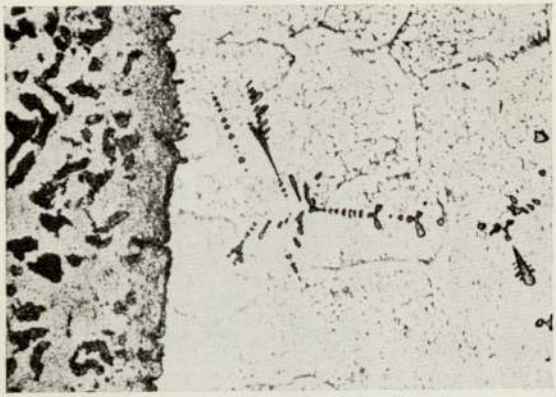

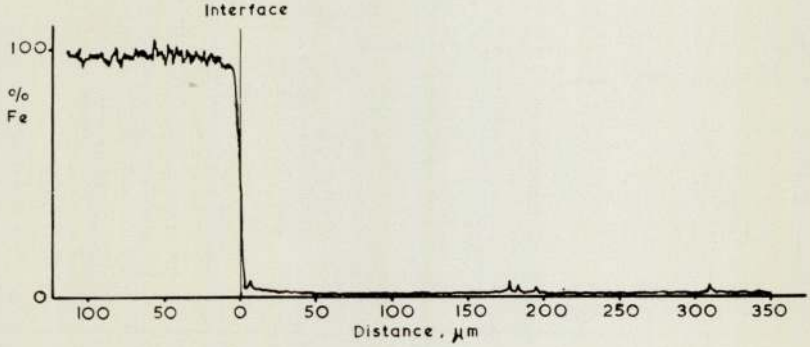

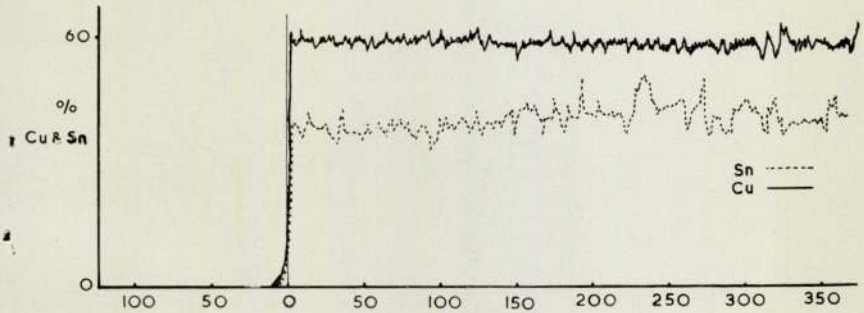

FIG. 14. Microstructure and electron-probe scan of section of the interface between Fe and 60–40 Cu–Sn alloy after diffusion.

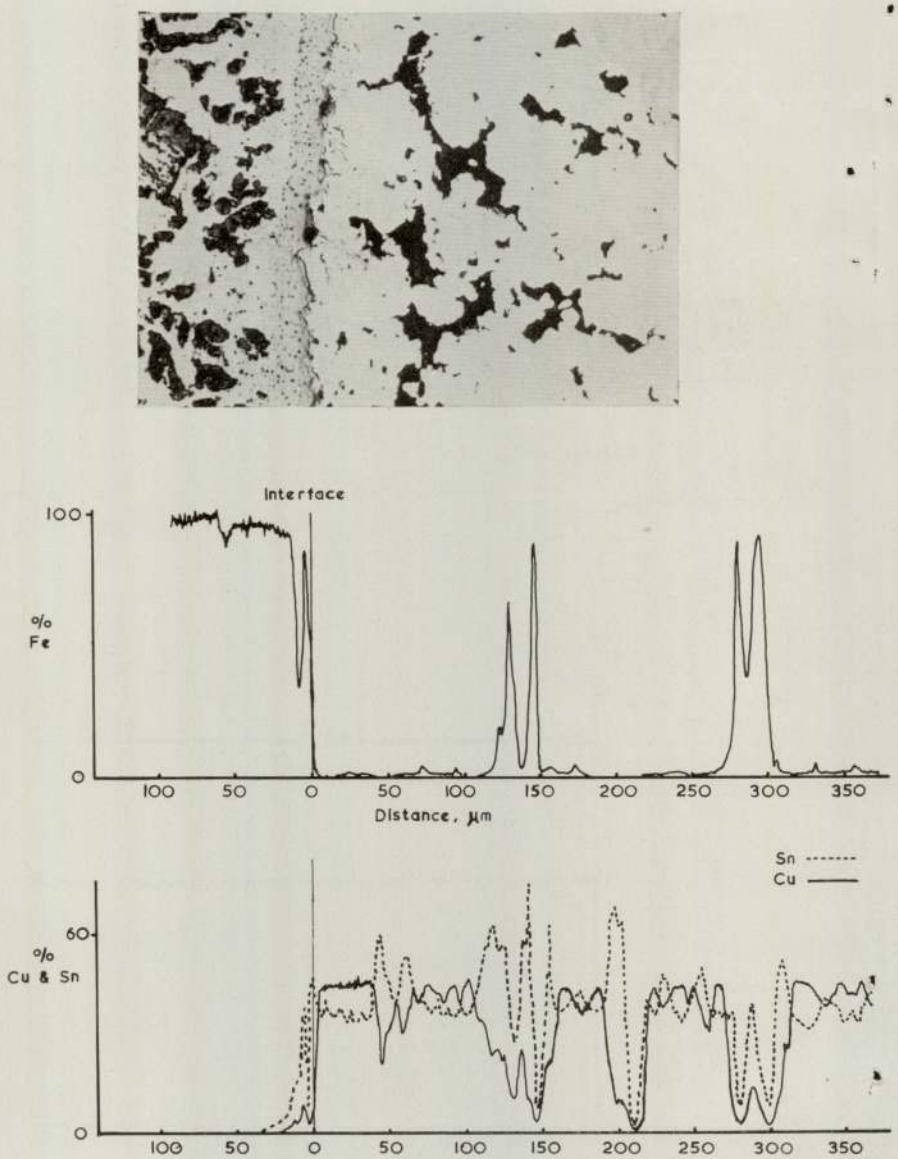

FIG. 15. Microstructure and electron-probe scan of section of the interface between Fe and 40:6 Cu–Sn alloy after diffusion.

The traces show no significant diffusion of either copper or tin into the iron, and the copper–tin matrix is a uniform ϵ phase Cu_3Sn. Near the interface a zone of apparent precipitation from the iron can be seen as was noted by Esper *et al.* within the grains of their sample sintered at 1050°C. However, this 'precipitation' was not noticeable in unetched specimens in the present work, and it is believed that it is an electrochemical effect produced by etching two dissimilar metals in 2% nital solution.

From the electron scan for Fe in Fig. 15 it can be seen that much more iron was dissolved in the copper–tin liquid, although no dendrites were etched-up in the photomicrograph. Porosity in the copper–tin-rich phase was due to the unavoidable break-up of the very brittle constituents during polishing. The electron-scan traces also show a diffusion gradient of copper and tin within the iron but only to a distance of ~30 μm. In the copper–tin matrix two intermetallic phases were present ϵ-Cu_3Sn and η-Cu_6Sn_5, as well as the iron-rich constituent.

Fig. 16 shows the results of an experiment in which pure tin was held in contact with iron for ½ h at 1100°C. Extensive reaction occurred. As well as the tin dissolving into the iron over a considerable distance (~120 μm), iron had dissolved into the tin to give dendrites of an iron–tin compound in the tin matrix. This experiment emphasizes that two-way solution occurs between the metallic phases. Note also that tin has pushed the small amount of carbon ahead of its diffusion front.

Fig. 17 illustrates the flow of molten tin around the grains of iron when a powder mix of 90% iron/10% tin with no added lubricant was sintered for only 15 min at 400°C. At high magnification (the white scale distance represents 10 μm), it is apparent that considerable reaction has occurred between iron and molten tin, causing precipitation of an iron–tin compound during cooling and solidification of the liquid phase, as reported by Esper *et al.*[3]

The tin lake shown in Fig. 17 was examined with the X-ray microprobe analyser and Fig. 18(*a*) shows an electron image of the lake. Figs 18 (*b*) and (*c*) are, respectively, a photograph of iron X-rays and an electron scan of the image along the line indicated. These confirm that the tin lakes contain iron and, therefore, that tin has reacted with iron in powder compacts after short periods at temperatures as low as 400°C.

Discussion

The diffusion experiments confirm the finding of other workers[1] that both copper and tin individually will diffuse into iron. At 1100°C the diffusion of tin is considerable, but with copper, diffusion is limited

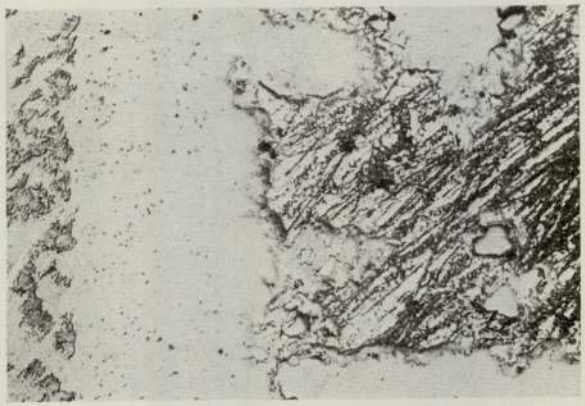

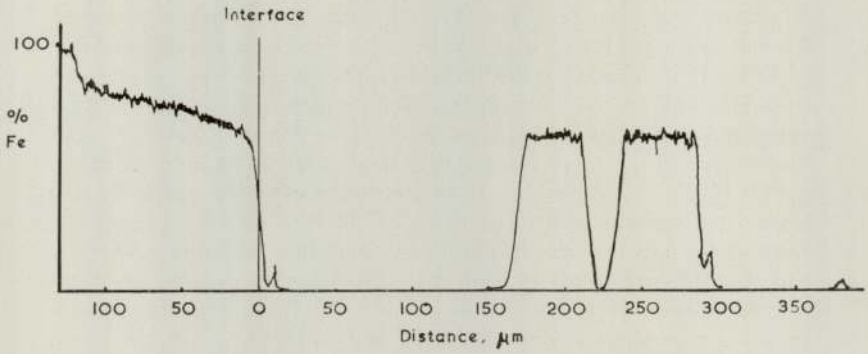

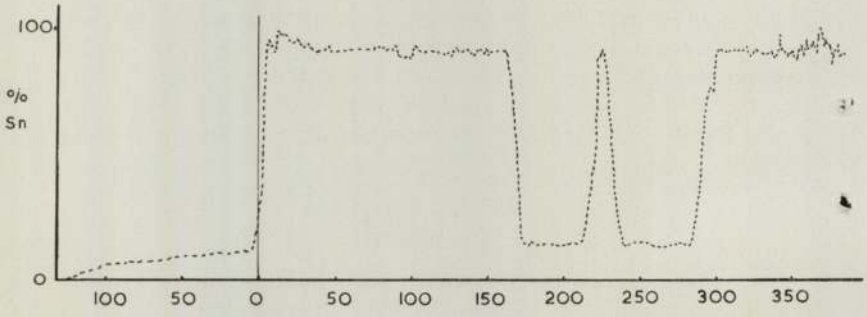

FIG. 16. Microstructure and electron-probe scan of section of the interface between Fe and Sn after heating at 1100°C.

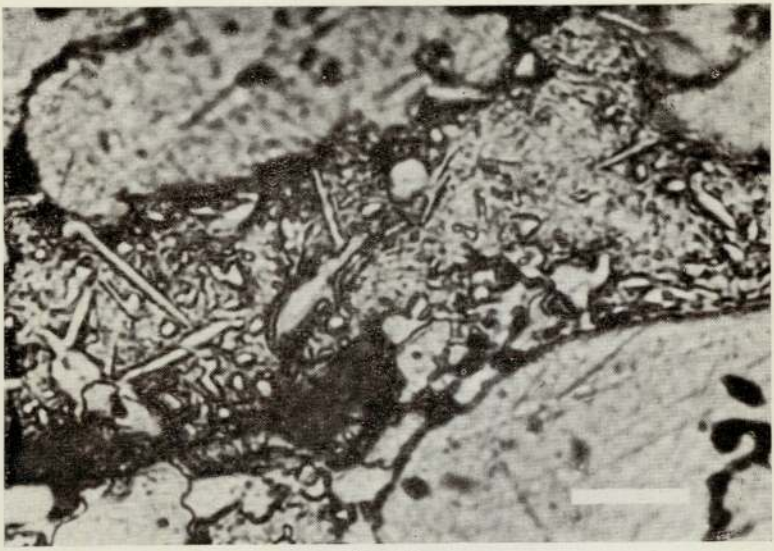

FIG. 17.

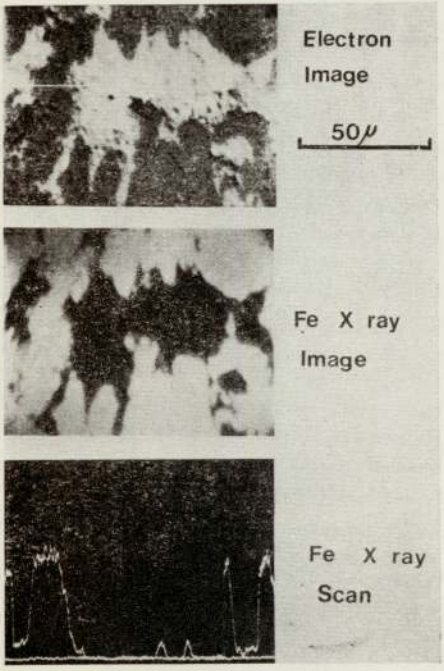

FIG. 18.

mainly to grain boundaries as the level of superheat in the molten copper is very low.

As tin is added to iron/copper mixes, diffusion of copper into the iron decreases to an almost undetectable level at the sintering temperature, while the solubility of iron in the liquid copper–tin increases. At high tin levels, its diffusion into the solid iron becomes noticeable simultaneously with increasing solubility of iron in the liquid. This restriction by tin on the copper diffusion and by copper on tin diffusion confirms the work by Robins *et al.*[5] and of Esper *et al.*[4] and helps to keep the copper–tin additions molten at the sintering temperatures, consequently aiding the sintering process. Intermediate copper–tin alloys seem to react with iron mainly by dissolving it rather than by diffusion into it to a significant extent. Dissolution of iron at the interface would tend also to remove any solid diffusion gradient that might be set up. According to Long and Robins[5] this would be disadvantageous to the sintering process, but the present work does not seem to substantiate this theory.

In all the investigations carried out at the authors' laboratories, it was found that a copper:tin ratio of 3:2 was the lowest that could be used before excessive brittleness began to affect the final mechanical properties. It was also found that only tin diffused significantly into the iron at lower copper:tin ratios. Long and Robins (*loc. cit.*) suggested that this was the major factor in improving the sintering characteristics of iron–copper–tin sintered compacts by increasing the self-diffusion rate of iron by stabilizing the α phase at the sintering temperature. Evidence for this theory was cited in the sintering behaviour of Fe–Cu–Sn compacts containing carbon.[6] The tensile strength of these compacts was decreased by increasing the carbon content, although a liquid phase was always present. It was suggested that because carbon is a strong γ stabilizer at the sintering temperature of 1000°C, its presence overruled α stabilization by tin, and consequently poorer sintering ensued together with lower final mechanical properties.

It has already been emphasized that the composition of the atmosphere is a major factor in controlling the sintering characteristics of Fe–Cu–Sn compacts, and that when carbon is associated with these elements in an attempt to improve final mechanical properties it is very important to control the dew-point of the sintering gases. Fairbank and Palethorpe[7] showed that the dew-point must be 270–256 K (−3–−17°C) for a steel containing 0·8% carbon potential at 900–1100°C, when using an endothermic gas. In recent work by one of the authors it has been shown that very different values of tensile strength can be obtained in iron–copper–tin compacts (3:2 and 15:2 ratios) sintered at 950°C according to whether the furnace atmosphere is hydrogen or carbon monoxide (Table IV).

TABLE IV. **Effect of Sintering Atmosphere on the UTS of Fe–Cu–Sn–C Compacts***

Copper:Tin Ratio (5% addition)	Added Carbon %	UTS kgf/mm²	UTS N/mm²	Sintering Atmosphere
3:2	0·2	18·1	178	H_2
,,	0·6	24·3	238	,,
,,	0·8	25·2	247	,,
,,	1·2	24·3	238	,,
3:2	0·2	24·9	244	CO
,,	0·6	28·0	275	,,
,,	0·8	28·0	275	,,
,,	1·2	33·2	326	,,
15:2	0·2	21·7	213	H_2
,,	0·6	21·4	210	,,
,,	0·8	18·1	178	,,
,,	1·2	19·8	195	,,
15:2	0·2	26·6	261	CO
,,	0·6	34·0	334	,,
,,	0·8	38·3	375	,,
,,	1·2	40·0	392	,,

* Sintered at 950°C. Compacting pressure 386 N/mm² (25 tonf/in²).

The results for 3:2 copper:tin compacts agree reasonably well with those of Barua and Thwaites,[6] determined on compacts sintered for 1h at 1000°C in hydrogen. They showed a decrease in final strength with increasing carbon. This suggested that there is no increased strengthening of the matrix by carbon solution, possibly because the extent of sintering is decreased by high carbon content. This cannot be the full explanation, as the results for carbon monoxide sintering show (especially in the case of 15:2 Cu:Sn compacts) that the UTS is raised considerably above that of compacts containing no carbon.

Esper and Zeller[4] could not detect any tin in the iron at copper:tin ratios of 3:1–5:1, but the UTS with the 4:1 Cu:Sn ratio was very similar to that obtained with the 3:2 ratio. Therefore it is suggested that α-phase stabilization by solution of tin in the iron matrix is unlikely to be the major factor affecting the sintering process. Only at very low Cu:Sn ratios can a phase stabilization occur to any significant extent, and at these tin levels, the brittleness of the tin rich phases nullifies any increase in sintering, due to the greater self-diffusion rates of iron in the α phase.

In the low-temperature sintering experiments it was shown that tin reacted very rapidly with iron particles even at 400°C. With copper present, this wetting of the iron enabled the tin to move around the

grains of iron more quickly and thus react with the copper as well, forming a ternary liquid of lower melting point. It is postulated that this interaction of tin with iron and copper delays its diffusion into the iron until complete liquid saturation occurs. Then sufficient time at the sintering temperature must elapse to allow a significant amount of tin to diffuse into the iron.

Conclusions

Tin additions to iron–copper compacts have four major effects:

(1) They increase iron solubility in the liquid phase and thereby cause very much higher rates of mass transfer of iron in the liquid.

(2) They decrease the rate of copper diffusion into iron, enabling much closer dimensional control as growth is reduced. (Figs. 8–10).

(3) They increase the wettability of the liquid by reducing the surface tension of the copper, permitting the liquid to disperse itself more fully within the matrix.

(4) They lower the liquidus temperature, allowing the above processes to occur at lower temperatures.

It appears that tin is the active constituent in controlling the sintering process but a major consideration is the type of atmosphere employed. With high tin contents mechanical properties are reduced because of the brittleness of the compounds produced, although the sintering rate in the absolute sense is increased. At high copper contents ductility is improved owing to the decrease in brittle compounds.

It would seem, therefore, that the mechanical properties, growth characteristics, and (to a lesser extent) the sintering temperature can be controlled effectively by correct choice of copper:tin ratio and of sintering atmosphere.

References

1. R. Duckett and D. A. Robins, *Metallurgia*, 1966, **74**, 163.
2. S. K. Barua, P. A. Ainsworth, and D. A. Robins, *Metallurgia*, 1969, **80**, 87.
3. F. Esper, K. H. Friese, and R. Zeller, *Int. J. Powder Met.*, 1969, **5**, 19.
4. F. Esper and R. Zeller, *Powder Met., Conference Suppl.* Part 1, **1971**, 311.
5. J. B. Long and D. A. Robins, 'Modern Developments in Powder Metallurgy', Vol. 4, 303, **1971**: New York (Plenum Press).
6. S. K. Barua and C. J. Thwaites, *Metall*, 1970, **24**, 460.
7. L. H. Fairbank and L. G. W. Palethorpe, 'Heat Treatment of Metals' (Special Rep. No. 95), p. 57. **1936**: London (Iron Steel Inst.).